A CASE STUDY ON SETTLEMENT ANALYSIS OF GEOTHERMAL POWER PLANT FOUNDATION

A Thesis Submitted to
the Graduate School of Engineering and Sciences of
İzmir Institute of Technology
in Partial Fulfillment of the Requirements for the Degree of

MASTER OF SCIENCE

in Civil Engineering

by
Hakan ELMAS

December 2018
İZMİR

We approve the thesis of **Hakan ELMAS**

Examining Committee Members:

Assoc. Prof. Dr. Nurhan ECEMİŞ
Department of Civil Engineering, İzmir Institute of Technology

Prof. Dr. Yeliz Yükselen AKSOY
Department of Civil Engineering, 9 Eylül University

Prof. Dr. Gökmen TAYFUR
Department of Civil Engineering, İzmir Institute of Technology

03 December 2018

Assoc. Prof. Dr. Nurhan ECEMİŞ
Supervisor, Department of Civil Engineering,
İzmir Institute of Technology

Prof. Dr. Şebnem Şeker ELÇİ
Head of the Department of
Civil Engineering

Prof. Dr. Aysun SOFUOĞLU
Dean of the Graduate School of
Engineering and Science

ACKNOWLEDGMENTS

I would like to thank Assoc. Prof. Dr. Nurhan Ecemiş, who has made great contributions to my academic development, for her knowledge, guidance and encouragement during the thesis study.

I would like to thank Mustafa Koç, who have been unsparing in help people, for providing opportunity to change my life and start the academic career.

I would like to thank Destech family for sharing their knowledge and experience with me.

I would like to thank my friend, Berk Demir, who is ambitious, clever and helpful engineer, for sharing source of geotechnical literature and geotechnical software with me.

I would like to thank Mümin Şen for his valuable friendship, encouragement and support in my life.

I would like to thank Yunus Emrah Karacan, who represents his management skills well.

I would like to thank Hüseyin Ergin and Ahmet Esen for help in plate load test, construction of measurement system and recording settlement value.

The deepest thanks to my father, Kemal Elmas, my sisters, Nazlı Özel and İlayda Elmas, my cousin Emre Elmas, my sister's husband, Sinan Özel, my niece, Eylül Ebrar Özel and my nephew, Emir Özel for being a real family in difficult periods of my life.

ABSTRACT

A CASE STUDY ON SETTLEMENT ANALYSIS OF GEOTHERMAL POWER PLANT FOUNDATION

Foundation settlement criteria are highly sensisitive for geothermal power plants. In geotechnical literature there are several settlement analyses which can be done by using elastic approaches, in-situ test results or numerical methods. Unfortunately, all these methods cannot give close results with each other. As a result, the unrepresentative analyses influence the safety, economy and time of the projects.

In this study, the settlement of the geothermal power plant located in Aydın / İncirliova which constructed on a raft foundation was investigated. According to soil investigations, the raft foundation is located on multilayer soil profile and a compacted high qualified fill layer is placed under the raft foundation. Soil parameters were obtained from in-situ tests (standard penetration tests, cone penetration tests, pressuremeter tests and plate load test and) and laboratory experiments.

Settlement results were obtained by 1D stress – strain analyses and 3D continuum numerical analyses (Hardening Soil Model with Small Strain Stiffness and Mohr Coulomb Soil Model) using the commercially available Settle 3D and Plaxis 3D software, respectively. The results of these analysis were also compared with the field monitoring data. The results show that Hardening Soil Model with Small Strain Stiffness gave more accurate result than other models due to the representation of real soil behavior, obtaining non-uniform stress distribution of foundation and obtaining effective stress depth accurately for settlement.

ÖZET

VAKA ANALİZİ: BİR JEOTERMAL ENERJİ SANTRALİNE AİT TEMEL OTURMASI

Temel oturma kriterleri jeotermal enerji santralleri için oldukça hassastır. Geoteknik literatürde elastik yaklaşımları, saha test sonuçlarını ya da nümerik yöntemleri kullanan bir çok oturma analiz yöntemi vardır. Maalesef bu yötemler birbirlerine yakın sonuçlar verememektedir. Saha oturmasını temsil etmeyen analizler projelerin güvenliğini, ekonomisini ve zamanını etkilemektedir.

Bu çalışmada, Aydın/İncirliova'da yer alan ve radye temel üzerine inşa edilmiş bir jeotermal enerji santralinin oturması incelenmiştir. Zemin araştırma çalışmalarına göre, radye temel çok tabakalı zemin profili üzerinde yer almaktadır ve temelin altında sıkıştırılmış nitelikli zemin dolgusu bulunmaktadır. Zemin parametreleri saha testlerinden (standard penetrasyon testi, koni penetrasyon testi, presiyometre testi ve plaka yükeleme testi) ve laboratuvar deneylerinden elde edilmiştir.

Oturma sonuçları tek boyutlu gerilme birim deformasyon analizleri ve üç boyutlu sürekli nümerik analizleri (Hardening Soil Model with Small Strain Stiffness ve Mohr Coulomb Soil Model) ile elde edilmiştir. Bu analizler sırasıyla ticari olarak ulaşılabilen Settle 3D ve Plaxis 3D yazılımları kullanılarak yapılmıştır. Analiz sonuçları sahada ölçülen oturma değerleri ile kıyaslamalı olarak verilmiştir. Oturma analiz sonuçları şunu göstermiştir: Hardening Soil Model with Small Strain Stiffness nümerik analizi zemin davranışını, temel altındaki farklı gerilme dağımlarını ve oturmanın gerçekleşeceği etkili derinliği daha doğru temsil etmesinden dolayı diğer analizlerden daha kesin sonuç vermiştir.

To my mother, Esma ELMAS who is the source of success in my life.

TABLE OF CONTENTS

LIST OF FIGURES

LIST OF TABLES

CHAPTER 1

INTRODUCTION

1.1 General

Geothermal power plants produce energy with using hydrothermal resources which include high water vapor pressure in the temperature range between 120° C and 320° C. The geothermal energy resources are renewable and are seen in 10% of earth show that it has a vital importance.

Vapor pressure, which has high temperatures, is transported with the help of steel pipelines. Especially in the part of the turbine where electricity is produced pipe stresses must be limited for safety concepts. Pipe stresses are affected by internal and external factors. Settlement of turbine foundation is an external effect which causes to stress in the pipes. Not only geothermal power plants but also other type power plants analyzing of settlement is very important. For example, in this total settlement values do not exceed 0.01 m to 0.02 m after piping and differential settlements ratio do not exceed 1/1000.

In this study, it has been investigated which of the settlement analysis methods will give more accurate results in projects with precise settlement criteria. But the selection of correct soil models is not sufficient also determination of soil parameters which are used in models, analyzing of stress distribution on soils and obtaining effective depth level of soils where stress increment decrease zero are just as important as settlement analysis methods.

Due to the non-uniform soil layer, settlement analysis based on in situ tests and empirical methods were not reasonable. Project soil profile in the order and thickness of the units as follows: silty clay 2.5-meter silty sand 4.5-meter silty clay 11.5-meter silty sand 3-meter silty clay 5.5-meter and clayey silt 2-meter. To analyze multilayer soil settlement correctly 1D Stress – Strain Relation analyses and 3D continuum numerical analyses (Hardening Small Strain Stiffness Soil Models and Mohr Coulomb Soil Models) was used.

The soil parameters to be used in the model were selected with the help of prominent correlations in the geotechnical literature by controlling their compatibility with one of the in situ tests, which were standard penetration tests, cone penetration tests, pressuremeter tests and plate load tests. For cohesive soils the compatibility of cone penetration tests and pressuremeter tests were examined and for cohesionless soils the compatibility of cone penetration tests and standard penetration tests were examined. Moreover, related laboratory works were evaluated.

In the project, nearly 220 points loads were applied on the raft foundation so that to obtain correct settlement value determination of soil structure interaction was important. Numerical continuum soil models were used to obtain the distribution of stress on soils. Moreover, effective depth level was evaluated with traditional methods and numerical continuum models.

1.2 Problem Statement

The analysis of the results that do not evaluate real settlements value directly affect the projects in terms of safety, time and economy. Especially, in power plant projects settlements criteria highly sensitive and lots of project choose soil improvement methods according to unrepresentative settlement results so that owners risk time commitments and project costs increase. The settlement analyses must have some criteria for such sensitive structures. In this study may provide how to evaluate necessary condition to obtain accurate settlement results.

1.3 Organization of the Thesis

The thesis consists of six chapters. The first chapter is the introduction includes general information, problem statement and organization of the thesis. The second chapter is background information includes differential settlement and total settlement of shallow foundation, determination of soil stiffness parameters and stress increment methods. The third chapter is the geothermal power plant project includes investigation area, the geology of the project area and site investigation tests and laboratory experiments. The fourth chapter is settlement analysis of the foundation which includes project information for settlement analyses, data analyses, settlement analyses with 1D stress – strain relation and settlement analyses with numerical methods, the fifth chapter is result and discussion includes settlement for stage loads, comparison of stress increment methods, the differential settlement result and determination of oedometric stress strain modulus of clay. The final chapter is conclusions and recommendations.

CHAPTER 2

BACKGROUND INFORMATION

2.1 Introduction

Service loads and own weight of structures statically generate compression which cause to sinking of structures into the underlying soil is described as settlement. (Terzaghi et al, 1996). Total settlement and differential settlement criteria should be checked for settlement analyses. In the project total settlement values should not exceed 0.01 m to 0.02 m after piping and differential settlements ratio should not exceed 1/1000. As a result, the shallow foundation is used to decrease differential settlement values, structure stresses on soils and balance hydrostatic uplift pressure.

In this chapter, firstly, the literature review about the settlement of shallow foundations for cohesive and cohesionless soils was presented. Then, the evaluation of soil stiffness parameters (stress strain modulus and Poisson's Ratio) from consolidation test, plate load test, standard penetration test, cone penetration test, the pressuremeter test and laboratory experiments were introduced. Finally, determination of the stress increment due to applied load at any depth was presented.

2.2 Differential Settlement of Shallow Foundation

Differential settlement is a different amount of settlement within the same structure. Figure 2.1 represents that points A – E on the same line but after settlement occurred point B was displaced more than other points.

Differential settlement in a structure is more undesirable than the total settlement or uniform settlement. Angular distortion the is ratio between vertical difference and displacement of two points. In Figure 2.1, maximum angular distortion is between point A and point B. Bjerrum (1963) classified limiting angular distortion in Figure 2.2. When foundation has no uniform loads disruption and nonhomogeneous soil stratum, continuum numerical methods are necessary to obtain an accurate differential settlement.

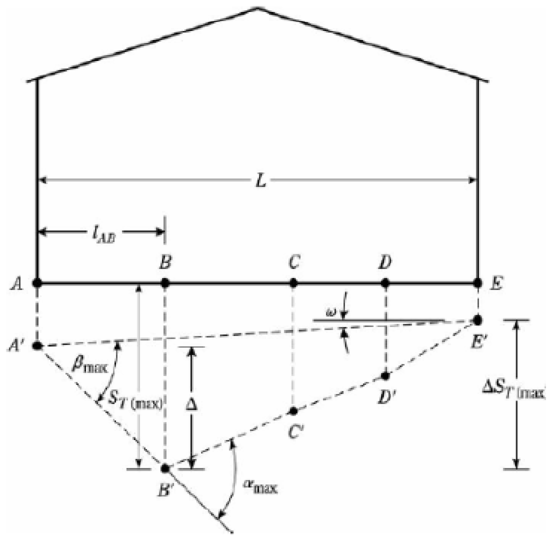

Figure 2.1 Representation of Differential Settlement

(Source: Kim, 2015)

Potential damage	β_{max}
Safe limit for flexible brick wall	1/150
Danger of structural damages to most buildings	1/150
Cracking of panel and brick walls	1/150
Visible tilting of tall rigid buildings	1/250
First cracking of panel walls	1/300
Safe limit for non-cracking of buildings	1/500
Danger to frame with diagonals	1/600

Figure 2.2 Limiting Angular Distortion for Structures

(Source: Bjerrum, 1963)

2.3 Total Settlement of Shallow Foundation

The magnitude of the service loads and own weight of the structure, size of the foundation, soil conditions and gradation, soil stiffness and soil strength affect the settlement of shallow foundation. In saturated fine soils, time and excess pore water pressure have significant effect on settlement rate depending gradation of soil. Consolidation settlement of the foundation increase with time during excess pore water dissipation (Becker and Moore, 2006).

Total settlement of shallow foundation usually categorized as initial settlement, primary consolidation settlement, and secondary consolidation settlement. Initial settlement (immediate / elastic settlement) is generally seen as occurring just after the implementation of the service loads and own weight of the structure. (Smith, 2014). In cohesionless soils the elastic settlement is the main part of the total settlement, however in the saturated cohesive soils primary consolidation settlement is the main part of the total settlement. Secondary consolidation settlement must be taken into consideration for plastic clays and organic soils. In overconsolidated inorganic clays, the secondary consolidation index is very small and of less practical importance. (Das, 2014)

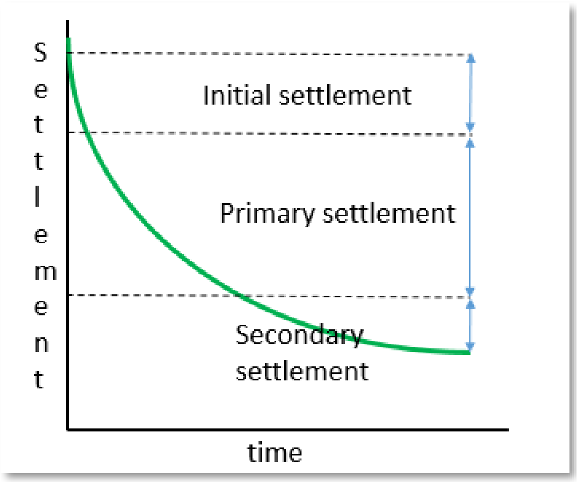

Figure 2.3. Parts of Total Settlement

$$S_T = S_i + S_c + S_s \tag{2.1}$$

Where;

S_T = Total Settlement, S_i = Initial Settlement, S_c = Primary (Consolidation) Settlement

S_s = Secondary (Consolidation) Settlement

2.3.1 Initial Settlement

Although total settlement calculation is divided into three parts for cohesive and cohesionless soil, some theoretical settlement analysis methods can be performed for each parts in view of the fact that the soil condition is drained or undrained. Theory of elasticity (Timoshenko and Goodier, 1951) mostly is used for initial (elastic or immediate) settlement calculations. The initial settlement has a big fraction rate in total settlement for cohesionless soil; on the contrary, it has a small fraction for normally consolidated cohesive soil. There are various formulations for initial settlement calculation, for example, Janbu et al. (1956) developed an equation for the flexible foundation on saturated clay soils or cohesionless soil settlement can be evaluated by strain influence factor proposed by Schmertmann et al. (1978). Most of these formulations are based on homogenous soil deposits so that cumulative elastic strain approach is introduced for the nonhomogeneous nature of soil deposits.

2.3.1.1 One Dimensional Cumulative Elastic Strain Approach

The initial settlement can be calculated by summing the vertical strains from the increase in effective stresses of sub layers. For multilayer nonhomogeneous soil deposits, cumulative elastic strain approach is useful and this calculation can be performed quickly using spreadsheet computer programs (Becker and Moore, 2006).

$$\varepsilon = \frac{\Delta\sigma}{E_s} \tag{2.2}$$

$$\mathrm{S}_i = \varepsilon \ . \ \mathrm{H} \tag{2.3}$$

Where;

ε = strain, $\Delta\sigma$ = the change in vertical total stress, E_s = stress strain modulus, H = depth of layers, S_i = Immediate or undrained settlement

The settlement of the i^{th} point is then the settlement of the point below (i+1) plus the settlement in sublayers i:

$$\mathrm{S}_i = \mathrm{S}_{i+1} \ . \ \varepsilon_i \ H_i \tag{2.4}$$

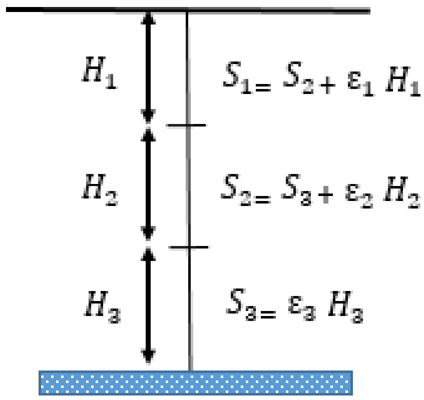

Figure 2.4. The Settlement of Any Soil Layer

2.3.1.2 Three Dimensional Cumulative Elastic Strain Approach

Poulos and Davis (1968) proposed using Eq. (2.5) to obtain an accurate initial settlement result because in a soil particular under one directional stress, strains occur in three directions. Three-dimensional cumulative elastic strain approach can be used for both cohesionless soils and overconsolidated cohesion soils.

$$Si=\sum\frac{1}{E}\left[\Delta\sigma_z-\nu(\Delta\sigma_x+\Delta\sigma_y\right]\ \delta h \qquad (2.5)$$

Where;

S_i = Immediate or undrained settlement, $\Delta\sigma_x$ = Stress increment in x direction, $\Delta\sigma_y$ = Stress increment in y direction, $\Delta\sigma_z$ = Stress increment in z direction, E = Drained or undrained stress strain modulus, δh = Unit height difference, ν = Undrained or drained Poisson's Ratio

The immediate or undrained settlement with mean stress can be used instead of Eq. (2.5) to perform more accurate three dimensional analyses.

$$Si=\sum\frac{1}{E}\left[(1+v)\Delta\sigma-3\Delta\sigma_m\right]\ \delta h \qquad (2.6)$$

Where;

$$\sigma_m=\sum\frac{1}{3}\ (\sigma_{xx}+\sigma_{yy}+\sigma_{zz})$$

S_i = Immediate or undrained settlement, $\Delta\sigma_m$ = Mean stress increment, E = Drained or undrained stress – strain modulus, ν = Undrained or drained Poisson's Ratio, Δσ = Total vertical stress increment

2.3.2 Primary Consolidation Settlement

In the previous chapter initial settlement was introduced for undrained cohesive soil and drained cohesionless soil. Primary consolidation settlement is only valid for fine cohesive soil in drain condition. In the primary settlement, 1D consolidation theory and degree of consolidation terms have an important place for understanding of the settlement of fine grained cohesive soil in time. Immediately after an applying a stress increment on the fine grained cohesive soil in fully saturated condition, the primary settlement will not be seen because water will carry whole stress increment. Sometime later, water starts to expel from soil pores and primary settlement starts to come to fruition. Piston Spring Analogy, which is given in Figure 2.5, is a good example to explain consolidation.

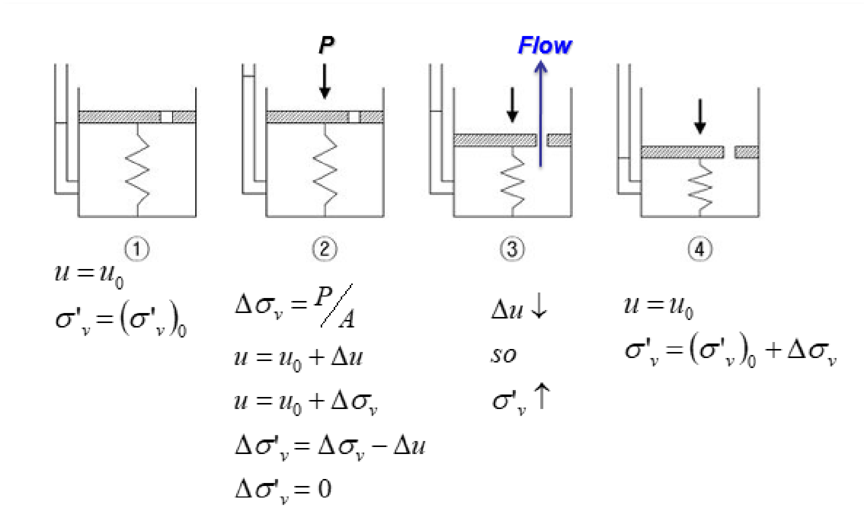

Figure 2.5. Piston Spring Analogy (Source: Likos, 2016)

Permeability, the thickness of stratum and the length of drainage path determine the expelling time of water and this time directly affect the rate of consolidation for a fine grained cohesive soil. (Budhu, 2010).

2.3.2.1 1D Consolidation Theory

Terzaghi (1944) developed the rate of 1D consolidation with some assumptions which are given below.

- Homogeneous clay layer.
- Fully saturated clay layer
- Accepting of Darcy's Law
- 1D compression is valid
- During consolidation process the coefficient of consolidation does not change.

Combining Darcy's law and volume change of soil element with time gives the equation;

$$\frac{k}{\gamma_w}\frac{\partial^2 u}{\partial z_2} = \frac{a_v}{1+e}\frac{\partial u}{\partial t} = m_v \frac{\partial u}{\partial t} \tag{2.7}$$

Where;

u= excess pore water pressure (Time and depth dependent), t=time, z=depth, k = permeability of soil, γ_w = unit weight of water, a_v = coefficient of compressibility, e = void ratio of soil, m_v = coefficient of volume compressibility

Volumetric Change

When consolidation load is applied on soil body, volume of soil will change in drain condition. Difference between initial volume ($V_1 = e_1 + 1$) and final volume ($V_2 = e_2 + 1$) over initial volume gives volumetric change.

$$\Delta V = \frac{V_1 - V_2}{V_1} = \frac{e_1 - e_2}{1 + e_1} \tag{2.8}$$

Coefficient of compressibility (a_v)

During consolidation compressibility of soil change and increasing of effective stress decreases soil compressibility. The rate of the void ratio – effective stress relation gives the coefficient of compressibility (a_v).

$$a_v = -\frac{\Delta e}{\Delta \sigma} \tag{2.9}$$

Coefficient of volume compressibility (m_v)

The coefficient of volume compressibility represents compression of a soil, per unit thickness, because of increasing pressure. Coefficient of compressibility over initial volume of soil gives the coefficient of volume compressibility.

$$m_v = -\frac{a_v}{1+e_1} \tag{2.10}$$

Excess pore water pressure (Δu)

To find excess pore water pressure at any time and depth after stress increment applied, the partial differential equation (2.7) can be solved with using separation of variable and with using boundary conditions. Moreover, Fourier series constant A_n can be determined with using orthogonality. Then excess pore water pressure equation is obtained as below;

$$u = \sum_{n=1}^{n=\infty} A_n \sin\frac{n\pi z}{2H} \exp(\frac{n^2\pi^2 T_v}{4}) \tag{2.11}$$

Where;

u = excess pore water pressure (Time and depth dependent)

$A_n = \frac{1}{H}\int_0^{2H} u_i \sin\frac{n\pi z}{2H} dz$ (Constant), $\quad T_v = \frac{dy}{dx}\frac{C_v t}{H^2}$ (*Time* Factor)

$C_v = \frac{k}{\gamma_w m_w}$ (Coefficient of consolidation)

t = time, z = depth, H = Stratum height (drainage type dependent)

Log of time method (Casagrande's Method), square root of time method (Taylor's Method), and some empirical methods can be used for determination of the coefficient of consolidation (C_v). If u_i is constant with depth Eq. (2.11) is determined as given below;

$$u = \sum_{m=0}^{m=\infty} \frac{2u_0}{M} \sin\frac{Mz}{H} \exp(-M^2 T_v) \quad (2.12)$$

Where;

M = (2m +1)

2.3.2.2 Degree of Consolidation

The degree of consolidation (U_z) is a ratio between current pore water pressure and initial excess pore water pressure and effective stress increment is equal to difference between current and initial excess pore water pressure. The degree of consolidation at a point is obtained with Eq. (2.13) or related chart is given in Figure 2.6.

$$U_z = 1 - \sum_{m=0}^{m=\infty} \frac{2}{M} \sin\frac{Mz}{H} \exp(-M^2 T_v) \quad (2.13)$$

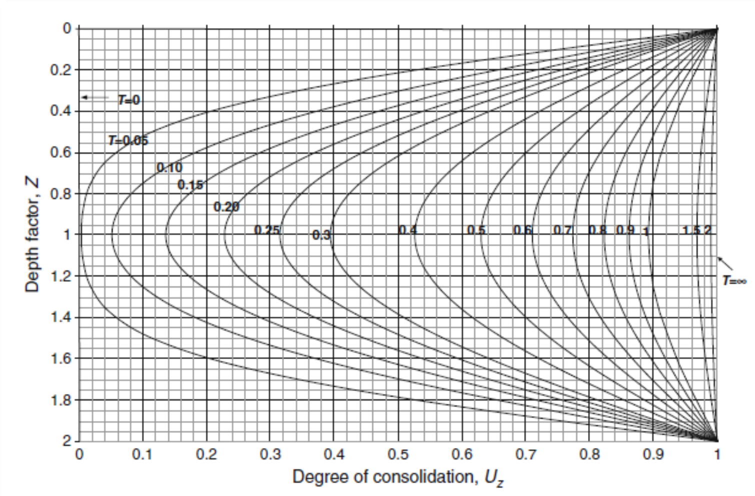

Figure 2.6. U_z , Z and T Relationship
(Source: Ameratunga et al, 2016)

In most cases, the average degree of consolidation is needed for the entire layer. The average degree of consolidation for a layer is obtained with Eq. (2.14) or related chart is given in Figure 2.7.

$$U_{avg} = 1 - \sum_{m=0}^{m=\infty} \frac{2}{M^2} \exp(-M^2 T) \quad (2.14)$$

Where;

$$T = \frac{\pi}{4} U^2_{avg} \text{ for } U_{avg} \leq 52.6\%$$

$$T = 1.781 - 0.933 \log (100 - U_{avg}) \text{ for } U_{avg} \geq 52.6\%$$

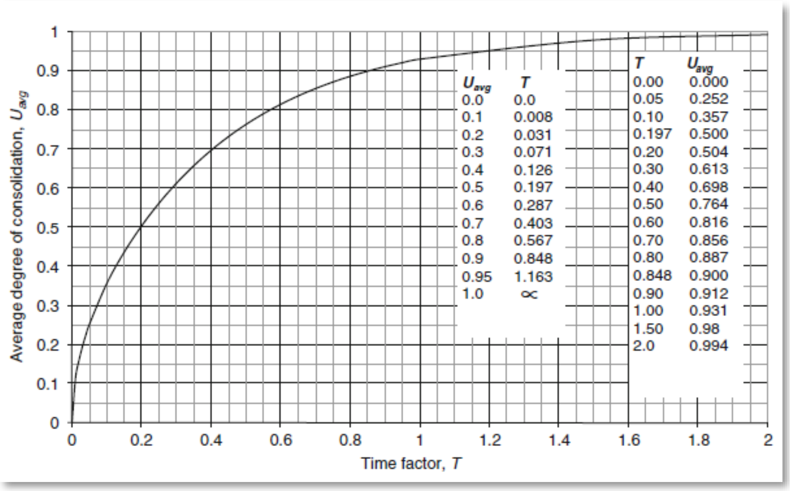

Figure 2.7. U_{avg} and T Relationship

(Source: Ameratunga et al, 2016)

2.3.2.3 Consolidation (Oedometer) Test

In consolidation test a soil sample is confined with a steel ring commonly has 75 mm diameter and 20 mm thick (ASTM D 2435-04). The consolidation test apparatus is given in Figure 2.8. Porous discs are placed at the top and bottom position of the soil sample for purpose of water expelling. Before the application of loading steps water is used for preventing pore suction. After that, compression is applied step by step with a load increment, which has commonly 0.25 kg/cm^2, 0.5 kg/cm^2, 1.0 kg/cm^2, 2.0 kg/cm^2, 4.0 kg/cm^2 (depending on project stresses), and periodically vertical settlement of soil sample is measured with the aid of transducer when settlement is over, the other load increment is passed (Figure 2.8.b). The consolidation test continues until reaching the required project stress levels and fully consolidation is achieved. For each increment steps void ratio of the specimen can be obtained and void ratio versus effective pressure graph can be drawn from test results as shown in Figure 2.9 a (Smith, 2014). Unloading process can be performed to obtain dilatation characteristic of the soil sample with releasing of the load in 24 hours intervals. Unloading process can be performed to obtain dilatation characteristic of the soil sample with releasing of the load in 24 hours intervals. Figure 2.9 b shows the expansion and recompression curves.

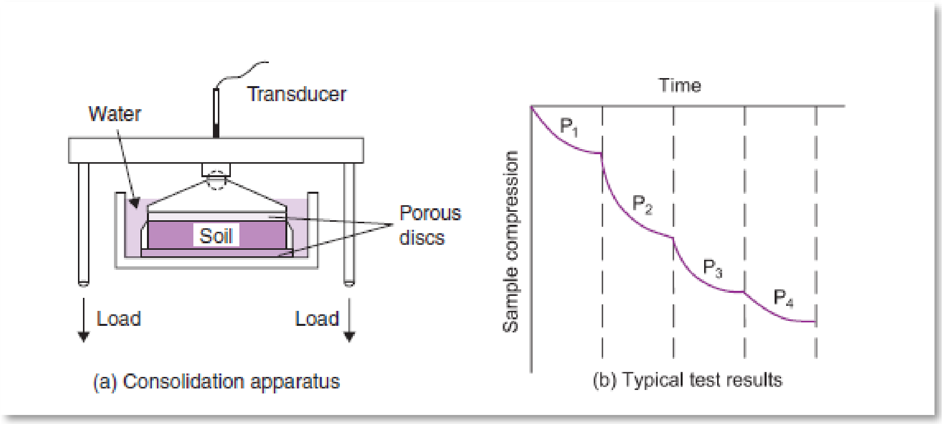

Figure 2.8. Consolidation Test Apparatus and Results
(Source: Smith, 2014)

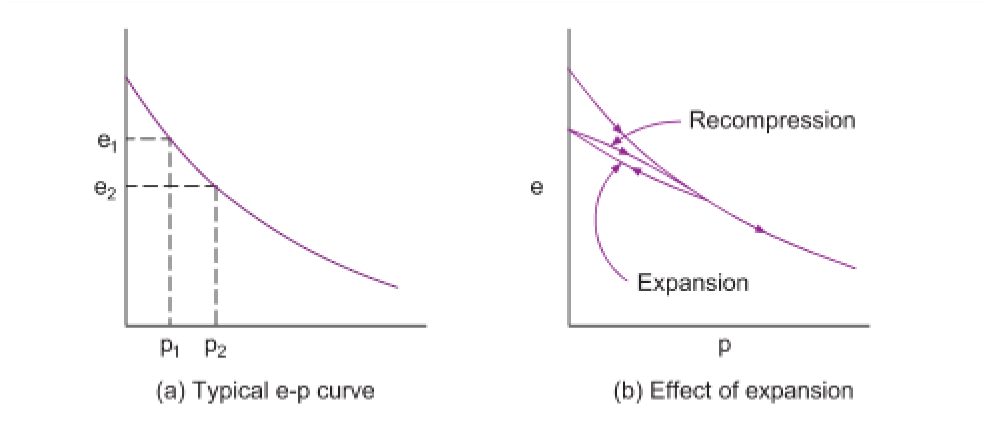

Figure 2.9. Void Ratio - Effective Pressure Graph
(Source: Smith, 2014)

Preconsolidation Pressure

Soil has a memory and remember the history of the past loading. If stress increment is in recompression zone, soil remembers past loading and less settlement will occur but in virgin compression, soil firstly is exposed to maximum stress level so that more settlement will occur as compared to recompression zone.

Preconsolidation pressure (σ_c') is equal to maximum past loading effective stress. Moreover, it is the midpoint recompression slope to compression slope. Preconsolidation pressure can be estimated with using Casagrande (1936)'s procedure, which has 4 steps given below.

- Extending the PR line from Point P which is the point of maximum curvature
- Drawing a horizontal line from Point P
- Drawing TS line as bisector of the angle
- The intersection point of bisector line and extending line (Slope = C_c) gives point T, its log stress component is equal to preconsolidation pressure

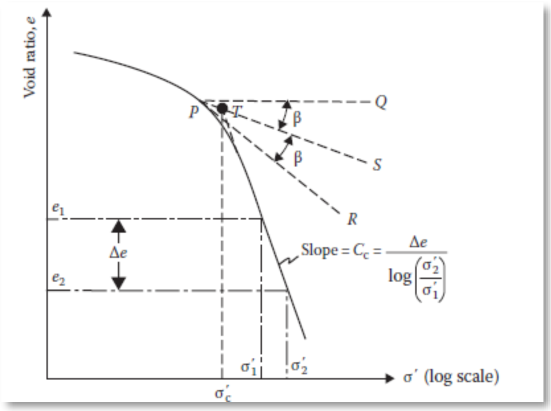

Figure 2.10. Preconsolidation Pressure

(Source: DAS, 2013)

The present effective overburden pressure is higher than the preconsolidation pressure which means that soil is normally consolidated. Normally consolidated soil volume is decreased by the increasing applied pressure. (Figure 2.11)

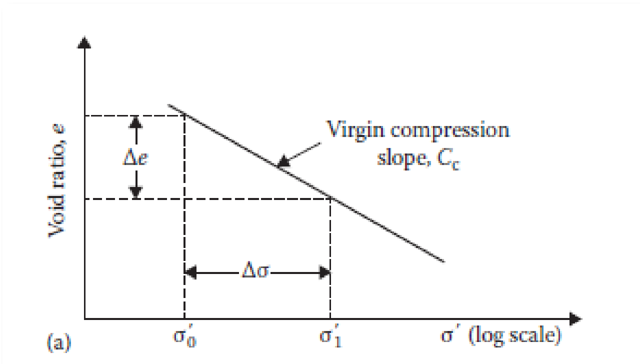

Figure 2.11. Void Ratio - Effective Stress Increment for NC Soil

(Source DAS, 2013)

If the present effective overburden pressure is lower than the preconsolidation pressure, the soil is overconsolidated and overconsolidation ratio is the ratio between the present effective overburden pressure and the preconsolidation pressure Eq. (2.15).

$$OCR = \frac{\sigma_c'}{\sigma_0'} \tag{2.15}$$

In overconsolidated soils volume change is calculated as cumulative of void ratio differences both recompression and virgin parts. (Figure 2.12)

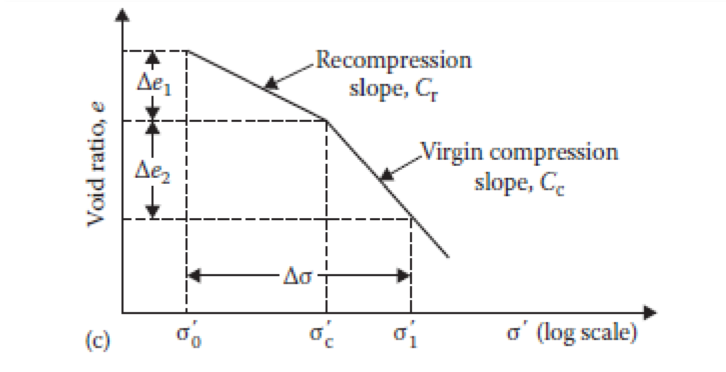

Figure 2.12. Effective Stress Increment in Recompression and Virgin Compression (Source: DAS,2013)

Compressibility Index (C_c, C_r)

In figure 2.11 slope of recompression slope and virgin compression slope gives compressibility index of soil. Compressibility index can be calculated also with some empirical correlations which are given in Table 2.1.

$$C_c = \frac{\Delta e}{\log\sigma_1' - \log\sigma_0'} \tag{2.16}$$

$$C_r = \frac{\Delta e}{\log\sigma_c' - \log\sigma_1'} \tag{2.17}$$

Table 2.1. Correlations for Compression Index

(Source: DAS,2013)

Reference	*Relation*	*Comments*
Terzaghi and Peck (1967)	$C_c = 0.009(LL - 10)$	Undisturbed clay
	$C_c = 0.007(LL - 10)$	Remolded clay
	LL = liquid limit (%)	
Azzouz et al. (1976)	$C_c = 0.01w_N$	Chicago clay
	w_N = natural moisture content (%)	
	$C_c = 0.0046(LL - 9)$	Brazilian clay
	LL = liquid limit (%)	
	$C_c = 1.21 + 1.005(e_0 - 1.87)$	Motley clays from Sao Paulo city
	e_0 = in situ void ratio	
	$C_c = 0.208e_0 + 0.0083$	Chicago city
	e_0 = in situ void ratio	
	$C_c = 0.0115w_N$	Organic soil, peat
	w_N = natural moisture content (%)	

Empirically recompression index (C_r) is equal to 0.1 C_c – 0.2 C_c.

2.3.2.4 Calculation of Consolidation Settlement

Basically, the settlement is calculated by multiplying strain with height of the soil. Strain depends on overconsolidation ratio of soil, stress increment, and compressibility index of soil. With using these factors three formulation can be used for primary consolidation settlement analysis.

1. Normally consolidated soil (OCR <= 1) and stress increment in the range of virgin compression zone (Look Figure 2.11)

$$S_c = \frac{C_c}{1+e_0} \log \frac{\sigma_1'}{\sigma_0'} H \qquad (2.18)$$

2. Overconsolidated soil and stress increment in the range of recompression zone (Look Figure 2.12)

$$S_c = \frac{C_r}{1+e_0} \log \frac{\sigma_1'}{\sigma_0'} H \qquad (2.19)$$

3. Overconsolidated soil and stress increment in the range of compression zone (Look Figure 2.12)

$$S_c = \frac{H}{1+e_0} \left(C_c \log \frac{\sigma_1^{'}}{\sigma_c^{'}} + C_r \log \frac{\sigma_c^{'}}{\sigma_0^{'}}\right) \tag{2.20}$$

These three formulas vary with stress level. Another formula can be used for constant stress level as using an average coefficient volume compressibility (m_v). These formula reduce the effects of nonlinearity. (Das, 2014).

$$S_c = m_v \; H \; \Delta\sigma \tag{2.21}$$

Poulos (1968) asserts that to obtain more accurate settlement analysis the three dimensional stress – strain modulus should be used and it can be derived with the given formula.

$$\frac{1}{m_v} = E = \frac{(1+v)\,(1\text{-}2v)\,E_{oed}}{(1\text{-}v)} \tag{2.22}$$

Where:

m_v = Coefficient volume compressibility, E = Stress strain modulus, E_{oed} = Oedometric stress strain modulus, υ = Poisson’s Ratio

2.4 Determination of Soil Stiffness Parameters

The stress-strain modulus (E_s) and Poisson's ratio (ν) are elastic properties of soil, which are widely used in the analysis of foundation settlements. (Bowles, 1997). In-situ tests and laboratory experiments were performed for determination of soil stiffness parameters for drained and undrained conditions. In this part of the thesis the Consolidation Test, Plate Load Test, Standard Penetration Test, Cone Penetration Test and the Pressuremeter Test are introduced for determination of stress-strain modulus of soils. Separately, determination of Poisson’s ratio is given in 2.4.6.

2.4.1 Stress – Strain Modulus from Consolidation Test

Details of the consolidation test are given in the part of chapter 2.3.2.3. Oedometric stress – strain modulus of soil is obtained from consolidation test and it used for both initial and primary settlement calculations. Drained stress – strain one dimensional modulus can be obtained with the inverse of the coefficient of volume compressibility Eq. (2.23) from consolidation test or directly taken from the correlation of in-situ tests.

$$\frac{1}{m_v} = D' \tag{2.23}$$

Where;

D': Oedometric Stress – Strain Modulus

2.4.2 Stress – Strain Modulus from Static Plate Load Test

In plate load tests, likely the consolidation test, load increment is applied step by step in the field. ASTM D1195 and TS 5744 are some related standards for static plate load tests. Load source is (truck or heavy construction equipment) applied incrementally on a rigid plate and periodically vertical settlement of soil or fill materials is measured with the aid of transducer. These data give the stress – strain modulus of soil or fill materials. Consists of applying a supposedly even pressure to the surface of the ground by means of a rigid plate. (Monnet, 2015) The size of the rigid plate affect settlement depth. (Two times diameter of plate equal to the depth of settlement). The depth of the test is the base level in buildings, unless stated otherwise; the upper level of the base for transportation structures.

Applied stress is not to exceed 1/10 project stress. Stress should be applied at least 30 s. The pressure should be changeless until the deformation is constant (<0.02 mm in 15 s). Then the settlement is measured as Δs. Then, stress is increased with the same value as before and the same procedure is applied. When loading value is reached project stress, which is increased by a safety factor, the unloading process can be applied to obtain unloading stress – strain deformation modulus. The related formula is given below for both cases. (TS 5744, 1988)

$$E_v = \frac{0.75\ D\ \Delta\sigma}{\Delta s} \tag{2.24}$$

Where;

E_v = Stress – Strain Modulus, D = Plate diameter (300 mm, 600 mm and 762 mm), $\Delta\sigma$ = Stress increment (kPa, kg/cm^2 ....), Δs = Settlement value (mm, cm ...)

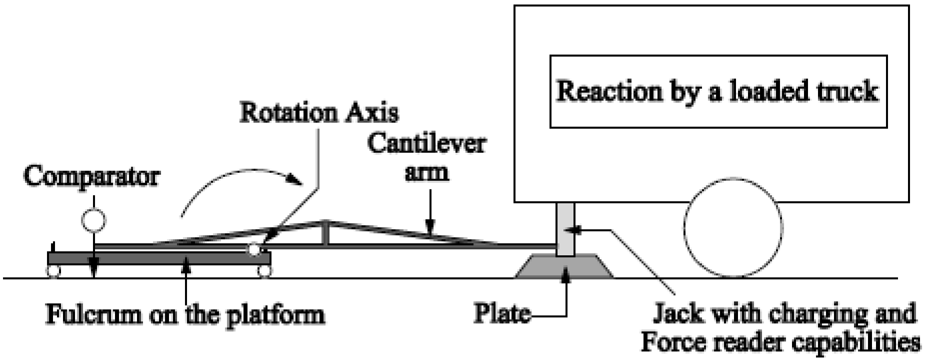

Figure 2.13. Installation of Plate Load Test

(Source: Monnet, 2015)

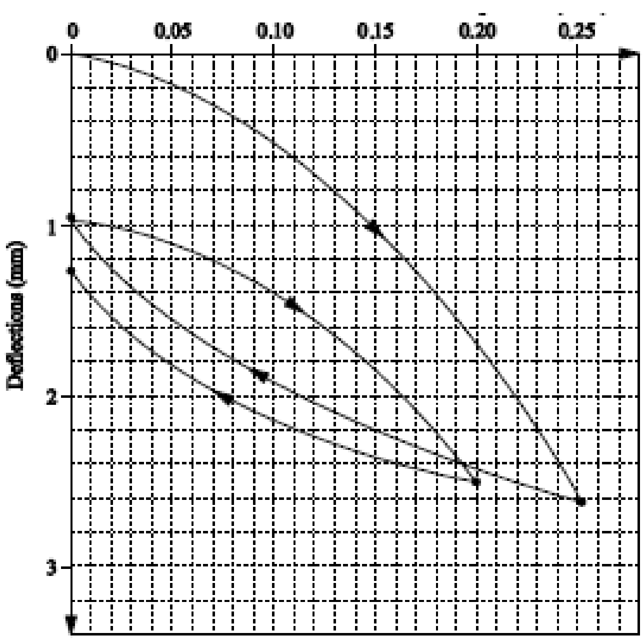

Figure 2.14. Plate Load Test Result Example

(Source: Monnet, 2015)

2.4.3 Stress – Strain Modulus from Standard Penetration Test

There are various site investigation methods in the geotechnics. The standard penetration test (SPT) still is the most popular site investigation testing all around the world due to simple performing, penetration into dense layers, gravel, and fill, common equipment and operators. (Schnaid, 2009). Penetration tests do not give soil stiffness directly because stress – strain values are not measured during tests so that empirical correlations are needed. Especially, for coarse – grained soils, stress strain modulus is obtained from in-situ tests due to difficulties of taking undisturbed sample for laboratory works.

In standard penetration test, a sample tube is driven into the soil layers by a hammer, its weight 63.5 kg, falling through 760 mm distance. The sampler's average outside diameter is 51 mm, inside diameter is 35 mm and length is greater than 457mm. (Figure 2.15). ASTM D 1586-99:1999, British BS 1377-9:1990 and TS 5744 are some related standards for SPT.

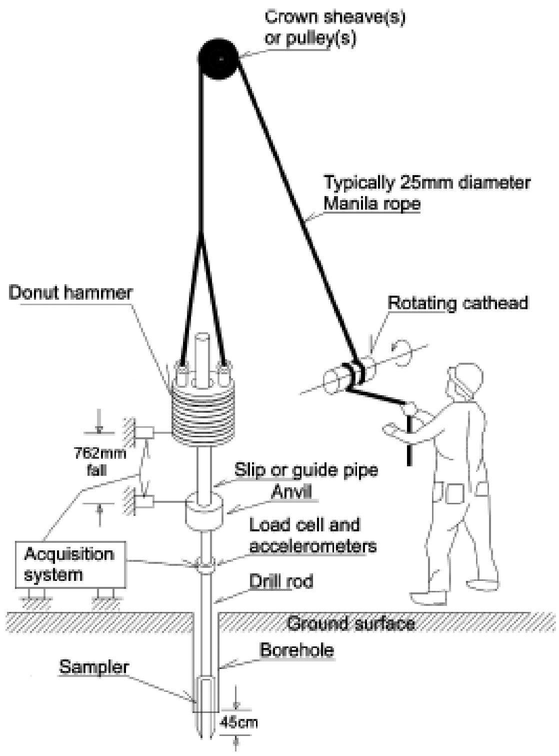

Figure 2.15. Equipment of Standard Penetration Test
(Source: Schnaid, 2009)

In geotechnical engineering most of the SPT correlations are related with SPT blow counts (N), which is total for the last 300 mm numbers of falling. SPT is applied commonly 1.5m depth interval. Theoretical penetration energy is higher than the measured energy due to implementation a factors so that some corrections are needed as factor of overburden pressure (for cohesive soil), a factor of energy ratio, a factor of borehole diameter, a factor of rode length and factor of sampling method, which are given in Figure 2.16.

$$N_{60} = \frac{C_H . C_B . C_C . C_R . N}{0.6} \tag{2.25}$$

$$(N_1)_{60} = N_{60} . C_N \tag{2.26}$$

Where;

N_{60} = Corrected SPTN-Value for field procedures

$(N_1)_{60}$ = Overburden Pressure Correction (for cohesionless soil)

Factor	Variable equipment	Term	Correction
Overburden pressure		C_N	$(P_a/s'_{vo})^{0.5}$ but $C_N \leq 2$
Energy ratio	Donut hammer	C_E	0.5-1.0
	Safety hammer		0.7-1.2
	Automatic hammer		0.8-1.5
Borehole diameter	65-115 mm	C_B	1.0
	150 mm		1.05
	200 mm		1.15
Rode length	3-4 m	C_R	0.75
	4-6 m		0.85
	6-10 m		0.95
	10-30 m		1.0
	> 30 m		< 1.0
Sampling method	Standard sampler		1.0
	Sampler without liners	C_S	1.1-1.3

Figure 2.16. Correction Factors for SPT blow counts, N
(Source: Monnet, 2015)

Determination of Stress – Strain Modulus from SPT for Cohesionless Soil

Standard penetration tests do not give soil stiffness directly because stress and strain is not measured during test application so that empirical correlations are needed. In

Table 2.2 related correlations in the geotechnical literature were given for cohesionless soils but when these formulations are used soil consistency should take be into consideration.

Table 2.2. Correlations between SPT(N_{60}) and Stress - Strain Modulus

Year and Researcher	Modulus (kPa)	Description
Webb (1969)	$E_s = 484(\mathrm{N} + 15)$	Sand (Below Water Table)
Schmertmann (1970)	$E_s = 766\ \mathrm{N}$	Sand (Saturated)
Bowles (1996)	$E_s = 500\ (\mathrm{N} + 15)$	Sand Normally Consolidated
Bowles (1996)	$E_s = 300\ (\mathrm{N} + 6)$	Sandy Silt or Clayey Silt
FHWA (2002)	$E_s = 400\ \mathrm{N}$	Sandy Silt
Kulhawy and Mayne (1990)	$\frac{E_s}{P_a} = \alpha N$	α = 5 for sand with fines; 10 for clean sand (NC)

*Bowles used N_{55} *Schmertmann, Webb, Kulhawy and Mayne used N
FHWA used N_{60}

2.4.4 Stress – Strain Modulus from Cone Penetration Test

The other popular in-situ test method is the cone penetration test (CPT). ASTM D3441 - 98 BS 1377-7:1990 and TS 5744 are some related standards for a cone penetration test. The cone penetration test was first used in 1934 to determine the location of the sand layers in soft alluvial clay deposits and the extent of these layers for pile design in the Dutch. (Erol and Cekinmez, 2014). In the CPT, a cone pushed into the soil layers with the aid of series of rods and during penetration continuous measurement are taken by the resistance of cone tip and surface sleeve. The CPT has enhanced versions such as the piezocone (CPTu), which is shown in Figure 2.17, and seismic cone penetration test (SCPT). CPTu is used for measurement of excess pore water pressure and SCPT is used to find dynamic soil parameters such as shear wave velocity (V_s). The main terminology of CPTu is given in Figure 2.19. Total forces are separated as two parts as cone tip force (Qc) and friction sleeve force (Fs). These forces can represent q_c and f_s with using cone area and surface area. (Robertson and Cabal, 2012).

Like all site investigation tests, CPT has some advantages and disadvantages. The main advantages of the CPT tests are (a) getting rapid and continuous soil profiling, (b) repeatability and reliability of the data, and (c) economic. The disadvantage of CPT are (a) Requiring skilled operators, (b) not able to take a soil sample and (c) restriction in gravel/cemented layers.

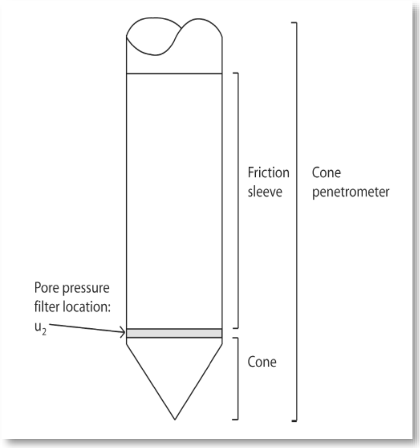

Figure 2.17. CPTu Probe
(Source: Robertson, 2012)

Figure 2.18 gives numerous semi-empirical correlation's reliability and applicability as like that 1 is equal to High, 2 is equal to High to Moderate, 3 is equal to Moderate, 4 is equal to Moderate to Low, 5 is equal to Low Reliability.

Soil Type	D_r	Ψ	K_o	OCR	S_t	s_u	ϕ'	E, G*	M	G_0*	k	c_h
Coarse-gained (sand)	2-3	2-3	5	5			2-3	2-3	2-3	2-3	3-4	3-4
Fine-grained (clay)			2	1	2	1-2	4	2-4	2-3	2-4	2-3	2-3

Where:

D_r	Relative density	ϕ'	Peak friction angle
Ψ	State Parameter	K_0	In-situ stress ratio
E, G	Young's and Shear moduli	G_0	Small strain shear moduli
OCR	Over consolidation ratio	M	1-D Compressibility
s_u	Undrained shear strength	S_t	Sensitivity
c_h	Coefficient of consolidation	k	Permeability

Figure 2.18. Reliability of Soil Parameters Obtained from CPT
(Source: Robertson, 2012)

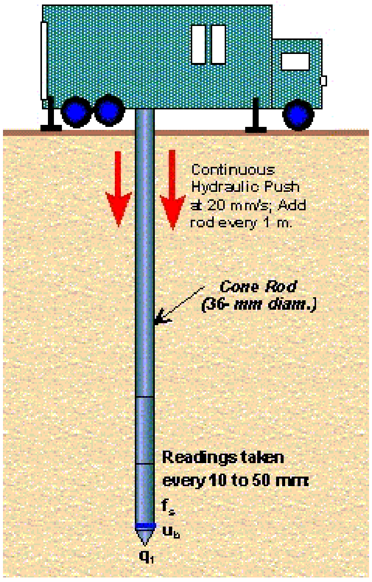

Figure 2.19. Test Procedure of CPT

Cone penetration tests do not give soil stiffness directly because stress and strain are not measured during test application so that empirical correlations are needed. In Table 2.3 related correlations in the geotechnical literature were given but when these formulations are used, soil consistency should take be into consideration.

Soil profiling and soil type can be obtained from CPT applications by using cone resistance and friction ratio (f_s/q_t) (Figure 2.20). Typically, the cone resistance for sands is high and for clays is low, (q_t) is high in sands) and low in clays, and the friction ratio (R_f). Moreover, the equivalent SPT N_{60} values were estimated using Table 2.4, which was suggested by Robertson (1986).

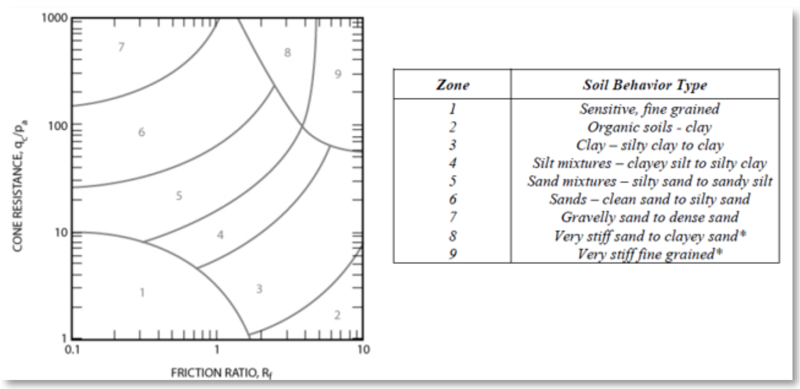

Figure 2.20. Soil Behaviour Type Chart

Table 2.3. Correlations between CPT (q_c) and Stress - Strain Modulus

Researcher	**Stress-Strain Modulus (kPa)**	**Cone Resistance Interval (kPa)**	**Description of Soil Type**
Bowles (1996)	$E_s = (1 \text{ to } 2)\ q_c$		Sandy Silt or Clayey Silt
Bowles (1996)	$E_s = (2 \text{ to } 4)\ q_c$		Normally Consolidated Sand
Schmertmann (1978)	$E_s = 2\ q_c$ $E_s = 3.5\ q_c$		Axisymmetric cases Plain strain cases
Sanglerat (1972)	$E_{oed} = 1.0\ to\ 3.0\ q_c$ $E_{oed} 3.0\ to\ 6.0\ q_c$	$q_c < 2\ MP_a$ $q_c > 2\ MP_a$	Low Plasticity Silt
Bogdanovi (1973)	$E_s = 1.5\ q_c$ $E_s = 1.5\ to\ 1.8\ q_c$ $E_s = 1.8\ to\ 2.5\ q_c$ $E_s = 2.5\ to\ 3.0\ q_c$	$q_c > 4MPa$ $2\ MP_a < q_c < 4\ MP_a$ $1\ MP_a < q_c < 2\ MP_a$ $q_c < 1\ MP_a$	Sand and Sandy Gravel Silty Saturated Sand Clayey Silt with Silty Sand Silty Saturated Sand
Sanglerat (1972)	$E_{oed} = 3.0\ to\ 8.0 q_c$ $E_{oed} = 2\ to\ 5\ q_c$ $E_{oed} = 1.0\ to\ 2.5\ q_c$ $E_{oed} = 2.0\ to\ 6.0\ q_c$	$q_c < 0.7\ MN/m^2$ $0.7MP_a < q_c < 2MP_a$ $q_c > 2MP_a$ $q_c < 2MP_a$	Low Plasticity Clay Low Plasticity Clay Low Plasticity Clay High Plasticity Clay
Erol (2004)	$E_{oed} = 4.0\ to\ 12\ q_c$ $E_{oed} = 2.7\ to\ 4.7\ q_c$	$0.20MP_a < q_c$ $< 0.75MP_a$ $0.75MP_a < q_c$ $< 2.40MP_a$	High Plasticity Clay Low Plasticity Clay

Table 2.4. Formulation for The Equivalent SPT N_{60} values (Robertson,1986)

Zone	*Soil Behavior Type (SBT)*	$\frac{(q_c/p_a)}{N_{60}}$
1	*Sensitive fine grained*	2.0
2	*Organic soils – clay*	1.0
3	*Clays: clay to silty clay*	1.5
4	*Silt mixtures: clayey silt & silty clay*	2.0
5	*Sand mixtures: silty sand to sandy silt*	3.0
6	*Sands: clean sands to silty sands*	5.0
7	*Dense sand to gravelly sand*	6.0
8	*Very stiff sand to clayey sand**	5.0
9	*Very stiff fine-grained**	1.0

2.4.5 Stress – Strain Modulus from Pressuremeter Test

The pressuremeter test (PMT) was developed in 1956 by Louis Menard in France. ASTM D4719 – 07 and BSI BS 5930 are some related standards for pressuremeter test. PMT results are empirically related to geotechnical characteristic of soil and weak rock parameters, which are used directly in foundation analysis.

The principal of the PMT is giving pressure in lateral direction and measurement volume change of cylindrical membrane, which is installed in the ground before giving pressure. With using pressure and volume change relation soil and weak rock parameters can be obtained as shear modulus, undrained strength for clays or weak rocks, angle of shearing resistance for sands, angle of dilation for sands. (Mair and Wood,1987). Table 2.5 shows reliability and applicability of that soil geotechnical parameters' reliability and applicability, which are obtained from PMT test results and Figure 2.21 gives schematic of PMT.

In the test procedure, fixed pressure increments are applied as commonly 15 kN/m^2 - 50 kN/m^2 for soft to stiff clays, 50 kN/m^2 - 100 kN/m^2 for weak rock and very stiff clays. Each pressure increment is applied for 15 secs, 30 secs, 60 secs and 120 secs and volume change is recorded. Three distinct zones are commonly obtained from tests in the soil, as given in Figure 2.22. The initial curved portion (expansion of membrane) is attributed to expansion of the membrane until it touch fully borehole's sides, the second curved portion (pseudo-elastic behaviour) has deformation of any softened zone and it is approximately linear until the starting point of the third curved portion which is in a plastic condition (plastic behavior)

The shear modulus, G, can be obtained from the slope of the pseudo- elastic behavior part and the related formula is given below;

$$G = \frac{V_0 \, dp}{dV} \tag{2.27}$$

Where;

G = Shear (Menard) Modulus, V_0 = Initial Volume, dp = pressure change, dV = volumetric change

Pressuremeter modulus can be obtained with Eq. (2.28) and typical pressuremeter test curve given in Figure 2.23.

$$E_p = 2(1+\nu)(V_0 + V_m)(\Delta P / \Delta V) \tag{2.28}$$

Where:

E_p = Pressuremeter (Menard) Modulus, υ = Poisson's Ratio, $V_0 + V_m$ = Volume of probe, ΔV = Volume increase in straight- line portion of test curve, ΔP = Pressure increase corresponding to ΔV volume increase.

It was observed that the settlements found by Menard based on the pressuremeter modulus were more than the measured real settlements so that a corrected factor (α) is suggested in Table 2.6. This factor (α) is useful to find stress – strain modulus (E) from Menard modulus (E_m).

$$E = E_m / \alpha \tag{2.29}$$

Table 2.5. Geotechnical Parameters from PMT
(Source: Mair and Wood,1987)

Parameter	Clays			Sands			Weak rocks		
	MPM	SBP	PIP (3,4)	MPM	SBP	PIP (3,4)	MPM	SBP (5)	PIP
In-situ horizontal stress, σ_{ho}	••(1)	•••	N/A	N/A	•	N/A	•	N/A	N/A
Elastic shear modulus, G	••	•••	••	•	•••	••	•••	N/A	N/A
Undrained shear strength, c_u	••(2)	••	••	N/A	N/A	N/A	••	N/A	N/A
Pore pressure, u_o	(3)	•	(3)	(3)	••	(3)	(3)	N/A	N/A
Angle of shearing resistance, ϕ'	(3)	(3)	(3)	•	••	•	N/A	N/A	N/A
Angle of dilation, ψ	N/A	N/A	N/A	•	••	•	N/A	N/A	N/A
Horizontal coefficient of consolidation, c_h	(3)	••	(3)	N/A	N/A	N/A	N/A	N/A	N/A

(1) MPM only suitable for stiff clays with linear elastic response and certain rocks. (2) Only suitable for certain stiff clays and rocks
(3) Little or no experience. (4) Greatest advantage of PIP is offshore when MPM and SNP are neither nor feasible or economic
(5) There is very little experience with SBP in weak rocks, Highest potential indicated by *** and N/A = Not applicable

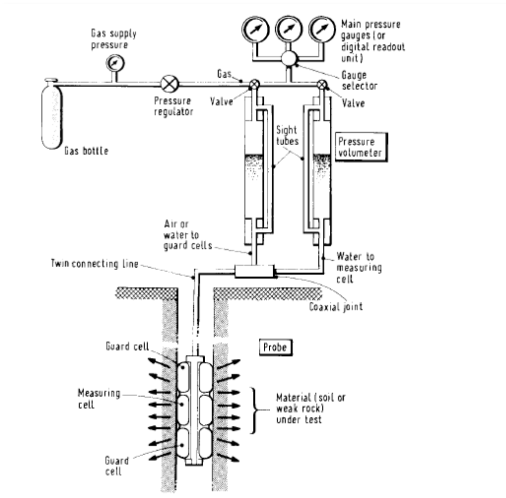

Figure 2.21. Schematic of PMT
(Source: Mair and Wood,1987)

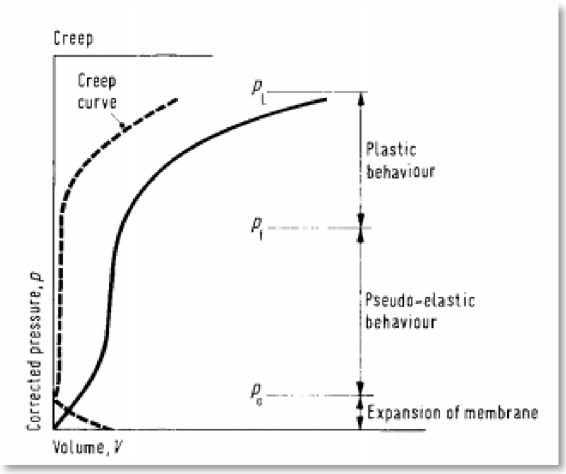

Figure 2.22. Pressuremeter Zones

(Source: Mair and Wood)

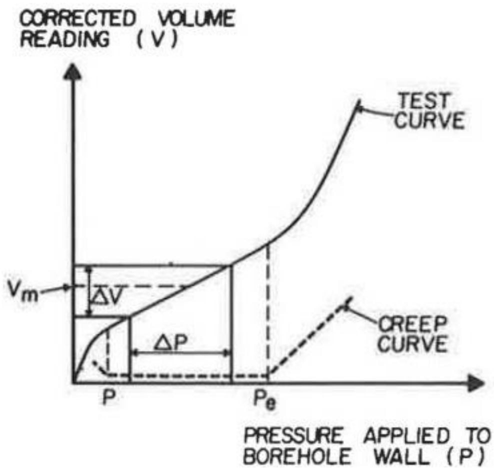

Figure 2.23. Typical Pressuremeter Test Curve

Table 2.6. Menard Factors

Soil Type	Peat		Clay		Silt		Sand		Sand and Gravel	
	E_o/p_L^*	α	E_o/p_L^*	α	E_o/p_L^*	α	E_o/p_L^*	α	E_o/p_L^*	α
Over-consolidated			> 16	1	> 14	2/3	> 12	1/2	> 10	1/3
Normally consolidated		1	9–16	2/3	8–14	1/2	7–12	1/3	6–10	1/4
Weathered and/or remoulded			7–9	1/2		1/2		1/3		1/4

Rock	Extremely fractured	Other	Slightly fractured or extremely weathered
	α = 1/3	α = 1/2	α = 2/3

2.4.6 Poisson's Ratio

It is difficult to determine the Poisson ratio in the laboratory. Poisson's ratio is defined as the ratio of axial strain (ε_V) to lateral strain (ε_L) and it is used commonly for settlement analysis of foundation. Poisson's ratio can be obtained from triaxial test or related charts. Mayne and Poulos (1999) assert that drained Poisson's ratio (υ') for elastic approach between 0.1 to 0.2 for all soil types and undrain Poisson's ratio (υ_u) for fine soils is equal to 0.5. Table 2.7 shows Poisson's ratio values for different soil types.

$$v = \in_L / \in_V \tag{2.30}$$

Table 2.7. Poisson's Ratio for Soil Type
(Sources: Bowles,1996)

Clay, saturated	0.4–0.5
Clay, unsaturated	0.1–0.3
Sandy clay	0.2–0.3
Silt	0.3–0.35
Sand, gravelly sand	−0.1–1.00
commonly used	0.3–0.4
Rock	0.1–0.4 (depends somewhat on type of rock)
Loess	0.1–0.3
Ice	0.36
Concrete	0.15
Steel	0.33

2.5 Stress Increment Methods

Settlement calculations are basically related to the stress-strain relationship of soils. Stress increment in a soil layer is happened due to adding load of external factors such as buildings, bridges, and embankments. These stress increments decrease throughout soil depth and settlement calculations start the point where stress is applied and finish the point where stress is ended. In this part three methods (Boussinesq's Method, Westergaard's Method and 2:1 Method), which are commonly used for calculation of stress increment in any depth of soil stratum, is presented.

2.5.1 The Boussinesq's Method

The Boussinesq's Method assumes the soil throughout the depth is semi-infinite, homogenous, isotropic and weightless. In 1885 Boussinesq solved the decreasing of a point load, which is applied on the surface, throughout the depth of soil, which is the semi-infinite, homogenous, isotropic and weightless, with depth position. His equation based on the Theory of Elasticity. Not only a point load on the surface, uniform loads on the rectangular and circular areas can be solved with the derivation of Boussinesq's Method (Bowles,1996).

Vertical Stress Due to Surface Loading

Figure 2.24 shows a rectangular area of length L and width B subjected to a uniform vertical load of q per unit area. The vertical stress increase at point P, which is located at a depth z below the rectangular area, can be obtained by using Eq. (2.31),

$$\sigma_z = q \cdot I \tag{2.31}$$

Where;

$$I = \frac{1}{4\pi}\left[\frac{2mn(m^2+n^2+1)^{1/2}}{m^2+n^2+m^2n^2+1}\,\frac{m^2+n^2+2}{m^2+n^2+1} + \tan^{-1}\frac{2mn(m^2+n^2+1)^{1/2}}{m^2+n^2-m^2n^2+1}\right]$$

$$m = \frac{B}{z} \qquad n = \frac{L}{z}$$

2.5.2 Westergaard's Method

In 1938 Westergaard solved the decreasing of a point load, which is applied on the surface, throughout the depth of soil. In Westergaard solution soil is not assumed homogenous therefore thin rigid reinforcements are placed in an elastic solid medium. This assumption represents stratified soils, where soft layers are strengthened by stiff or dense soil layers. Therefore, this method can be used for pavement or layered with clay and sand stratum of soil.

Vertical Stress Due to Surface Loading

A rectangular area of length L and width B subjected to a uniform vertical load of q per unit area. The vertical stress increase at a depth z below the rectangular area, can be obtained by using equation (2.32),

$$\sigma_z = \frac{q}{2\pi}\left\{\cot^{-1}\left[\eta^2\left(\frac{1}{m^2}+\frac{1}{n^2}\right)+\eta^4\left(\frac{1}{m^2n^2}\right)\right]^{0.5}\right\} \tag{2.32}$$

Where;

$$\eta = \sqrt{\frac{1-2v}{2-2v}} \qquad m = \frac{B}{z} \qquad n = \frac{L}{z}$$

2.5.3 2:1 Method

2:1 method is an approximated method to determine the increase in stress with depth caused by the construction of a foundation. The increase in stress at depth z is given by using Eq. (2.33) and the representative figure is given below.

$$\Delta\sigma = \frac{q_0.B.L}{(B+z).(L+z)} \tag{2.33}$$

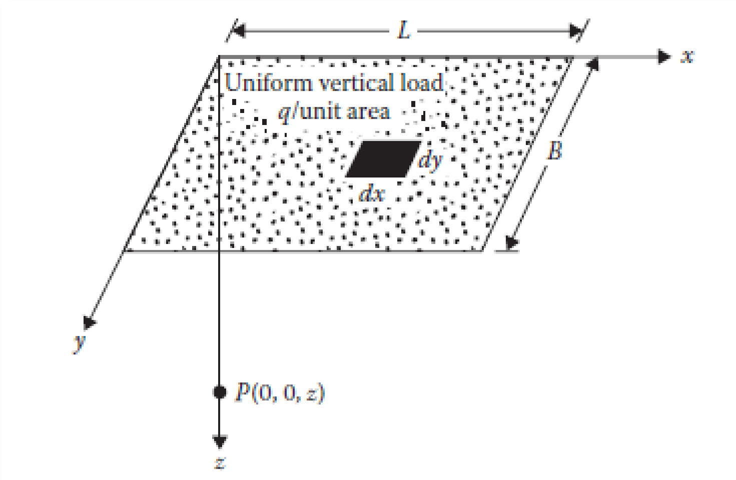

Figure 2.24. Area Load on the Surface
(Source: DAS, 2013)

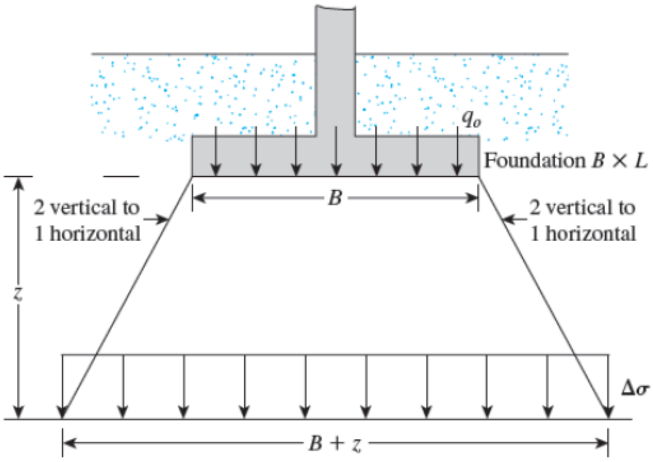

Figure 2.25. Stress Increment in 2:1 Method

CHAPTER 3

GEOTHERMAL POWER PLANT PROJECT

3.1 Introduction

Geothermal power plants product energy with using hydrothermal resources which include high water vapor pressure in the temperature range between 120° C and 320° C. The geothermal energy resources are renewable and are seen in 10% of earth shows that it has vital importance.

The geothermal power plant project is placed in Aydin, Turkey. The power plant project has 6 production wells and 6 re-injection wells. The energy production capacity of the project is 25MW and total investment cost is amount 84 million USD.

In this chapter, first, the area of the investigation is introduced with the geology of the project. Than performed site investigations and laboratory experiments are presented in detail.

3.2 Investigation of Project Area

Investigation area is 11 km away from Aydın province. Investigation area is at the south of İzmir – Aydın Highway, at the northwest of Acarlar Neighborhood and Osmanbükü Neighborhood. Location of the project is shown in Figure 3.1 and Figure 3.2.

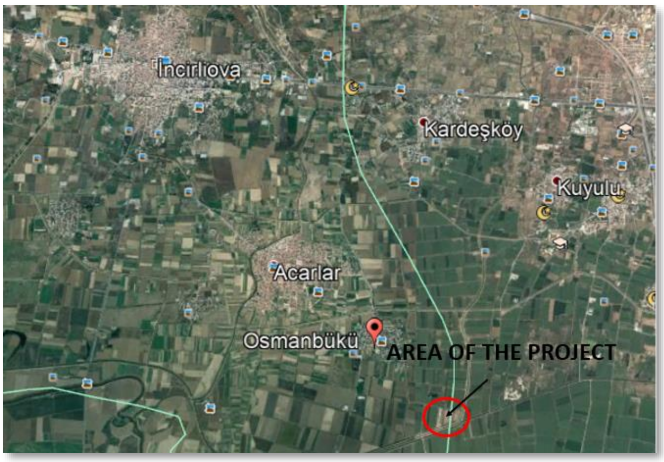

Figure 3.1. Location of The Project (Source: Google Earth Pro)

Figure 3.2. Location of The Project (Source: Google Earth Pro)

3.2.1 Environmental Information

In the study area, the characteristics of the temperate is Mediterranean climate, which has warm and rainy winters as well as hot and dry summers. The rains in this region are mostly downpours and short - heavy rainfalls. According to meteorological measurements, the average annual temperature is about 17.1 ˚C

3.2.2 Project Information

Production energy in the geothermal power plant comes true in five steps which are given in Figure 3.3. For settlement analysis the main part of the project is Air Cooler Condenser and Turbine Generator part due to having static and dynamic heavy loaded structural and mechanical elements.

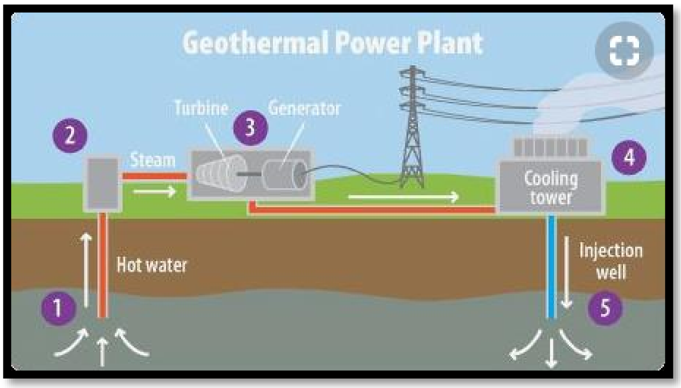

Figure 3.3. Organization Chart of the Geothermal Power Plant

The Air Cooler Condenser and Turbine Generator's area is around 7700 m^2. Vapor pressure, which has high temperatures, is transported with the help of pipelines. Shallow foundation (mostly raft foundation) is preferred to avoid differential settlement of pipelines. The project's raft foundation height is 90 cm beneath of Turbine – Generator Part. The maximum loaded element is 1615 kN as dead load. Detailed project loads are given in Chapter 4.

Figure 3.4. Air Cooler Condenser and Turbine-Generator

3.3 Geology of The Project Area

3.3.1 General Geology

A parcel of Menderes, which has complex mass nappe that is formed by compressive tectonic of Geç Alpin, is exposed in the west of Anatolia. This complex crystal is separated into two main parts, namely, Pan – African and Paleozoic Early. Paragneisses and mica schists are seen in the main parts of Parcel and Menderes. In Cenozoic of Erathemn mid Miocene is formed by marly sandstone, top Miocene and Miocene is formed by sandstone and claystone, in quaternary of erathemn Pleistocene are formed by gravel and sandstone and Holocene is formed by alluvial deposit (Sınıflama and Kuralları,1986). Stratigraphic section of the project area was given in Figure 3.5.

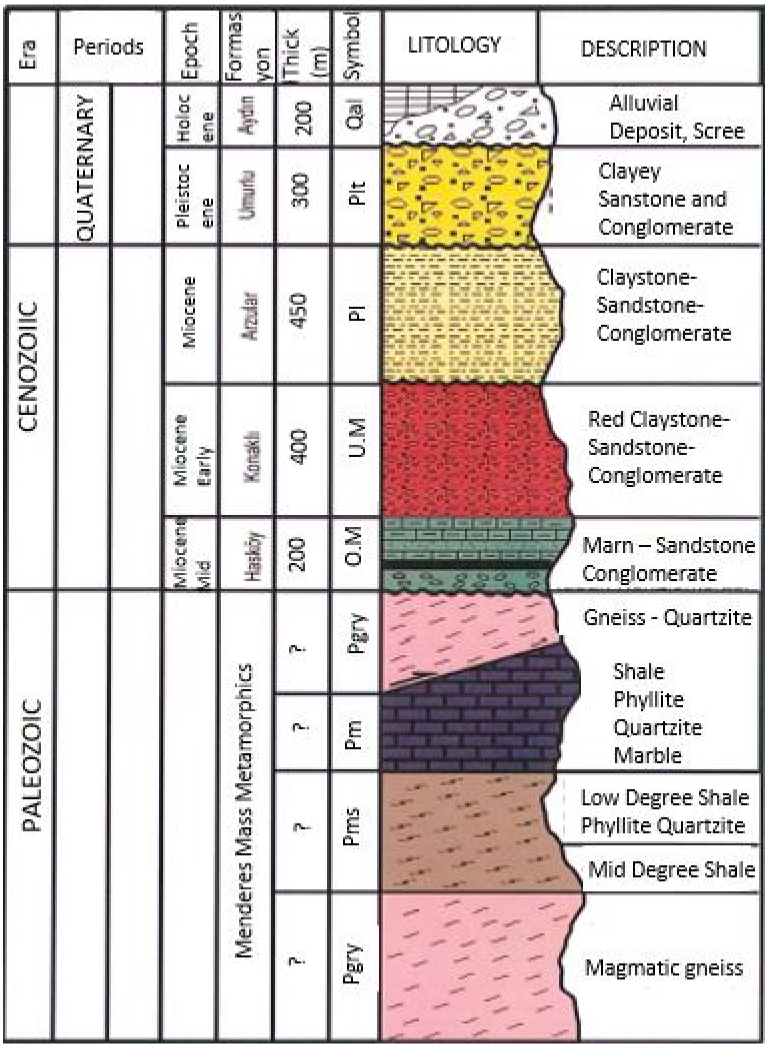

Figure 3.5. Stratigraphic Section of Project Area

3.3.2 Engineering Geology

The surveying area drilling logs works shows that the whole project area has old quaternary alluvium. The old quaternary is formed by the accumulation of alluvial deposit (sand, silt and clay) which is transported by Buyuk Menderes and its streamlets.

In surveying area drilling works shows that yellowish brown, brownish grey and greenish grey mid – high plastic silty clay (CL), greyish brown mid dense silty sand (SM) and brownish grey, greenish grey, nonplastic clayey sandy silt (ML) are seen. SPTN values are commonly 3 – 13 for first 7 m – 10 m depth and 13 – 44 for remained depth.

The altitude above sea level of the project area is 23 m – 24 m. The ground water level is seen at the depth of 1.8 m and 2.0 m from ground level. Depending on the geological conditions, the site has not been observed to have a large topographic anomaly or mass movement (landslide, soil flow, rockfall, etc.) is not observed in the site.

3.4 Site Investigation Tests and Laboratory Experiments

The site investigation tests include Standard Penetration Test, Cone Penetration Test, Pressuremeter Test and Plate Load Test. The disturbed and undisturbed samples were collected to perform consolidation tests and physical tests at the laboratory. The physical properties of the soils were obtained by performing tests on disturbed samples. The consolidation tests were performed on undisturbed samples. In this part of Chapter 3, the details of in-situ tests and laboratory tests and essential soil parameters, which were obtained from these tests and experiment for settlement analysis, are presented

3.4.1 Standard Penetration Test

In Chapter 2 the procedure and uses of the standard penetration tests were given with details. In this part of Chapter 3 implementation of the standard penetration tests and its results were given. According to the layout plan of boreholes which are given in Figure 3.6, 9 drilling works were done with SPT for each 1.5 m depth in the ACC and Turbine Generator Zone. Totally, 264.5m drilling works were done. The depth of the boreholes was between 26 m and 30.5 m, the number of the SPT was 168 and 7 undisturbed samples were collected. The tables in Appendix A2 show the corrected N values at 1.5m depth intervals.

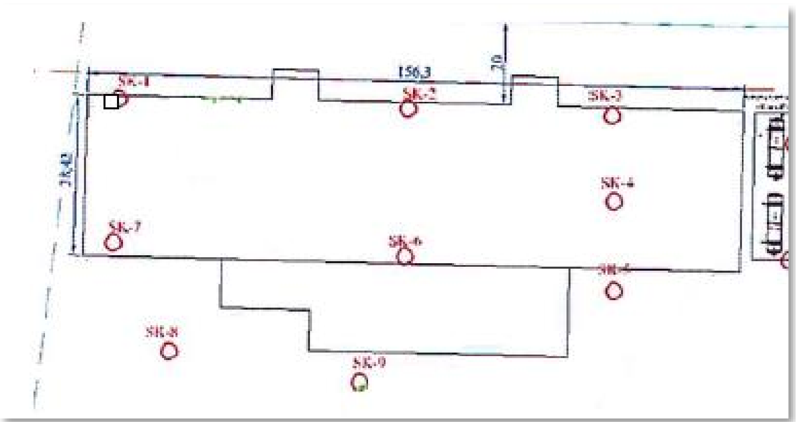

Figure 3.6. The Layout Plan of Boreholes

Figure 3.7. Standard Penetration Test in the Geothermal Project

These number of blows (N_{60}) were used to determine the consistency and relative density (D_r) of soils. Terzaghi and Peck suggests Table 3.1 and Table 3.2 for determination of soil consistency for clays and relative density for granular soils, respectively. Thus, the consistency of clay and relative density of granular soils were estimated using the SPT-N data. SPT logs were given in Appendix A1 - A2.

As a result of the drilling works, alluvial ground layers formed by alternation of silt, clay and sand units are located along the depths of the boreholes. It was generally observed in yellowish brown, brownish gray, and greenish gray. The clay unit, which had a wide spread in the field, was yellowish brown, grayish brown and brown. As a result of the USCS classification, it was determined that the clay units have low plasticity (CL), medium plasticity (CI) and high plasticity (CH). In general clays include silt layers and sand layers. The silt unit observed in the study area was gray and brown. According to the USCS classification, it was determined that silt units were medium, high plastic and non-plastic in ML and MI types. Gray silt units were clayey, sandy, and in some cases had fine sand layer, while brown silt units were observed as sandy, clayey. Sand units were observed in greenish gray, grayish and brownish gray colors. Sand units contain silt and clay and there were clay layers in the unit. In addition, yellowish and blackish traces were observed in brownish sand units. According to the USCS classification tests, SM, SP-SM type sand units were determined.

Table 3.1. The Relation Between N_{60} and Consistency
(Source: Terzaghi and Peck,1967)

	q_u (kPa)					
Consistency	Very Soft	Soft	Medium	Stiff	Very Stiff	Hard
N_{60}	<2	2–4	4–8	8–15	15–30	>30
q_u	<25	25–50	50–100	100–200	200–400	>400

Table 3.2. The Relation Between N_{60} and Relative Density
(Source: Terzaghi and Peck,1967)

No. of Blows, N_{60}	Relative Density
0–4	Very loose
4–10	Loose
10–30	Medium
30–50	Dense
Over 50	Very dense

3.4.2 Cone Penetration Test

In Chapter 2 the procedure and uses of the cone penetration tests (CPT) were given in details. In this part of the thesis implementation of the CPT tests and its results were given. CPT tests layout plan were given in Figure 3.8. Two CPT tests were performed at Air Cooler Area (ACC) and Turbine Generator Region. CPT1 at a depth of 36m test was conducted at Turbine Generator Region. Cone resistance and skin friction results, dynamic pore pressure, equivalent SPT N_{60} value and soil classification detailed results were given in Appendix B1 and Appendix B2.

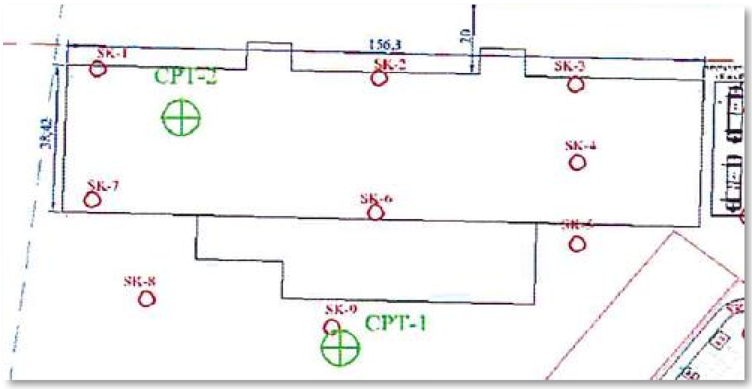

Figure 3.8. Cone Penetration Tests Layout Plan

Figure 3.9. Application of CPT in The Geothermal Project

3.4.3 Pressuremeter Test

In Chapter 2 the procedure and uses of the pressuremeter tests (PMT) was given with details. Normally, only 1 PMT test was conducted in the ACC – Turbine generator parts (labeled as SK 7). However, SK 14, SK 16 and SK 19-20 pressuremeters tests results were also given because same alluvial soil types were seen in all regions of the Geothermal Power Plant Project. Stress – strain modulus and limit pressure for each PMT were given in Appendix C.

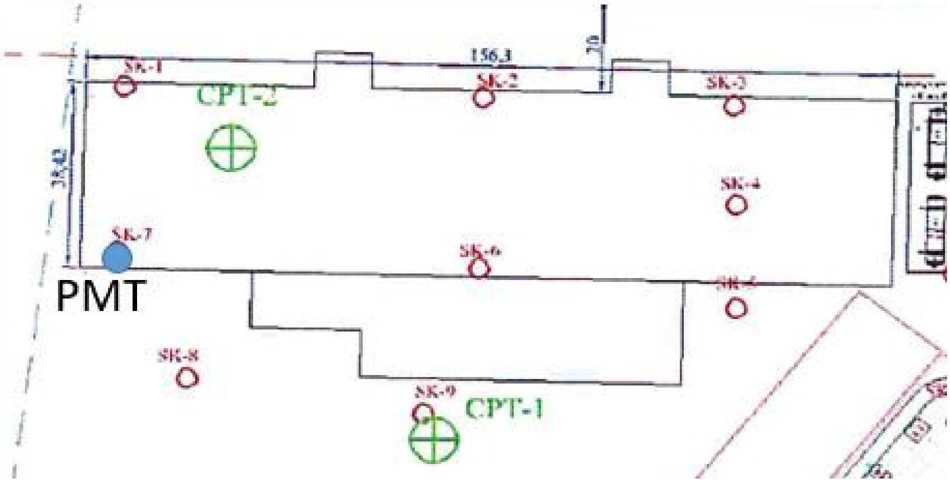

Figure 3.10. Pressuremeter Tests Layout Plan

Figure 3.11. Application of PMT in The Geothermal Project

3.4.4 Plate Load Test

In Chapter 2 the procedure and uses of plate load tests (PLT) were given in detail. In this part of the chapter implementation of the load test and its results (applied pressure and settlement values) are given. Only one plate load test was applied for high quality filled material which underlies the foundation of the power plants in ACC Turbine Generator area. Three 30 mm thick circular plates with a diameter of 450 mm, 600 mm and 762 mm were placed at the top of the fill material and a 30-ton weight excavator was used as a load source and plate load test were applied for fill material. The photo of the PLT was given in Figure 3.12.

The pressure was increased up to 2.1 t/m^2 which is three times higher than maximum service stresses and settlement readings were given in Table 3.3 and the graph of applied pressure – plate settlement was given in Figure 3.13.

Figure 3.12. Plate Load Test in The Geothermal Project

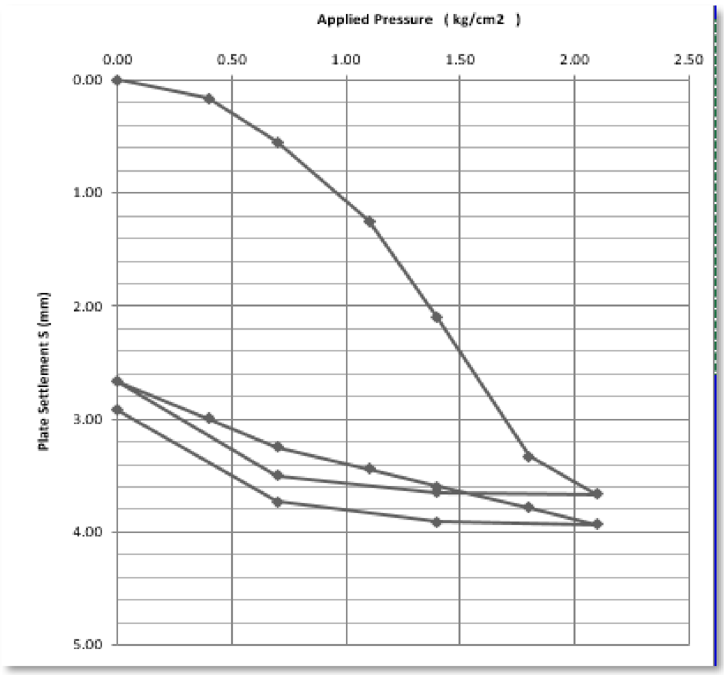

Figure 3.13. The Graph of Applied Pressure - Plate Settlement

Table 3.3. Plate Load Test Readings

Pressure (kg/cm^2)	Settlement (mm)	Pressure (kg/cm^2)	Settlement (mm)
0.00	0.00	0.70	3.25
0.40	0.16	1.10	3.44
0.70	0.55	1.40	3.60
1.10	1.25	1.80	3.78
1.40	2.10	2.10	3.93
1.80	3.33	1.40	3.91
2.10	3.67	0.70	3.73
1.40	3.65	0.00	2.92
0.70	3.50		
0.00	2.67		
0.40	3.00		

In Appendix D, PLT results were given in details. Stress – strain modulus for high qualified fill material under raft foundation was calculated as 57000 kPa.

3.4.5 Consolidation Test

In Chapter 2 the procedure and uses of consolidation tests were given with details. In this part of Chapter 3 implementation of the consolidation tests and its results were given. Totally, three undisturbed samples were taken during borehole drilling and consolidation tests were performed on these samples. The first undisturbed samples obtained from SK 2 at 6 m depth. The consolidation test result and related graph were given in Table 3.4 and in Figure 3.14.

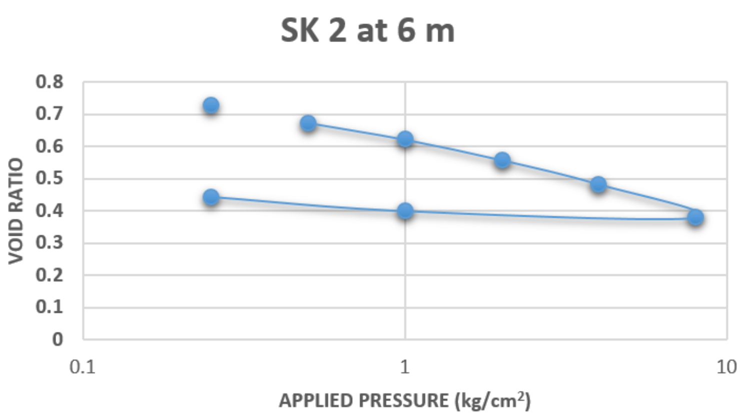

Figure 3.14. Pressure Void Ratio Graph for SK 2 at 6 m

Table 3.4. The Consolidation Test Results for SK 2 at 6 m

Applied Pressure (kg/cm^2)	Settlement (cm)	Void Ratio	m_v (cm^2/kg)	Cc
0	0	0.921		0.22
0.25	0.070	0.854	0.140	
0.50	0.122	0.804	0.107	
1	0.183	0.745	0.065	
2	0.260	0.671	0.042	
4	0.348	0.586	0.025	
8	0.425	0.513	0.011	
1	0.435	0.503		
0.25	0.392	0.544		

The first undisturbed samples obtained from SK 2 at 6 m depth. The consolidation test result and related graph were given in Table 3.5 and in Figure 3.15.

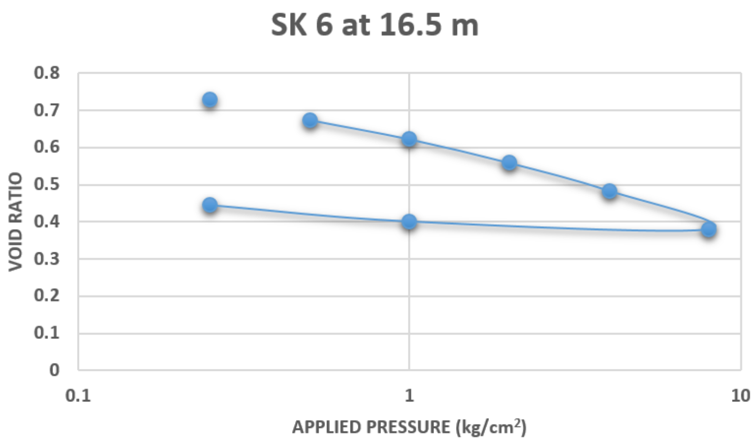

Figure 3.15. Pressure Void Ratio Graph for SK 6 at 16.5 m

Table 3.5. The Consolidation Test Results for SK 6 at 16.5 m

Applied Pressure (kg/cm^2)	Settlement (cm)	Void Ratio	m_v (cm^2/kg)	Cc
0	0	0.794		0.182
0.25	0.07	0.73	0.142	
0.5	0.132	0.675	0.128	
1	0.19	0.623	0.061	
2	0.262	0.559	0.039	
4	0.345	0.484	0.024	
8	0.461	0.38	0.017	
1	0.438	0.401		
0.25	0.388	0.445		

The third undisturbed samples obtained from SK 25 at 4.5 m. The consolidation test result and related graph were given in Table 3.6 and in Figure 3.16.

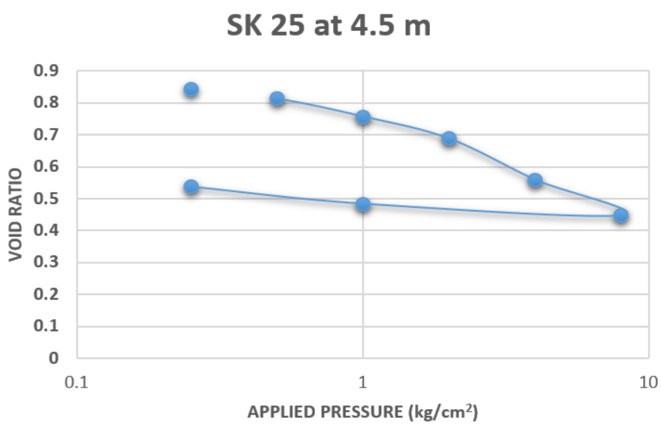

Figure 3.16. Pressure Void Ratio Graph for SK 25 at 4.5 m

Table 3.6. The Consolidation Test Results for SK 25 at 4.5 m

Applied Pressure (kg/cm^2)	Settlement (cm)	Void Ratio	mv (cm^2/kg)	Cc
0	0	0.923		0.26
0.25	0.08	0.844	0.164	
0.5	0.114	0.813	0.067	
1	0.173	0.757	0.0526	
2	0.244	0.688	0.039	
4	0.378	0.559	0.038	
8	0.494	0.448	0.0179	
1	0.456	0.484		
0.25	0.401	0.445		

3.4.6 Soil Experiments

The physical properties of the soils were obtained from the disturbed samples collected from ACC and Turbine Generator Region's boreholes (SK1 – SK9). The plasticity index (PI), soil classification (USCS), water content (w), unit weight (g) and specific gravity (Gs) of the soils were determined. In Table 3.7 the physical properties of soils collected from SK1-SK3 were given. In Table 3.8 the physical properties of soils collected from SK4-SK6 were given. In Table 3.9 the physical properties of soils collected from SK7-SK9 were given.

Table 3.7. The Physical properties of the soils SK1 – SK 3

Borehole No	Sample	Depth	wn	γ	Gs	Atterberg Limits			Sieve Analysis		Classification of Soils
						LL	PL	PI	10 (+)	200 (-)	
SK-1	SPT	3.00-3.45	35.3			52.1	20.6	31.5	0	95.8	CH
SK-1	UD	4.50-4.00	32.1	18.2		N.P	N.P	N.P	0	9.2	SP-SM
SK-1	SPT	9.00-9.45	25.2			N.P	N.P	N.P	0	47.6	SM
SK-1	SPT	16.50-16.95	44.5			59.4	28	31.4	0	98.6	CH
SK-1	SPT	21.00-21.45	31.5			37.2	18.9	18.3	0.33	93.73	CI
SK-1	SPT	25.50-25.95	33			58.4	24.7	33.7	0	87.7	CH
SK-1	SPT	28.50-28.95	28.8			N.P	N.P	N.P	0	62.2	ML
SK-2	SPT	3.00-3.45	30.6			51.6	20.1	31.5	0	82	CH
SK-2	UD	6.00-6.50	30.3	18.1	2.7	34.3	21.3	13	0	97.2	CL
SK-2	SPT	9.00-9.45	25.3			N.P	N.P	N.P	0	34.6	SM
SK-2	SPT	15.00-15.45	28.8			N.P	N.P	N.P	6.7	44	SM
SK-2	SPT	21.00-21.45	31.4			36.4	19.2	17.2	0.3	96	CI
SK-2	SPT	27.00-27.45	34.6			33.4	20	9	0.3	93	CL
SK-3	SPT	3.00-3.45	23.7			29	20	9	0	93.7	CL
SK-3	SPT	9.00-9.45	33.3			37.3	21.9	15.4	0.2	90.7	CI
SK-3	SPT	13.50-13.95	28			37.5	23.2	14.2	0	97.9	CI
SK-3	SPT	16.50-16.95	32.8			49.9	20.6	29.3	0	81.3	CI
SK-3	SPT	21.00-21.45	29.3			30.4	21.4	8.9	0	92.8	CL
SK-3	SPT	28.50-28.95	30.9			31.2	21	10.1	0	89	CL

Table 3.8. The Physical properties of the soils SK 4 – SK 6

Borehole No	Sample	Depth	wn	γ	Gs	Atterberg Limits			Sieve Analysis		Classification of Soils
						LL	PL	PI	10 (+)	200 (-)	
SK-4	SPT	1.50-1.95	31			51.4	20.3	31.1	0	90.3	CH
SK-4	SPT	6.00-6.45	32.2			52.4	20.9	31.4	0	90.1	CH
SK-4	SPT	9.00-9.45	43.2			45.1	18.3	26.8	0	98.1	CI
SK-4	UD	12.00-12.50	27	18.5		N.P	N.P	N.P	0.16	38.9	SM
SK-4	SPT	18.00-18.45	25.7			N.P	N.P	N.P	0	51.6	ML
SK-4	SPT	21.00-21.45	23.4			N.P	N.P	N.P	0	20.4	SM
SK-4	SPT	25.00-25.45	27.3			32.4	17.3	15	0	91	CL
SK-5	SPT	1.50-1.95	36.8			48.6	18.4	30.2	0.14	98.1	CI
SK-5	SPT	10.50-10.95	35.8		2.7	37	21	16	0	99.5	CI
SK-5	SPT	16.50-16.95	44.6			66.2	24.1	42	0	98.9	CH
SK-5	SPT	22.50-22.95	21.1			N.P	N.P	N.P	0	81.5	ML
SK-5	SPT	25.50-25.95	25.2			N.P	N.P	N.P	0.32	77.1	ML
SK-5	SPT	30.00-30.45	30.7			N.P	N.P	N.P	0.14	89	ML
SK-6	SPT	1.50-1.95	37.5			56.7	23.8	32.8	0	99	CH
SK-6	SPT	4.50-4.95	25.6			N.P	N.P	N.P	0	7.8	SP-SM
SK-6	SPT	10.50-10.95	37.4			44.9	19	25.9	0	87.3	CI
SK-6	UD	16.50-17.00	42.8	18.1		55.1	24	31	0	99.3	CH
SK-6	SPT	19.50-19.95	32.5			37	18.3	18.7	0	94.5	CI
SK-6	SPT	21.00-21.45	28.4			N.P	N.P	N.P	0	44.4	SM
SK-6	SPT	25.50-25.95	35.6			58.7	26.3	32.4	0	93.2	CH
SK-6	SPT	30.00-30.45	25.6			N.P	N.P	N.P	0	59.1	ML

Table 3.9. The Physical properties of the soils SK 7 – SK 9

Borehole No	Sample	Depth	wn	γ	Gs	Atterberg Limits			Sieve Analysis		Classification of Soils
						LL	PL	PI	10 (+)	200 (-)	
SK-7	SPT	1.50-1.95	31			52	19.8	32.2	0.22	98.6	CH
SK-7	SPT	4.50-4.95	32.2			52.2	20.8	31.3	0	99	CH
SK-7	SPT	9.00-9.45	43.2			37.6	23.4	14.1	0	95	CI
SK-7	UD	15.00-15.45	27	17.8		N.P	N.P	N.P	0	75.6	ML
SK-7	SPT	19.50-19.95	25.7			N.P	N.P	N.P	0	73.2	ML
SK-7	SPT	24.00-24.45	23.4			66.2	23.1	43.1	0	97	CH
SK-7	SPT	30.00-30.45	27.3			N.P	N.P	N.P	0	79	ML
SK-8	SPT	3.00-3.45	36.8			44	21.1	22.9	0	95.1	CI
SK-8	SPT	7.50-7.95	35.8			34.2	17.1	17	0	91.8	CL
SK-8	SPT	10.50-10.95	44.6		2.7	26.3	18	8.2	0	73.1	CL
SK-8	UD	15.00-15.45	21.1	17.8		N.P	N.P	N.P	0	94.1	ML
SK-8	SPT	21.00-21.45	25.2			46.2	17.4	28.8	0.5	98.7	CI
SK-8	SPT	24.00-24.45	30.7			30.4	20	10.4	0.4	97	CL
SK-9	SPT	4.50-4.95	37.5			32.6	19.7	12.9	0.5	82.7	CL
SK-9	SPT	10.50-10.95	25.6			37.1	20.6	16.4	0	99.3	CI
SK-9	SPT	16.50-16.95	37.4			65.2	24.1	41.1	0	98.8	CH
SK-9	UD	25.50-25.95	42.8			N.P	N.P	N.P	0	23.4	SM
SK-9	SPT	30.00-30.45	32.5			N.P	N.P	N.P	0.2	84.8	ML

CHAPTER 4

SETTLEMENT ANALYSIS OF THE RAFT FOUNDATION

4.1 Introduction

Vapor pressure, which has high temperatures, is transported with the help of pipelines in the geothermal power plant project. Pipes are affected by internal and external factors such as temperature, pressure and settlement of foundation and these cause to extra stress in pipelines. Especially, pipe stresses must be limited for safety concepts in the turbine and generator area, where electricity is produced.

Settlement problem is considered as total settlement and differential settlement from the point of geotechnical engineering. Shallow foundation (especially raft foundation) is selected to decrease settlements due to decreasing structure stress and balancing hydrostatic uplift pressure. In this project raft foundation is selected with height is 90 cm beneath of Turbine – Generator Part.

In this chapter, settlement analysis of the foundation in Turbine – Generator Area was performed with using soil stiffness parameters (stress – strain modulus and Poisson's ratio) soil stratum information and service loads. Settlement analyses were performed with Settle 3D software based on 1-D stress – strain relation and with Plaxis 3D software based on advanced numerical continuum models (Mohr Coulomb Soil Model and Hardening Soil Model with Small Strain Stiffness)

4.2 Soil Properties

In this part of the chapter soil properties were determined with the correlations detailed in Chapter 2 and the results of field tests and laboratory experiment detailed in Chapter 3. In the geothermal area, there were three types of soil (silty sand, sandy silt and silty clay), and one types of qualified fill material (PMT).

4.2.1 Stress Strain Modulus

In real soil behavior, commonly observed phenomena of increasing stiffness modulus with increasing confining stress or increasing depth but related some stiffness formulations (SPT correlations) in Chapter 2 does not take account of this. Soil consistency also is related to the stress level of soil for normally consolidated soil. Consistency is increased with depth so that typical values of stress – strain modulus and consistency for cohesionless and cohesive materials are given in Table 4.1 and Table 4.2. These tables were used to check stress – strain modulus from correlations that were given in Chapter 2.

Table 4.1. Stress – Strain Modulus of Cohesionless with Consistency
(Source: Kezdi 1974 and Prat et al. 1995)

USCS	Description	Loose	Medium	Dense
GW, SW	Gravels/Sand well-graded	30-80	80-160	160-320
SP	Sand, uniform	10-30	30-50	50-80
GM , SM	Sand/Gravel silty	7-12	12-20	20-30

Table 4.2. Stress – Strain Modulus of Cohesive with Consistency
(Source: Kezdi 1974 and Prat et al. 1995)

USCS	Description	Very soft to soft	Medium	Stiff to very stiff	Hard
ML	Silts with slight plasticity	2.5 - 8	10 - 15	15 -40	40 - 80
ML, CL	Silts with low plasticity	1.5 - 6	6 -10	10 - 30	30 -60
CL	Clays with low-medium plasticity	0.5 - 5	5 -8	8 - 30	30 - 70
CH	Clays with high plasticity	0.35 - 4	4 -7	7 - 20	20 - 32
OL	Organic silts	-	0.5 -5	-	-
OH	Organic clays	-	0.5 -4	-	-

Atterberg limits show that silty sand layers were non plastic (NP) so that the silty sand layers were considered as cohesionless. SPT and CPT correlations were used to determine stress-strain modulus at several depths. Figure 4.1a shows the stress-strain modulus with depth using the SPT test data with correlations Webb (1969), Bowles (1996), Schmertmann (1970), Kulhawy and Mayne (1990) and Figure 4.1b shows the stress-strain modulus with depth using the CPT test data with correlations Bowles (1996), Schmertmann (1978), Bogdanovi (1990). The consistency of sand layers, which were classified as SP and SM, were loose and medium dense soils. SPT and CPT stiffness results for silty sand materials were almost compatible with expected stiffness in Table 4.1.

Atterberg limits show that sandy silt layers were non plastic (NP) so that the sandy silt layers were considered as cohesionless. SPT and CPT correlations were used to determine stress-strain modulus at several depths. Figure 4.2a shows the stress-strain modulus with depth using the SPT test data with FHWA (2002), Bowles (1996), Kulhawy and Mayne (1990) correlations and Figure 4.2b shows the stress-strain modulus with depth using the CPT test data with Bowles (1996), Bogdanovi (1990) and Sanglerat (1972) correlations. The consistency of silt layers, which were classified as ML, were stiff to very stiff. SPT and CPT stiffness results for silty sand materials were almost compatible with stiffness in Table 4.1.

For cohesive soil obtaining drained stress strain modulus is complicated because in-situ tests are quick but cohesive soil needs time to dissipate water; otherwise, undrained condition affect the test results. Although consolidation tests are suitable for drained stiffness parameters, generally obtained stiffness parameters value are lower than actual value due to difficulties in obtaining undisturbed samples, working on very small volume of soil particles and operator errors. When pressuremeter test results were taken into consideration as undrained stress – strain modulus, these values are four times greater than consolidation drained stress – strain modulus but for normally consolidated medium clays undrained / drained stress – strain modulus ratio is expected to be in the value range of 1.07 to 1.34 (Truty and Obrzud, 2011). As a result, CPT results were used to make comparesion. Oedometric stress – strain modulus is obtained from multiplying cone resistance with α factor for cohesive soil (Table 2.3). The α factor ranges from 2 to 12 and it is not consensus. The α factor was taken as 7 to be compatible with undrained stress – strain modulus and settlement results, related work was given in Chapter 5. In this part PMT results was given in Figure 4.3 and oedometric stress – strain modulus from CPT and Consolidation Test were given in Figure 4.4. According to PMT and CPT results, undrained / drained stress – strain modulus ratio was compatible with the value range of 1.07 to 1.34.

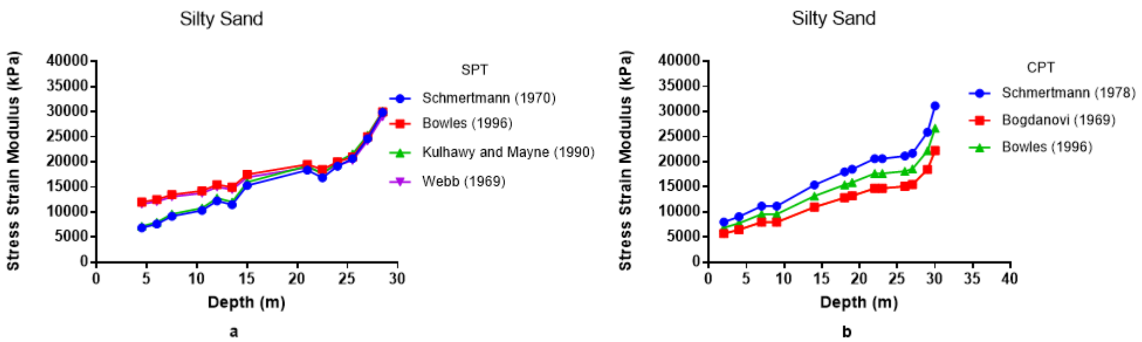

Figure 4.1. Stress Strain Modulus of Silty Sand (a) SPT Correlations (b) CPT Correlations

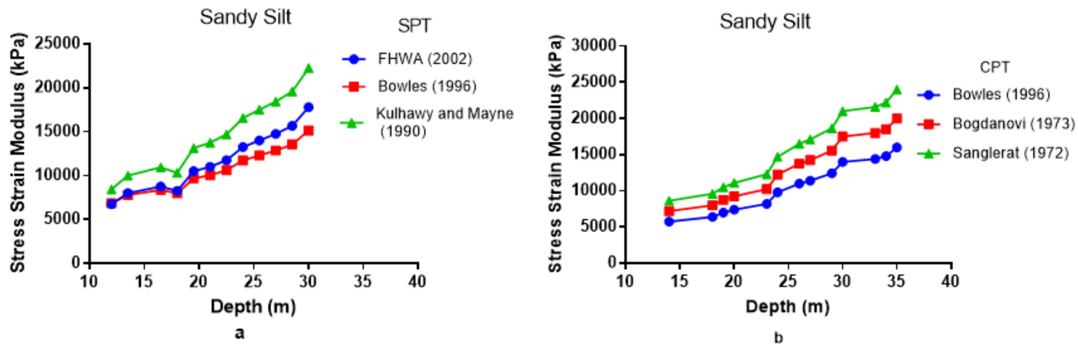

Figure 4.2. Stress Strain Modulus of Sandy Silt (a) SPT Correlations (b) CPT Correlations

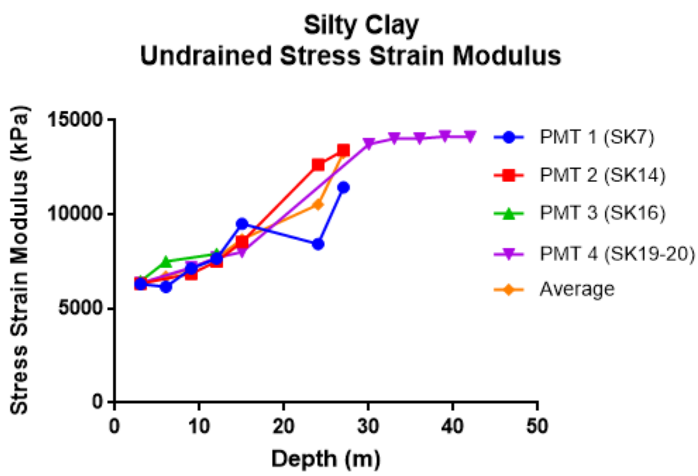

Figure 4.3. Undrained Stress Strain Modulus for Silty Clay

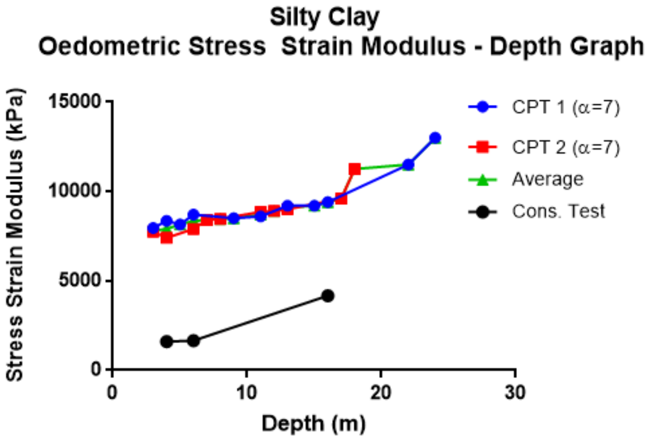

Figure 4.4. Oedometric Stress – Strain Modulus for Silty Clay

Table 4.3. Fill Material Stress Strain Modulus

Deformation Module: *Ev = [0,75 x D x (Δσ / ΔS)], kg/cm²								
	σ_{02} kgf/cm²	σ_{01} kgf/cm²	$\Delta\sigma$ kgf/cm²	S_2 cm	S_1 cm	ΔS cm	$*E_{v1}$ Mpa	$*E_{v2}$ Mpa
$*E_{v1}$	1.80	1.10	0.70	0.333	0.263	0.070	57.00	
$*E_{v2}$	1.40	0.70	0.70	0.365	0.350	0.015		266.00
E_{v2}/E_{v1} =	4.67							

4.2.2 Compressibility Index

Compressibility indexes were obtained from consolidation test and related Terzaghi and Peck's (1967) correlations which were given in Chapter 2. Mean compressibility index data, which were obtained by using liquid limits and water contents, were given in Figure 4.5. Consolidation tests results are compatible with correlation.

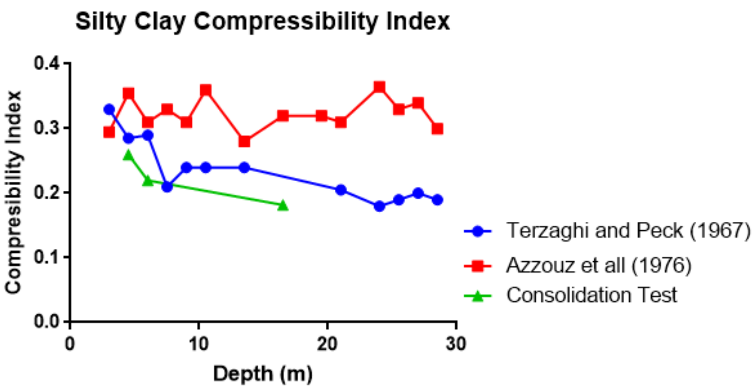

Figure 4.5. Compressibility Index of Silty Clay

4.2.3 Void Ratio

Direct measurement of void ratio in the laboratory is a difficult task. Therefore, void ratios for silty clay were obtained from undisturbed samples by using specific gravity and water content for fully saturated case. The void ratio values in the range of 0.80 to 0.96 for silty clay were given in Figure 4.6.

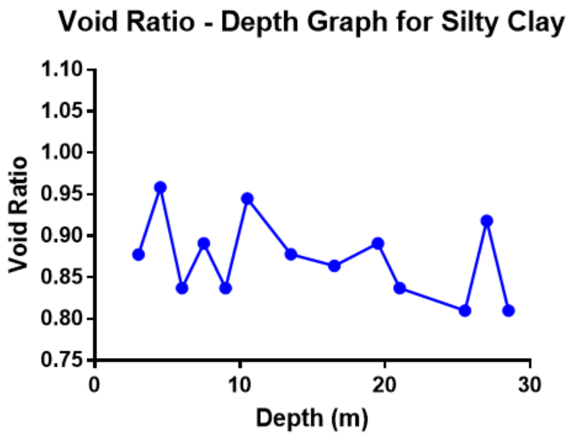

Figure 4.6. Void Ratio for Silty Clay

4.3 Project Information for Settlement Analysis

In this part of Chapter 4 determination of stratum of the soil in the project area and introduction service loads of the project is given. These data directly affect the settlement analyses.

4.3.1 Stratum of the Soils in the Project

A stratum of the soil in the project gives useful information such as boundary condition (drain or undrain) for consolidation, determination of soil consistency which affect the selection of settlement types (initial settlement, primary settlement, and secondary settlement), selection of soil stiffness parameters (stress – strain modulus and Poisson's ratio). The plan view of the A-A cross, the cross sectional views of Section A-A in Figure 4.7. The side view of A-A cross section was given in Figure 4.8. Logs of borehole SK 1, SK6 and SK 5 were used. The representative soil profile with soil stiffness parameters was given in Figure 4.9. For cohesive layers, void ratio also was given.

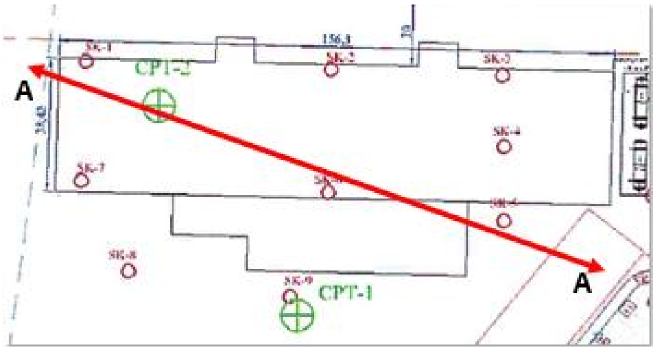

Figure 4.7. The Plan View of Section A-A

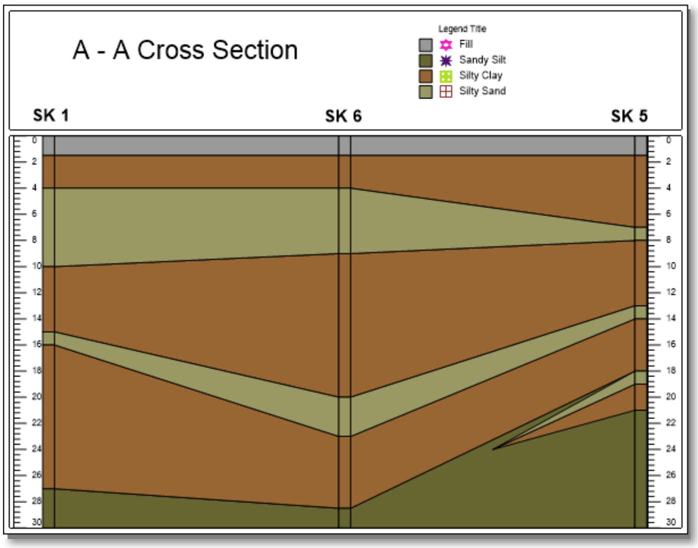

Figure 4.8. The Side View of Cross Section A-A

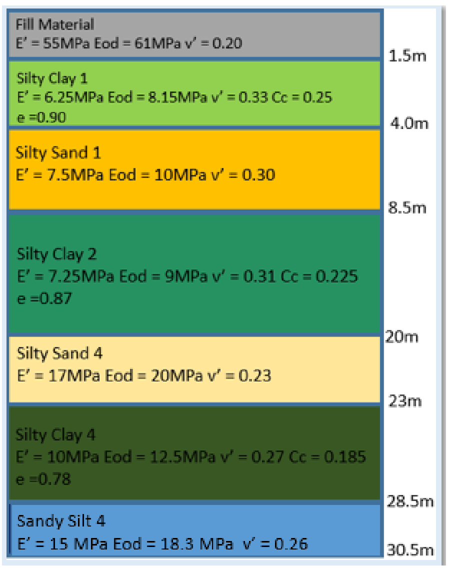

Figure 4.9. Representative Soil Profil

It is clearly seen from Figure 4.8 that first depth of 25 m silty clay layers were divided with layers of silty sand and sandy silt and between depth of 25 m a silty layer was encountered. Due to the existence of sand and silty layers at silty clay consolidation time of clays is supposed to be short.

4.3.2 Service Loads of the Project

In the project, structural and mechanical elements loads, which is shown in Figure 4.10, divided as Recuperator Loads, Air Cooler Condenser Loads, Pipe Support Loads, Heat Exchanger Loads, and Turbine and Generator Loads. For settlement analyses death loads, which were given in between Table 4.4 and Table 4.8.

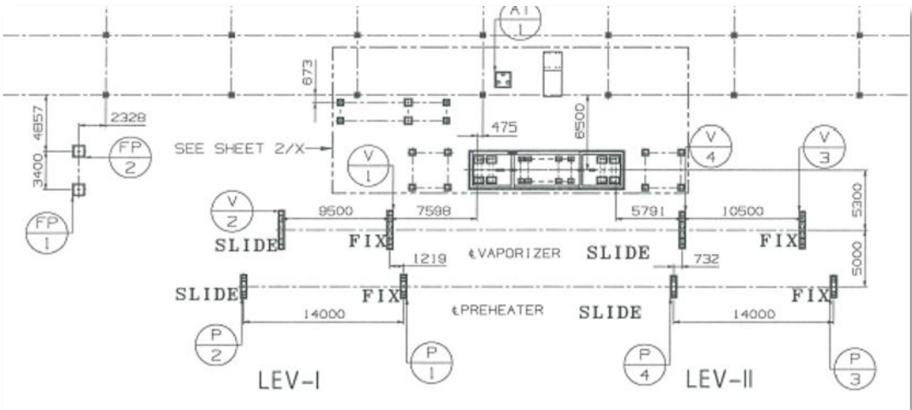

Figure 4.10. Structural and Mechanical elements loads

Table 4.4 Heat Exchanger Loads

Description	Index	F_y [N]
Condensate Separator Tank	CS1	-34,777.9
	CS2	-32,777.9
Condensate Separator Tank	CS3	-31,254.5
	CS4	-30,254.5
Preheater	P1	-583,432
	P2	-548,201
Preheater	P3	-602,720
	P4	-590,436
Vaporizer	V1	-1,377,466
	V2	-1,615,961
Vaporizer	V3	-1,359,876
	V4	-1,435,348

Table 4.5. Air Cooler Condenser Loads

ACC	Load Case	F_x [N]	F_y [N]	F_z [N]
AC1/ 5	TDW	-21,128.4	-188,294.3	-15,640.2
AC1/ 6	TDW	-21,120.7	-186,485.3	-14,744.9
AC1/ 7	TDW	-21,070.3	-187,332.6	-15,184.5
AC1/ 8	TDW	-21,114.1	-188,304.5	-15,706.0
AC1/ 9	TDW	-20,960.7	-185,374.0	-15,091.4
AC1/ 10	TDW	-21,134.9	-188,082.8	-15,197.0
AC1/ 11	TDW	-21,116.5	-186,292.8	-14,661.6
AC2/ 5	TDW	-24,703.1	-168,406.2	-14,192.3
AC2/ 6	TDW	-24,697.0	-167,019.3	-13,504.6
AC2/ 7	TDW	-24,611.0	-167,841.1	-13,847.5
AC2/ 8	TDW	-24,674.9	-167,872.5	-14,023.2
AC2/ 9	TDW	-24,373.6	-166,074.0	-13,705.4
AC2/ 10	TDW	-24,741.6	-168,596.3	-13,960.1
AC2/ 11	TDW	-24,693.2	-166,729.5	--13,365.6

Table 4.6. Turbine and Generator Loads

<table>
<tr><th rowspan="2">Description</th><th rowspan="2">Mark</th><th colspan="2">L (Normal)</th></tr>
<tr><th>F_x [N]</th><th>F_y [N]</th></tr>
<tr><td rowspan="2">Turbine L1</td><td>T1</td><td>-2,893</td><td>-40,972</td></tr>
<tr><td>T2</td><td>-2,893</td><td>-13,916</td></tr>
<tr><td rowspan="2">Turbine L2</td><td>T3</td><td>-2,893</td><td>-40,972</td></tr>
<tr><td>T4</td><td>-2,893</td><td>-13,916</td></tr>
<tr><td rowspan="8">Generator</td><td>G1</td><td>-12,115</td><td>-102,110</td></tr>
<tr><td>G2</td><td>-12,115</td><td>-137,110</td></tr>
<tr><td>G3</td><td>-12,115</td><td>-150,110</td></tr>
<tr><td>G4</td><td>-12,115</td><td>-87,110</td></tr>
<tr><td>G5</td><td>-12,115</td><td>-72,110</td></tr>
<tr><td>G6</td><td>-12,115</td><td>-73,110</td></tr>
<tr><td>G7</td><td>-12,115</td><td>-78,110</td></tr>
<tr><td>G8</td><td>-12,115</td><td>-69,110</td></tr>
<tr><td rowspan="2">L1 Feed Pump</td><td rowspan="2">FP1-2</td><td rowspan="2">11,139</td><td>-50,890</td></tr>
<tr><td>8,394</td></tr>
<tr><td rowspan="2">L2 Feed Pump</td><td rowspan="2">FP3-4</td><td rowspan="2">10,210</td><td>-38,647</td></tr>
<tr><td>10,718</td></tr>
<tr><td>Generator Cooling Pumps</td><td>GC</td><td>-129</td><td>-1,350</td></tr>
</table>

Table 4.7. Pipe Support Loads

Pipe Supports	Load Case	F_x(N)	F_y(N)	F_z(N)
S1	TDW	0	-13,424	-110
S2	TDW	205	-3,026	-524
S4	TDW	-861	-35,286	-1,860
S7	TDW	5,494	-36,698	6,790
S8	TDW	-49,722	-77,529	-29,642
S9	TDW	184	-2637	-632
S16	TDW	-5,283	-59,803	16,916
S17	TDW	-2,114	-31,845	9,436
S34	TDW	-1,766	-75,049	2,462
S41	TDW	5,963	-25,125	-2,186
S42	TDW	-1,006	-11,854	843
S46	TDW	-23,178	-55,208	66,217

Table 4.8. Recuperator Loads

Recuperator	Load Case	Force		
		F_x N	F_y N	F_z N
R1	TDW	1,171.6	-184,926.0	0.0
R2	TDW	-1,1663	-184,869.1	-0.7
R3	TDW	-22.4	-4,020.5	-76.5
R4	TDW	-23.1	-4,343.1	79.4
R5	TDW	1,219.4	-187,205.0	-7.9
R6	TDW	-1,179.1	-186,422.9	5.8

4.4 Settlement Analysis with 1D (Vertical) Stress – Strain Relation

In geotechnical literature many methods can be used for settlement analysis, however, many of methods are based on homogenous soil types such as only sand layer or clay layer. For example, Schmertmann (1977) developed a settlement analysis and influence factor for sand layers. Woefully, most of the cases stratums are formed with different soil types. In this project, silty clay layers are divided by sandy silt layers and silty sand layers. For such a multilayer (non-homogenous) soils using vertical stress strain relation with convenient stress distribution factor such as Boussinesq's method can provide closed solution for settlement analysis. In chapter 2, detailed formulations are based on vertical stress strain relation for elastic and consolidation settlement and next part of this chapter settlement analyses with vertical stress strain relation were done with Settle 3D Software.

4.4.1 Settle 3D Software

Settle 3D is a user friendly software for analysis of vertical consolidation settlement, foundation settlement, and embankment settlement analysis due to easily creation of complex soil stratum, selection of loading conditions, and obtaining results in 3D. Moreover, construction stages can be defined, time intervals can be used for primary and secondary settlement analysis and pre-load fill height or required time is obtained with back analysis option.

Although Settle 3D makes sense using 3D stress strain relation, the software uses only 1D vertical stress strain relation but Settle 3D take into consideration 3D effects such as using modified stress strain modulus with Eq. 2.22, using loads effects in 3D format and using 3D non-homogeneous soil stratums.

4.4.2 The Selected Soil Parameters for Settle 3D Software

In the geothermal area, there were three types of soil (silty sand, sandy silt and silty clay), and one types of qualified fill material (PMT). It is pointed out an important matter that soil physical and stiffness properties such as void ratio, compressibility index, stress strain modulus and Poisson’s ratio can change with depth for the same type of soil. For accurate analysis soil types should be divided into groups and each group has depth dependent physical and stiffness properties. The depth dependent stress – strain modulus, Poisson’s ratio, compression index, void ratio and overconsolidation ratio were given in Table 4.9.

4.4.3 Modelling of Project in Settle 3D for Settlement Analysis

In this part of chapter 4, modelling the of project in Settle 3D is given with four subtitles as project settings, soil layers and properties, services load and auto field grids

Project Settings

In Project Settings dialog stress computation methods (Boussinesq, Westergaard and 2:1 Method), time dependent consolidation, SI and British Units, staging, groundwater properties and advanced settings are found. In the project four steps were applied as the application of fill, settlement due to fill, application of foundation load and application of service loads.

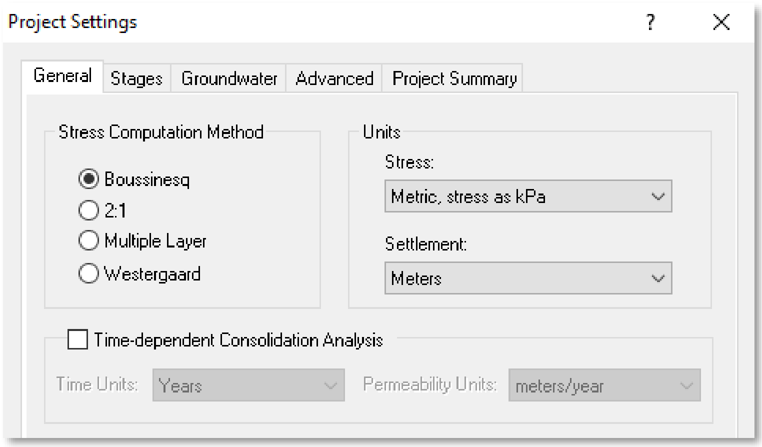

Figure 4.11. Project Settings in Settle 3D Software

Soil Layers and Properties

Seven soil layers were defined as fill material, silty clay 1, silty sand 1, silty clay 2, silty sand 4, sandy silt 4 and silty clay 4. Moreover, the height of each layers was defined in Figure 4.12.

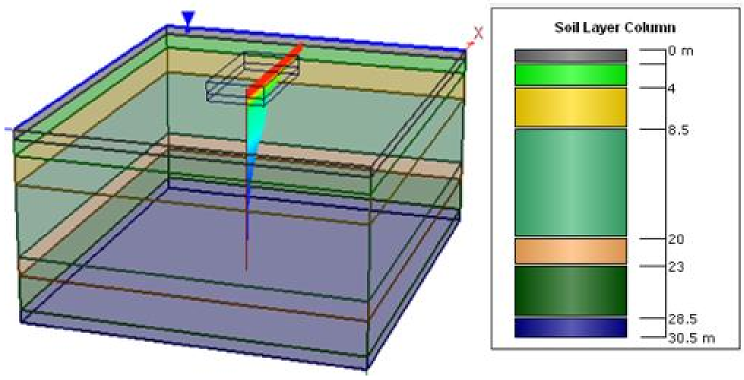

Figure 4.12. Soil Layers of Project

Primary consolidation is activated for clay layers and immediate settlement is activated for silts and sands layer in Figure 4.13. For clay layers linear and nonlinear options can be selected. Linear analysis uses coefficient of volume compressibility Eq. (2.21) and nonlinear analysis use Eq. (2.18), Eq. (2.19) and Eq. (2.20). The coefficient of volume compressibility was obtained from in-situ tests as inverse of stress – strain modulus and compression index was taken from consolidation tests results so that this gave the possibility to compare the settlement results obtained with the field test data with the settlement results obtained from the consolidation test.

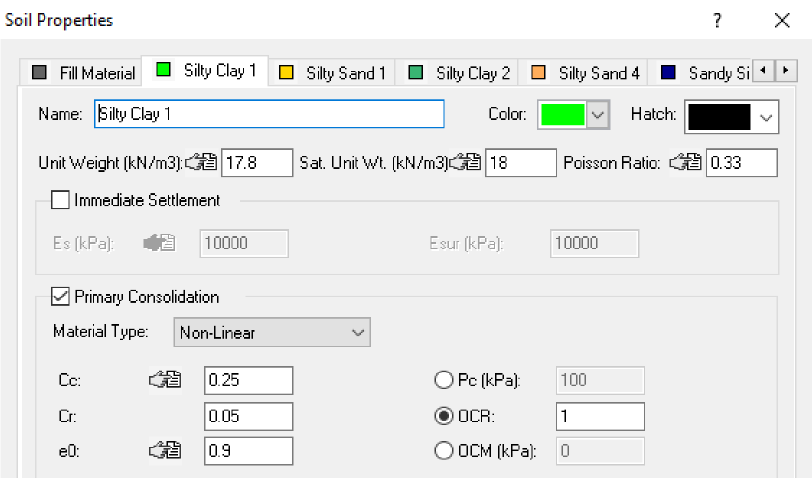

Figure 4.13. Soil Properties of Project

Services Loads and Auto Field Point Grid

Foundation loads and service loads are main loads for settlement. Moreover, application of fill material cause settlement on soil layers. Unit weight of foundation should be specified as subtracting the unit soil weight from the real unit weight of plate because of the fact that the foundation does not occupy any volume and overlaps with the soil elements. Foundation height is 90 cm and decreased unit weight of foundation is 15.5 kN/m^3 so that foundation pressure calculated as 0.9 x 15.5 = 14 kPa as given in Figure 4.14. Raft foundation (which is used to decrease differential settlement) dimensions higher than strip footing; on the other hand, last stress increment level is increased under same stress because Boussinesq's, Westergaard's and 2:1 method depends on length and width of foundation. Normally, length of foundation is 55 m and width of foundation is 27 m, but width is chosen as 10 m and length is chosen 20 m in order to obtain accurate last stress increment level which was obtained from numerical continuum model. In Chapter 5, relation between foundation dimensions and settlement results were given.

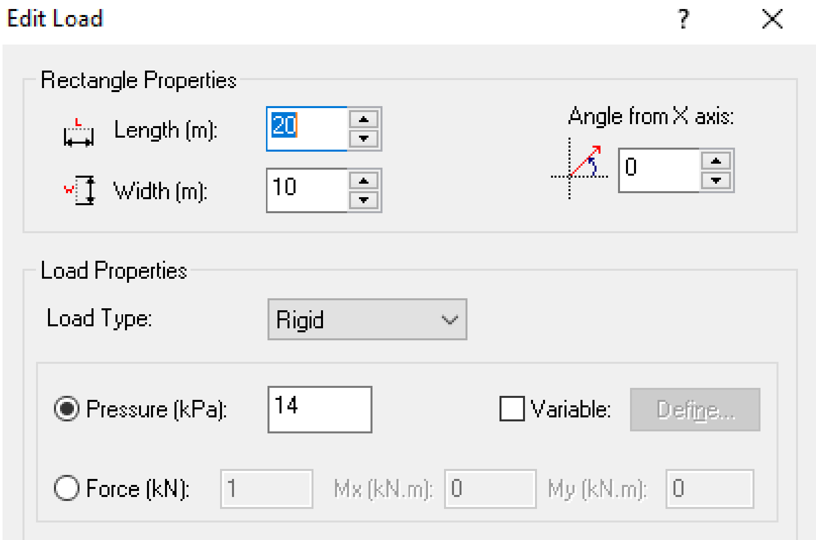

Figure 4.14. Foundation Load Input

Table 4.9. Soil Parameters for Settlement Analyses

Depth Interval (m)	Soil Type	Stress-Strain Modulus E (kPa)	Oedometric Modulus E_{oed} (kPa)	Poisson Ratio v	Compres. Index C_C	Void Ratio e_0	OCR
3-10	Silty Clay	6250	8150	0.33	0.25	0.90	1
10-15	Silty Clay	7250	9000	0.31	0.225	0.87	1
15-20	Silty Clay	8250	9800	0.29	0.2	0.83	1
20-25	Silty Clay	10000	12500	0.27	0.185	0.80	1
0-5	Silty Sand	7500	10000	0.30			1
5-10	Silty Sand	10000	12750	0.28			1
10-20	Silty Sand	13500	16500	0.26			1
20-30	Silty Sand	17000	20000	0.23			1
10-15	Sandy Silt	7500	10100	0.30			1
15-20	Sandy Silt	10000	12800	0.28			1
20-25	Sandy Silt	12000	15000	0.27			1
25-30	Sandy Silt	15000	18350	0.26			1
0-1.5	Fill	55000	61000	0.2			1

4.5 Settlement Analysis with Numeric Methods

For a complete theoretical solution, the equilibrium, compatibility, material constitutive behavior and boundary conditions should be satisfied. A closed form analytical solution cannot satisfy real constitutive soil behavior which include four fundamental requirements. On the other hand, numerical methods can provide information for design requirements and complete construction history (Potts et al, 2001).

Most numerical techniques such as finite difference method and finite element method are based on the principle of discretization which means that a complex problem is divided, or discretized, into smaller equivalent units, or components. In these methods, real soil behavior is defined with some material models which include elastic and plastic strain contribution, yield surfaces and soil strength parameters. (Townsend et al, 2001),

In this part of the chapter, introduction to Finite Element Method, Plaxis 3D software, Mohr Coulomb and Hardening Soil with Small Stiffness soil models, selected soil parameters for each soil model and input steps for the settlement analysis were given.

4.5.1 Finite Element Method (FEM)

Generating a finite element (FE) mesh is the first stage in any FE analysis. A mesh consists of elements connected together at nodes. Calculations are done in the nodes which were given in Figure 4.15, and some sort of mathematical equation are used to estimate the solution inside the elements. In geotechnical problems, finite element method mostly is based on finding displacement. (Potts and Zdravković, 2001)

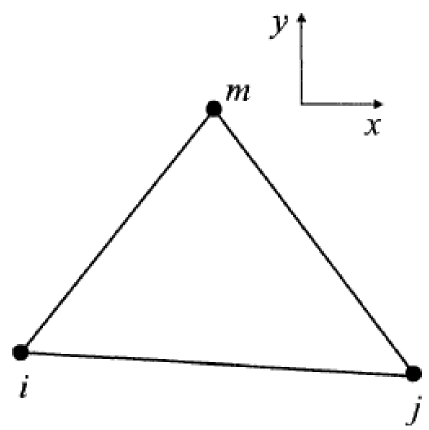

Figure 4.15. Three Noded Element

Displacement equations for three noded triangular element are given below:

$$u = a_1 + a_2 x + a_3 y \tag{4.1}$$

$$v = b_1 + b_2 x + b_3 y \tag{4.2}$$

The equations are solved in terms of the nodal displacements u_i, u_j, u_m, v_i, v_j, and v_m which are given below:

$$\begin{Bmatrix} u \\ v \end{Bmatrix} = [N]\{u_i \; u_j \; u_m \; v_i \; v_j \; v_m\}^T \tag{4.3}$$

Where:

[N] is known as the matrix of shape functions.

Briefly, element equations combine the compatibility, equilibrium and constitutive conditions in the Eq.(4.4)

$$[K_E]\{\Delta d\}_n = \{\Delta R_E\} \tag{4.4}$$

Where:

$[K_E] = \int_{Vol} [B]^T [D][B] dVol = Element$ stiffness matrix;

$\{\Delta R_E\} = \int_{Vol} [N]^T [\Delta F] dVol + \int_{Vol} [N]^T \{\Delta T\} dSrf = Right$ hand side load vector

[B] = derivatives of the shape functions, [D] = constitutive matrix, ΔF^T = Body Forces, ΔT^T = Surface Tractions (Line Loads, Surcharges)

4.5.2 Plaxis 3D Software

Plaxis, one of the worldwide geotechnical design software, use finite element method (FEM) to obtain analysis of deformation, stability and groundwater flow in geotechnical engineering. Plaxis has products such as Plaxis 2D, Plaxis 3D, Dynamics, Plaxflow, Thermal and Plaxis Vip.

The Plaxis's development began in 1987 at Delft University. Initially 2D finite element code was developed to analysis lowlands Holland's river embankments on the soft soil. In following years, Plaxis was introduced in many geotechnical engineering areas due to continuously expanding activities. Extended to cover most other areas of geotechnical engineering. Because of continuously growing activities. Plaxis was founded as a company in 1993 as a result of these developments. Plaxis 3D is a full three-dimensional finite element program which combines an easy to use interface with full 3D modelling facilities. The first Plaxis 3D program was released in 2010.

Non-linear, time-dependent and anisotropic behavior of soils or rock are simulated as a constitutive model with Plaxis. Moreover, pore pressures and (partial) saturation in the soil are introduced with multi-phase soil layer properties in Plaxis. Soil structure interaction is very important issue for geotechnical project and Plaxis involves the modelling of structure and the interaction between the soils and structures. Plaxis carries out various aspects of complex geotechnical requirements (Brinkgreve, 2017). Plaxis has sufficient soil models, namely, Linear Elastic, Mohr-Coulomb, Hardening Soil, Hardening Soil Model with Small Strain Stiffness, Soft Soil, Soft Soil Creep, Jointed Rock and Modified Cam – Clay. Mohr-Coulomb, Hardening Soil, Hardening Soil Model with Small Strain Stiffness were used in analyses.

4.5.3 Mohr Coulomb Material Model

The Mohr-Coulomb model is a linear elastic perfectly plastic model. This model is widely used to determine soil strength, estimation of the ultimate limit state (e.g. stability analyses) or modeling of less influential, massive soil bed layers, and a first approximation of soil behavior where the number of soil tests and the parameter database are limited. (Truty and Obrzud, 2011). The linear elastic part of the Mohr-Coulomb model is based on Hooke's law of isotropic elasticity.

In the Mohr-Coulomb constant elastic stiffness parameters are used. In figure 4.16, it is seen that deviatoric stress strain curve (Young Modulus) is constant until the yield point, after reaching yield stress perfectly strain is obtained. Moreover, unloading stiffness ($E_{ur)}$ has the same curve with loading condition.

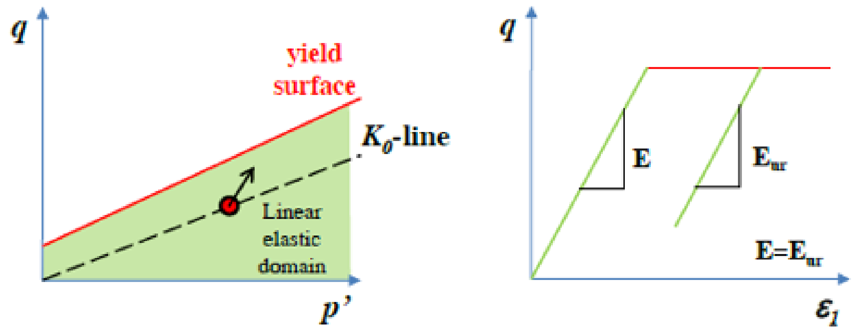

Figure 4.16. Mohr Coulomb Soil Model
(Source: Truty, 2009)

The Mohr-Coulomb model needs two elastic stiffness parameters (Young Modulus, E and Poisson's ratio, υ) and three strength parameters (cohesion, c, friction angle, φ, and dilatancy angle, ψ).

4.5.3.1 The Selected Soil Parameters for Mohr Coulomb Model

Soil parameters which are obtained from field and laboratory works were given below for Mohr Coulomb Soil Model. Stress strain modulus and Poisson's ratio were taken from Table 4.7. Determination of cohesion, friction angle and dilatancy angle is same with Hardening Soil Model with Small Strain Stiffness.

Table 4.10. The Selected Mohr Coulomb Parameters

Letter	E' (kPa)	υ'	c' (kPa)	φ' (o)	Ψ (o)
Silty Clay 1	6250	0.33	4	24	0
Silty Sand 1	7500	0.30	1	33	0
Silty Clay 2	7250	0.31	5	26	0
Silty Sand 4	17000	0.23	4	35	0
Silty Clay 4	10000	0.27	7	30	0
Sandy Silt 4	15000	0.26	6	32	0
Fill Material	55000	0.20	0	40	0

E': Stress - strain modulus, υ: Poisson's ratio, c: Cohesion, φ: Friction angle, ψ: Dilatancy angle,

4.5.4 Hardening Soil Model with Small Strain Stiffness (HSMSSS)

Soil behavior is non-linear when subjected to changes in stress or strain. In reality, the stiffness of soil depends at least on the stress level, the stress path and the strain level. Some such features are included in the advanced soil models. (Brinkgreve, 2017). The hardening soil model is an advanced soil model which was designed by Schanz in 1998. The hardening soil standard model covers densification, stress dependent stiffness, soil stress history, plastic yielding, dilatation in details. In Figure 4.17(a), hardening mechanism was given. In Figure 4.17b plastic yielding and unloading stiffness was given.

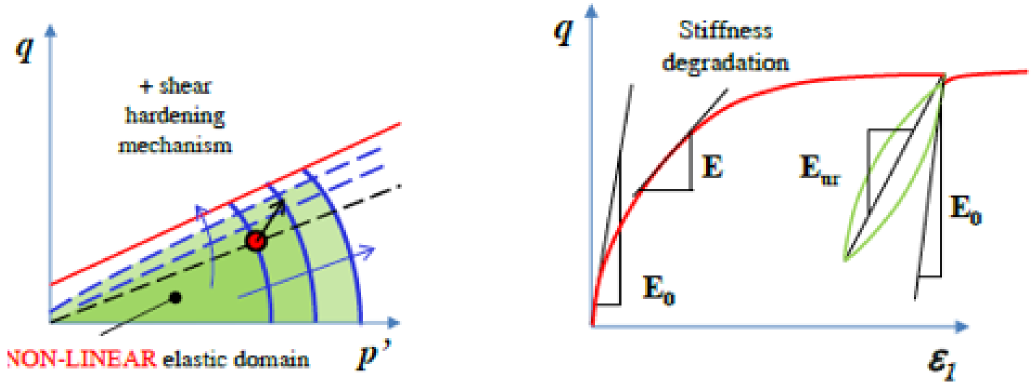

Figure 4.17. HS-Small Strain Soil Model (a) Hardening Mechanism, (b) Plastic Yielding and Unloading Stiffness (Source: Truty, 2009)

The Hardening Soil with Small Stiffness is an improved version of the Hardening Soil Standard by Benz (2007). Two important soil behavior was included. The first behavior is strong stiffness variation with increasing shear strain (Figure 4.18) and the second one is hysteretic soil behavior (Figure 4.19). These features mean that the HSMSSS is a useful soil model with these properties to produce a more accurate and reliable approximation of displacements for dynamic analysis or unloading case such as deep excavations with retaining walls and tunnels. The HSMSSS parameters were reference shear modulus at very small strain (G_0), threshold shear strain ($\gamma_{0.7}$), secant stiffness in standard drained triaxial test (E_{50}^{ref}), tangent stiffness for primary oedometer loading (E_{oed}^{ref}) , unloading / reloading stiffness from drained triaxial test (E_{ur}^{ref}), Poisson's ratio for unloading-reloading υ_{ur}, power for stress-level dependency of stiffness (m), cohesion (c) , friction angle (φ), dilatancy angle (ψ).

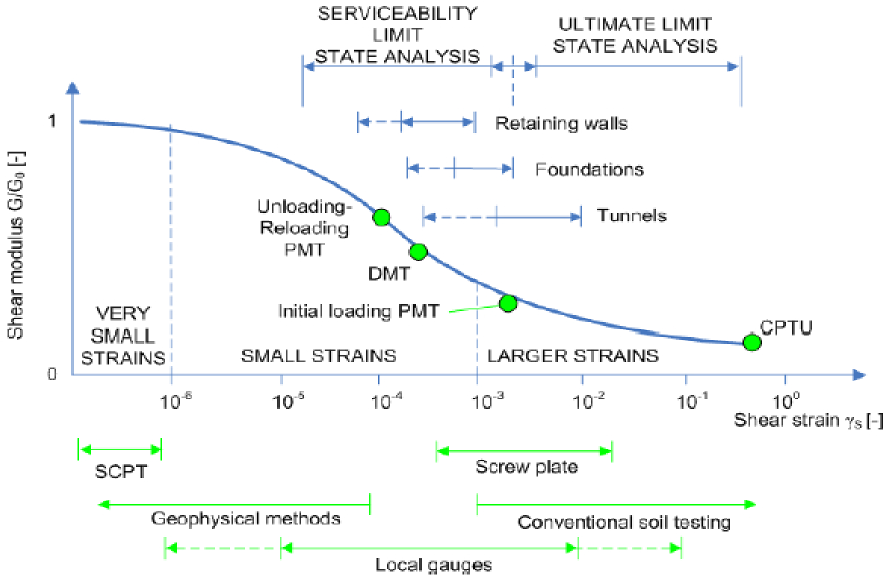

Figure 4.18. Stiffness Variation and Shear Strain for Geotechnical Analysis

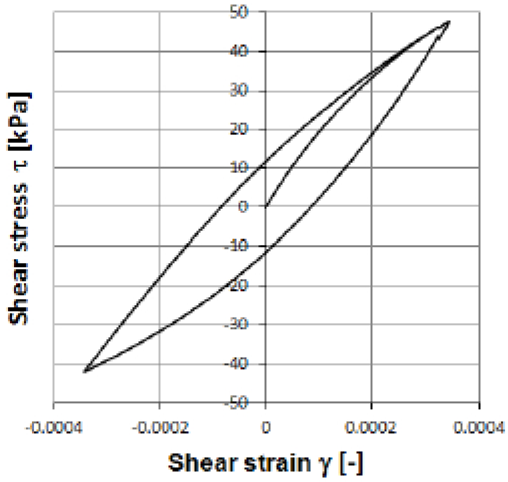

Figure 4.19. Hysteretic Soil Behavior

4.5.4.1 Parameter Determination for HSMSSS

The HSMSSS parameters can be obtained by laboratory tests such as oedometer test and triaxial shear test. However, most of the time testing natural soil is difficult due to sampling problem and soil characteristic. For example, dependently site condition getting undisturbed sample from cohesionless soils under groundwater level is so difficult or low permeable clay's drainage time is so long. Therefore, some model parameters can be derived directly from the experimental curves or using correlations from in-situ test results. In this part, the determination of soil parameters for cohesionless and cohesive materials were given.

Reference shear modulus (G_0)

Biarez and Hicher (1994) proposed a simple relationship for all soils with w_L < 50 %:

$$G_0 = \frac{140}{e}\left(\frac{p'}{p_{ref}}\right)^{0.5} / \left(2(1+v_{ur})\right) \tag{4.5}$$

Where;

p_{ref}: reference pressure, p': mean effective stress, e: void ratio

Threshold shear strain ($\gamma_{0.7}$)

In a more practical point of view, the reference threshold shear strain defines the beginning of significant stiffness degradation. (Santos and Correia,2001). A well-known experimental database was reported by Vucetic and Dobry (1991) illustrates the relationship between $\gamma_{0.7}$ and plasticity index (PI < 100) for cohesive soils.

$$\gamma_{0.7} = \gamma_{0.7}^{ref} + 5.10^{-6} IP \quad \text{for PI} < 15 \tag{4.6}$$

$$\gamma_{0.7} = 10^{1.15\log(IP)-5.1} \quad \text{for PI} \geq 15 \tag{4.7}$$

$$\gamma_{0.7}^{ref}(\mathrm{I}_p = 0) = 10^{-4} \tag{4.8}$$

Darendeli and Stokoe (2001) suggests threshold shear strain as given below for cohesionless soil:

$$\gamma_{0.7} = \gamma_{0.7}^{ref} + \left(\frac{p'}{p_a}\right)^{0.35} \tag{4.9}$$

$$\gamma_{0.7}^{ref}(p_a) = 1.26 \times 10^{-4} \tag{4.10}$$

Stiffness Modulus (E_{50}^{ref} E_{oed}^{ref} E_{ur}^{ref}) and Stiffness Exponent (m)

Experimentally ratio between unloading stiffness modulus and secant stiffness modulus is given below for lack of triaxial tests and the oedometric modulus can be approximately taken as secant stiffness modulus.

$$\frac{E_{ur}^{ref}}{E_{50}^{ref}} = 3 \text{ to } 6 \quad \text{(4 can be taken for cohesive soil)} \tag{4.11}$$

$$\frac{E_{ur}^{ref}}{E_{50}^{ref}} = 2 \text{ to } 6 \quad \text{(3 can be taken for cohesionless soil)} \tag{4.12}$$

$$E_{oed}^{ref} \cong E_{50}^{ref} \tag{4.13}$$

An important point is that the secant stiffness modulus is determined by using static deformation modulus (E_s) and mean effective stress (p’) in equation 4.14. In chapter 2, the determination of static deformation modulus (E_s) is given in detail with using in situ tests (SPT, CPT, PMT and PLT). Moreover, the depth of modulus is also known so that with using the coefficient of in situ of earth pressure at rest (K_0), mean effective stress can be obtained as;

$$E = E_{50}^{ref}\left(\frac{p' + c\,\cot\phi}{p_{ref} + c\,\cot\varphi}\right)^{m} \tag{4.14}$$

Mayne and Kulhawy (1982) and Meyerhof (1976) suggested stiffness exponent as given below

m = sin φ’ (for cohesive soil) (4.15)

m = 0.5 (for cohesionless soil) (4.16)

Friction Angle and Cohesion

The exception of cemented soils, in drained condition cohesion value is small and it is known that in effective stress condition clay's strength is frictional. In Table 4.11, representative clay's friction angle values are given by Carter and Bentley (1991).

Table 4.11. Friction Angle of Clay

Soil Type	USCS	φ(◦)
Silty Clays, Sand – Silt Mix	SM	34
Clayey Sands, Sandy – Clay Mix	SC	31
Silts and Clayey Silts	ML	32
Clays of Low Plasticity	CL	28
Clayey Silts	MH	25
Clays of High Plasticity	CH	19

In drained condition cohesion value is zero for cohesionless soils. In Table 4.12, friction angle of sands is given by Peck at al. (1974) and Meyerhof (1956).

Table 4.12. Friction Angle of Sand

Soil Type	N_{60}	Peck at al. (φ)	Meyerhof (φ)
Very Loose Sand	< 4	< 30	< 29
Loose Sand	$4 - 10$	$29 - 30$	$30 - 35$
Medium Sand	$10 - 30$	$30 - 36$	$35 - 40$
Dense Sand	$30 - 50$	$36 - 41$	$40 - 45$
Very Dense Sand	> 50	> 41	> 45

Failure Ratio

Failure ratio is the ratio between asymptotic deviatoric stress and ultimate deviatoric stress. In Figure 4.21, hyperbolic stress – strain relation in primary for a standard drained triaxial test shows asymptote and failure line.

$$R_f = \frac{q_f}{q_a} \tag{4.17}$$

R_f value is experimentally in the range of 0.75 and 1.00. (Truty and Obrzud, 2011).

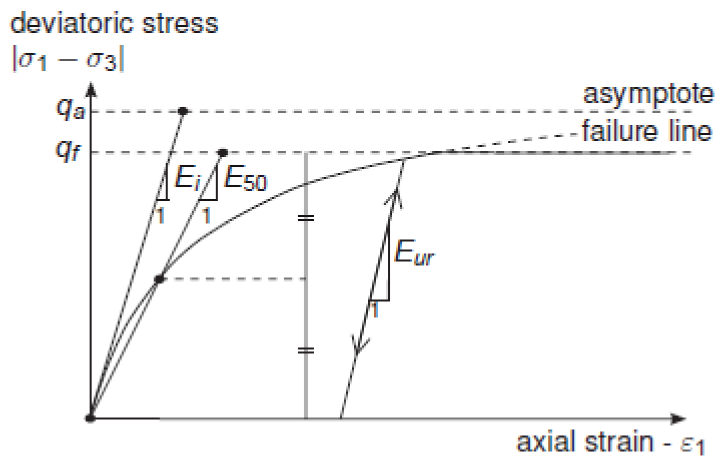

Figure 4.20. Hyperbolic Stress – Strain Relation in Primary for a Standard Drained Triaxial Test

Dilatancy Angle

Dilatation is an occurrence of negative volumetric strains under shear stress. For cohesive soils dilatancy angle depends on the preconsolidation ratio, which was chosen by Truty and Obrzud (2011) as given below:

$$\psi = 0^{\circ} \text{ for NC and LOC} \tag{4.18}$$

$$\psi = \varphi'/6 \text{ for OC} \tag{4.19}$$

$$\psi = \varphi'/3 \text{ for HOC} \tag{4.20}$$

Dilatation is seen in very dense sand and its value is equal to 1/3 of the peak friction angle.

$$\psi = \varphi'/3 \text{ for Dense Sand} \tag{4.21}$$

4.5.4.2 The Selected Soil Parameters for HSMSSS

Soil parameters which are obtained from field and laboratory works are given below for HS-Small Stiffness Material Model.

Table 4.13. The Selected Soil Parameters for HSMSSS

Letter	E_{oed}^{ref} (kPa)	E_{50}^{ref} (kPa)	E_{ur}^{ref} (kPa)	G_{o}^{ref} (kPa)	c' (kPa)	φ' (o)	Ψ (o)	$\gamma_{0.7}$	υ_{ur}	p_{ref} (kPa)	m	R_f
Silty Clay 1	14000	14000	42000	74000	4	24	0	2.6×10^{-4}	0.2	100	0.5	0.9
Silty Sand 1	12600	12600	37800	100000	1	33	0	1.4×10^{-4}	0.2	100	0.5	0.9
Silty Clay 2	8000	8000	24000	77000	5	26	0	2.3×10^{-4}	0.2	100	0.5	0.9
Silty Sand 4	15500	15500	46500	77000	4	35	0	2.1×10^{-4}	0.2	100	0.5	0.9
Silty Clay 4	8500	8500	25000	85000	7	30	0	2.6×10^{-4}	0.2	100	0.5	0.9
Sandy Silt 4	12000	12000	36000	104000	6	32	0	3.5×10^{-4}	0.2	100	0.5	0.9
Fill Material	155000	155000	155000	465000	0	40	0	2.6×10^{-4}	0.2	100	0.5	0.9

G_0: Reference shear modulus at very small strain , $\gamma_{0.7}$: Threshold shear strain , E_{50}^{ref}: Secant stiffness in standard drained triaxial test , E_{oed}^{ref}: Tangent stiffness for primary oedometer loading , E_{ur}^{ref}: Unloading / reloading stiffness from drained triaxial test , υ_{ur}: Poisson's ratio for unloading-reloading, m: Power for stress-level dependency of stiffness c: Cohesion , φ: Friction angle , ψ: Dilatancy angle, R_f : Failure Ratio

4.5.5 Modelling of Project in Plaxis 3D for Settlement Analysis

In this part of chapter 4, modelling of the project in Plaxis 3D is given with seven subtitles as properties of the project, the geometry of project, borehole of project, soils of project, structural elements and projects loads, mesh generation and staged construction.

Properties of the Project

In project properties option, length and force units can be chosen as English system of units and the SI (Systems International) system of units. Furthermore, earth gravity and unit weight of water are defined manually and contour limits can be defined manually as it is shown in Figure 4.21.

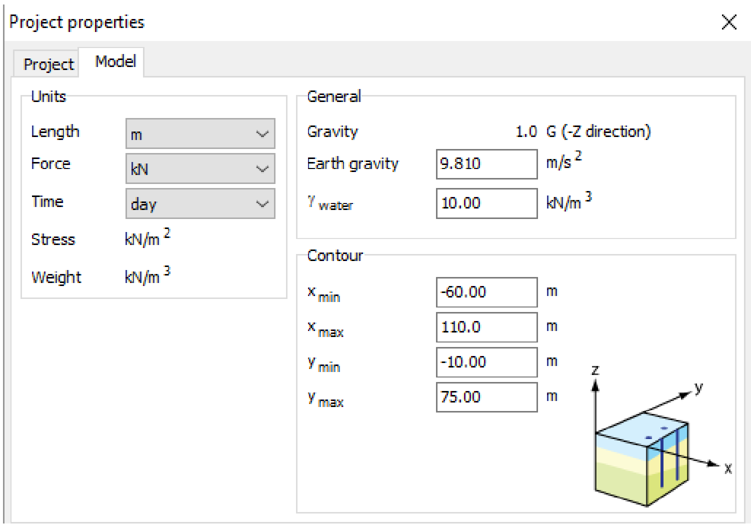

Figure 4.21. Properties of Project

Geometry of the Project

Points, surfaces, volumes, and soil volumes can be generated in Plaxis 3D. In this project points were used as points loads, volumes were used as excavation and fill volume, soil volumes used as soil layers as it is shown in Figure 4.22.

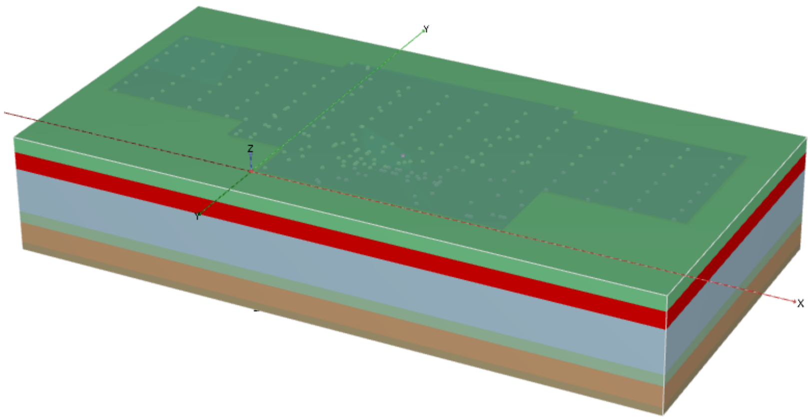

Figure 4.22. Geometry of the Project

Borehole of Project

The instrumentation system for observation of settlement was placed under the supports which were exposed to carry maximum service loads of around 1600 kN, and borehole SK6 was drilled in the same area where the service loads were maximum. As a result, SK6 borehole data was used to define the soil layers defined as it is shown in Figure 4.23.

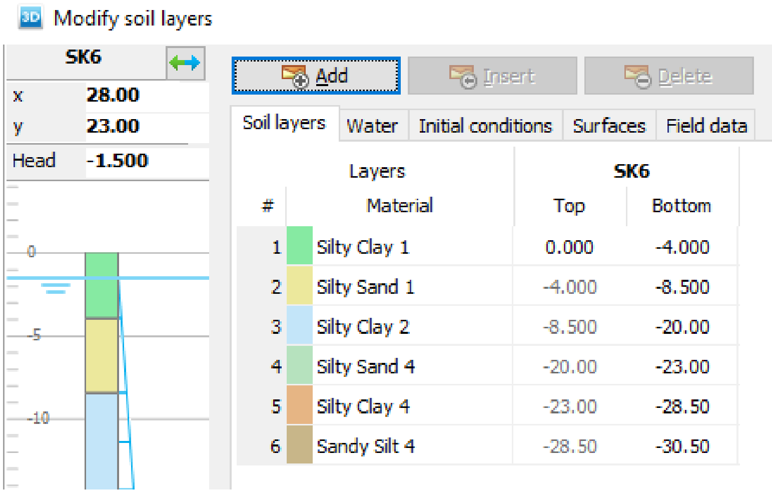

Figure 4.23. Defining Borehole SK6

Soils of Project

Soil layers were defined as Silty Clay 1, Silty Sand 1, Silty Clay 2, Silty Sand 4, Silty Clay4, Sandy Silt 4 and Fill Material. Material model is HSMSSS with drainage type. In parameter option, selected soil parameters given in part 4.5.4 were defined for all soil types as it was shown in Figure 4.24.

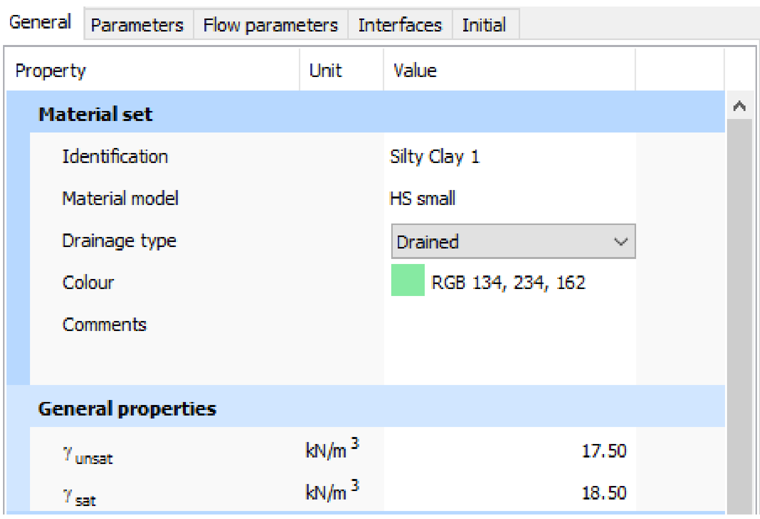

Figure 4.24. Defining Soil Types and Parameters

Structural Elements and Project Loads

In the model, plate and points are used as structural element. The plate is defined as a foundation with concrete properties and points are defined as point loads. Moreover, there were 217 points loads, its details were given in 4.3.2, as it is shown in Figure 4.25.

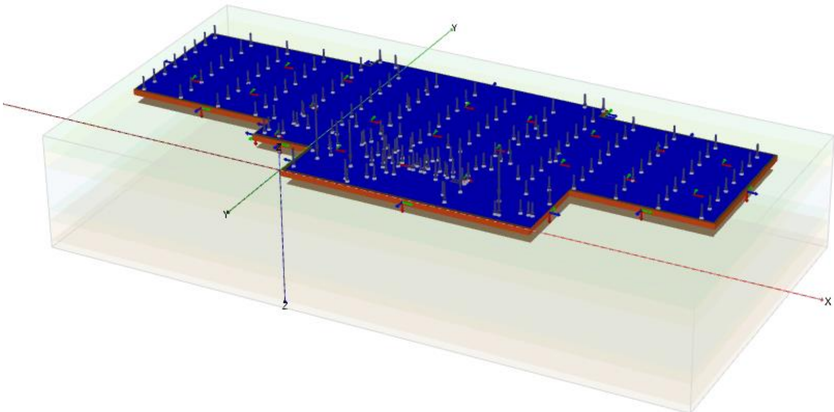

Figure 4.25. Structural Elements and Project Loads

Mesh Generation

37556 soil elements were obtained in mesh generation as it was shown in Figure 4.26. Element distribution can be chosen from very coarse to very fine. The very fine mesh was selected for analysis. Although calculation time is increased with very fine mesh, more accurate analyses were performed.

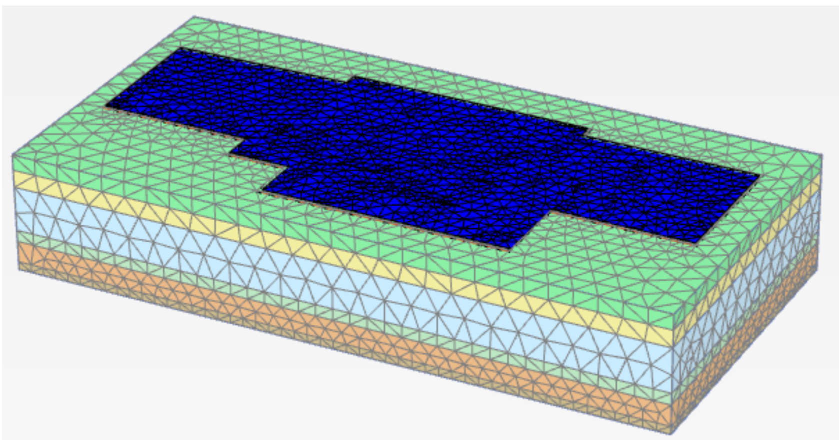

Figure 4.26. Very Fine Mesh Generation of Project

Staged Construction

In the project four steps were applied as application of fill, settlement due to fill, application of foundation load and application of service loads. In the application of fill stage a 0.5 m height soil was excavated as it is shown in Figure 4.27.

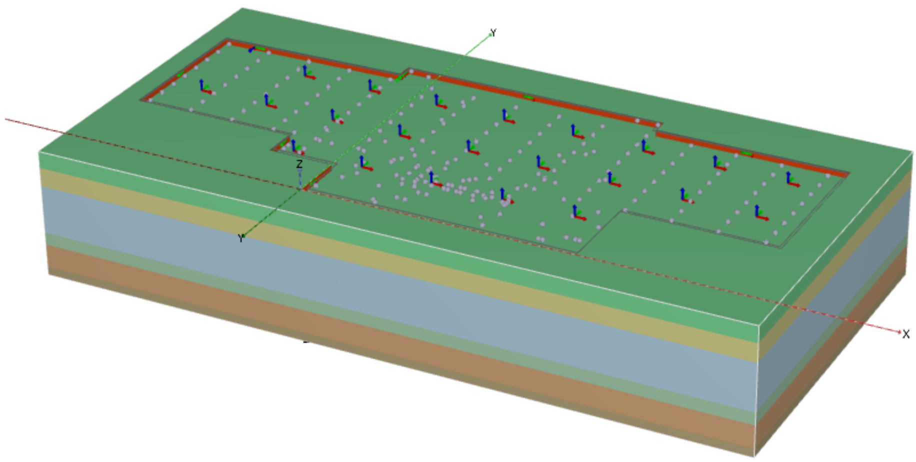

Figure 4.27. The Application Of Fill Stage

Then, a 1.5m height high qualified fill material was placed in the first stage (Figure 4.27).

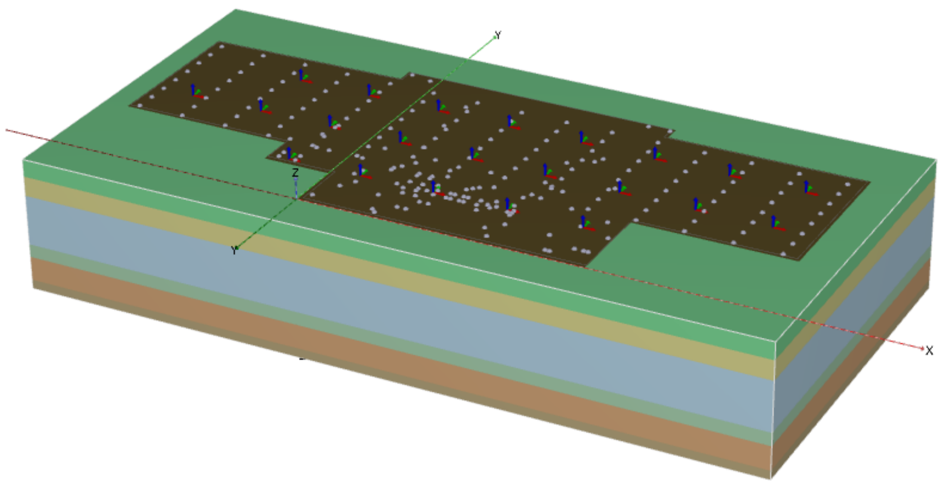

Figure 4.28. High Qualified Fill Material Application

In the application of foundation's loads, a 90 cm height foundation was constructed on the high qualified fill material as it was shown in Figure 4.39.

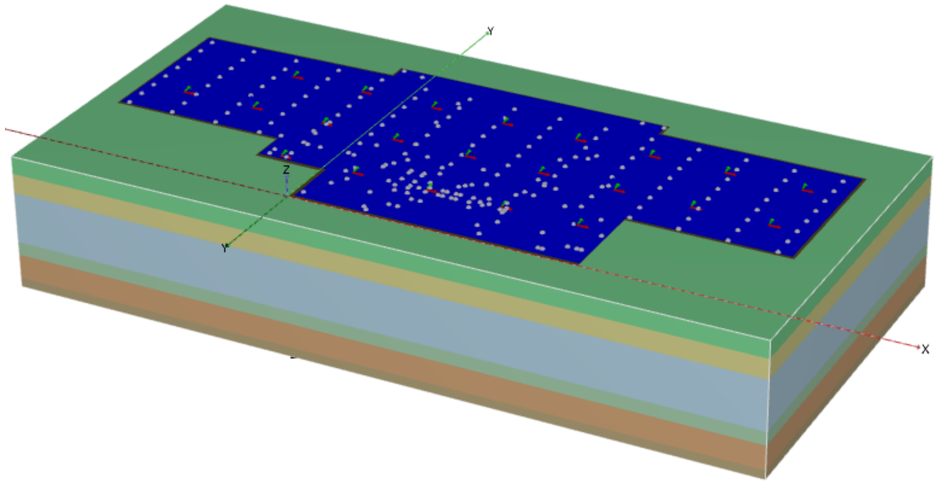

Figure 4.29. Construction of Foundation

In the application of service loads stage, the service loads were generated on the foundation. (Figure 4.30)

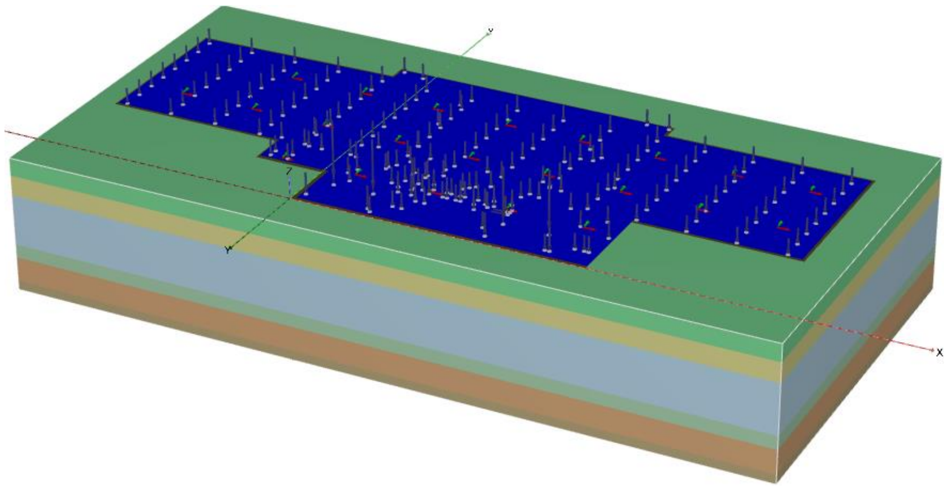

Figure 4.30. Application of Service Loads

CHAPTER 5

SETTLEMENT ANALYSES RESULTS AND DISCUSSION

5.1 Introduction

In this chapter, the settlement results of 1-D stress – strain relation and numerical continuum model were given for all stages of the project; namely, settlement due to fill material, settlement due to foundation weight, settlement due to service loads. 1D total settlement analyses were performed separately by using stiffness parameters based on in-situ tests and consolidation tests for cohesive layers. Mohr Coulomb Material Model and Hardening Soil Model with Small Strain Stiffness were used for numerical analyses. For each stages four analyses were performed and results were compared with measured field settlement data. Differential settlement value was obtained with HSMSSS. Moreover, stress increment levels and settlement relation with traditional methods (Boussinesq, Westergaard and 2:1) were compared with the 3D numerical continuum model. Finally, settlement and stress strain modulus relation for cohesive layer was presented.

5.2 Settlement Due to Fill Material

At the site, high qualified fill materials were compacted at 30 cm intervals and total height of fill layer was 1.5 m. Application of fill material increased stresses on the soil; thus, application of fill material caused settlement. All settlement analyses results were compared in Figure 5.1. As a result, maximum settlement value was 3.5 cm that was obtained from 1 D total settlement analysis based on consolidation test results (1D TSBCT). Second high value was 1.8 cm that is obtained from Mohr Coulomb Model. 1D total settlement analysis based on in-situ test results (1D TSBIT) gave settlement value as 0.85 cm and minimum settlement value was 0.35 cm in HS-Small Strain Stiffness Model. It is clear that maximum settlement obtained from 1D TSBCT and minimum settlement from the HSMSSS. The measurement system started to read settlement value after this application so that which model gave accurate result was not known. It is clearly seen that though TSBIT has not solved with numerical method, it gave more accurate result with HSMSSS then Mohr Coulomb Model.

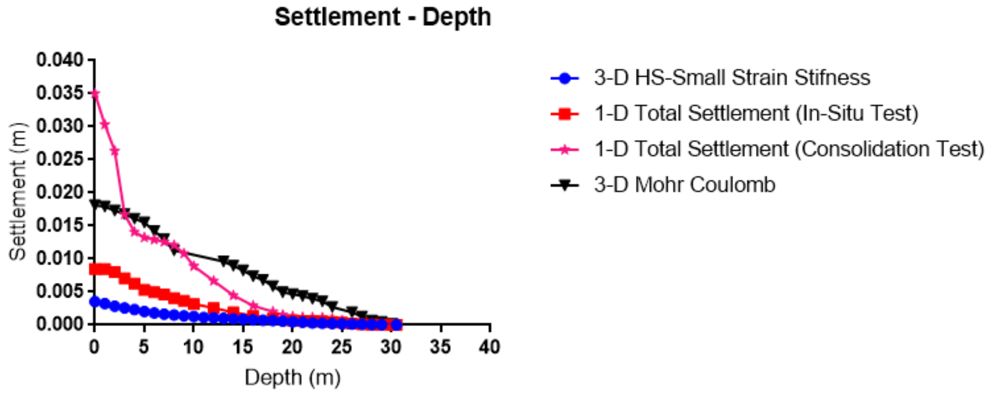

Figure 5.1. Settlement Values Due to Application of Fill Material

5.3 Settlement Due to Foundation Weight

In the site, foundation thickness was 90 cm under the turbine generator region, which is the most critical part of project for differential settlement criteria. Settlement analyses results were given in Figure 5.2. As a result, maximum total settlement value was 6.7 cm that was obtained from 1D total settlement analysis based on consolidation test results (1D TSBCT). Second high total value was 0.53 cm that was obtained from Mohr Coulomb Model. 1D total settlement analysis based on in-situ test results (1D TSBIT) gave total settlement value as 0.020 m and minimum total settlement value was 0.014 m in Hardening Soil Model with Small Strain Stiffness Model. The measured settlement was 0.008 m for this stage and minimum settlement value was 0.0105 in HSMSSS. Similar to the previous stage, 1D TSBIT gave a more accurate result with HSMSSS.

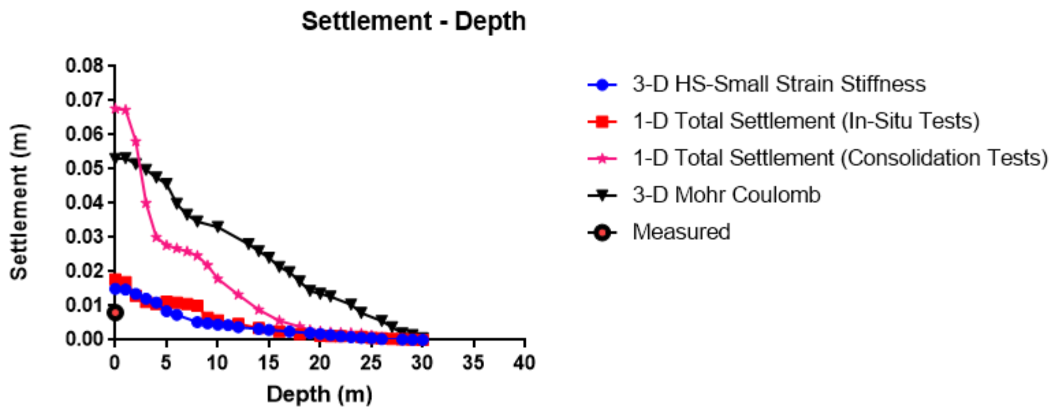

Figure 5.2. Settlement Values Due to Foundation Weight

5.4 Settlement Due to Service Loads

In the project, foundation thickness is 90 cm under the turbine generator region, which is the most critical part of project for differential settlement criteria. Settlement analyses results are given in Figure 5.3. As a result, the maximum total settlement value was 0.134 m obtained from 1 D total settlement analysis based on consolidation test results (1D TSBCT). Second high total value was 0.055 m obtained from Mohr Coulomb Model. Total settlement analysis based on in-situ test results (1D TSBIT) gave total settlement value as 0.033 m and minimum total settlement value was 0.022 m in Hardening Soil Model with Small Strain Stiffness. The measured total settlement was 0.018 m. The measured settlement was 0.01 m for this stage and minimum settlement value was 0.008 m in HSMSSS. Similarly, previous stage 1D TSBIT gave more accurate result with HSMSSS. Difference between measured settlement value and HSMSSS was equal to 0.004 m, which is close to equal first settlement value of Hardening Soil Model with Small Strain Stiffness.

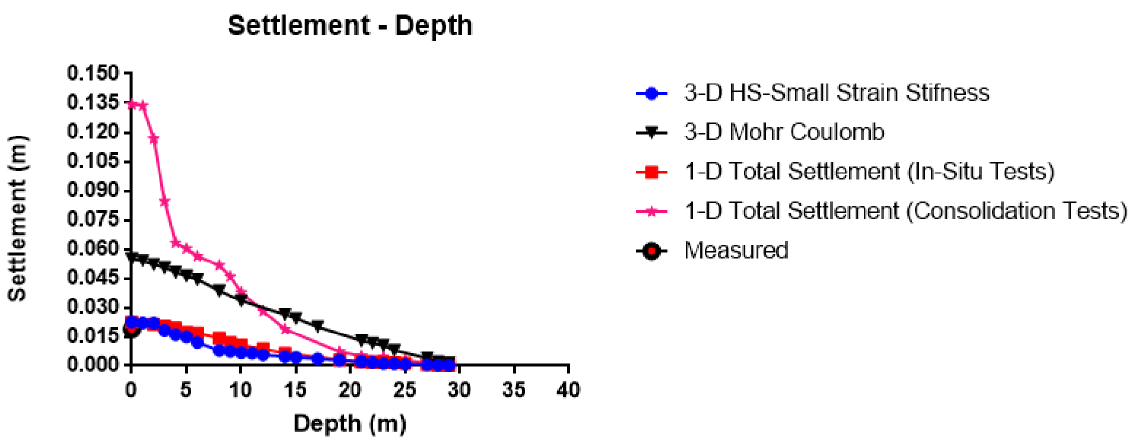

Figure 5.3. Settlement Values Due to Service Loads

The settlement measurement system (Figure 5.4) was set in the turbine area to measure the settlement by time. It was a simple system to measure the settlement during and after the construction of the foundation and the construction of the mechanical equipments. A steel reinforcement fixed into a concrete prism with 40 cm x 40 cm x 15 cm diameters and a plastic pipe isolated the steel from soils for free movement. Top of steel reinforcement was measured until the end of the settlement.

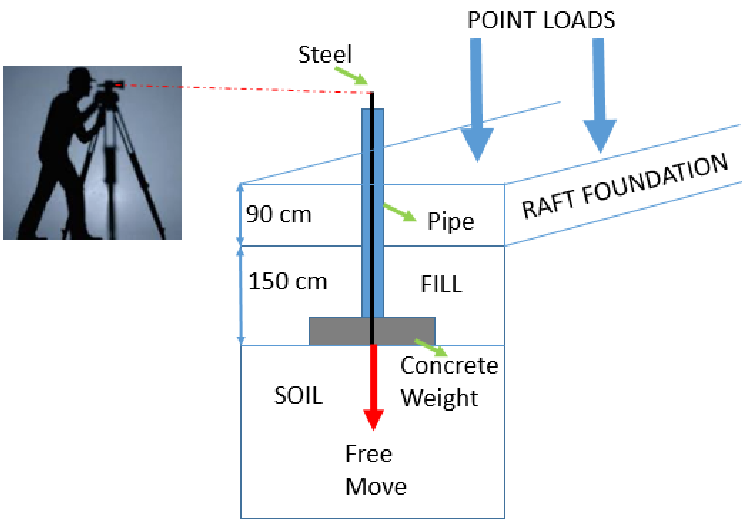

Figure 5.4. The Settlement Measurement System

The settlement has been measured for 8 months. Measured values were given with dates in Table 5.1.

Table 5.1. Construction Application and Measured Settlement by Time

Date	**Construction Application**	**Measured Value**	**Settlement**
11.12.2017		25.802	
12.12.2017	Construction of Foundation	25.799	0.003 m
11.01.2018	-	25.794	0.008 m
17.01.2018	-	25.794	0.008 m
10.03.2018	Service Loads (Turbine Area)	25.790	0.012 m
16.04.2018	Service Loads (Turbine Area)	25.784	0.014 m
15.05.2018	-	25.785	0.017 m
18.06.2018	-	25.784	0.018 m
13.08.2018	-	25.784	0.018 m

The summary of the settlement values for each stages were given in Table 5.2. Field measurement system started to read settlement after the applying fill material stage but there is an unknown settlement value which is represented by letter of x. Logically, if the first stage of field settlement value is close to HSMSSS, total settlement of foundation almost equal to result of HSMSSS.

Table 5.2. The Settlement Results For Each Stage

Stage	Stage Name	TSBCT	MOHR.C	TSBIT	HS-SMALL	FIELD DATA
#		m	m	m	m	m
1	Fill Material	0.035	0.018	0.0085	0.0035	x
2	Found. Weight	0.067	0.053	0.020	0.014	0.008 +x
3	Service Load	0.134	0.055	0.033	0.022	0.018 +x

5.5 Stress Increment Level and Settlement

Raft foundation (which is used to decrease differential settlement) dimensions are higher than strip footing; on the other hand, last stress increment level is increased under same stress because Boussinesq's, Westergaard's and 2:1 method depends on length and width of the foundation. In Table 5.3, settlement and last stress increment level were calculated using all given methods. It was seen that 2:1 method gave a more accurate result with 10 m width and 20 m length in dimensions than Boussinesq's and Westergaard's methods. Last accurate stress increment level obtained from the numerical continuum model was 30.5 m.

Table 5.3. Stress Increment Level and Settlement by 2:1 Method, Boussinesq and Westergad Methods

Length (m)	Width (m)	2:1 METHOD		BOUSSINESQ		WESTERGAARD	
		Stress Inc. Level (m)	Settlement (m)	Stress Inc. Level (m)	Settlement (m)	Stress Inc. Level (m)	Settlement (m)
55	27	62	0.069	63	0.092	62	0.078
40	20	52	0.057	53	0.076	53	0.065
30	15	42	0.047	45	0.063	43	0.053
20	10	30.5	0.033	35	0.046	31.5	0.039

Another important point is that there are lots of non-uniform loading area and these distributions were obtained with the help of numerical continuum model which were given in Figure 5.5. The contours in the figure shows per unit load value.

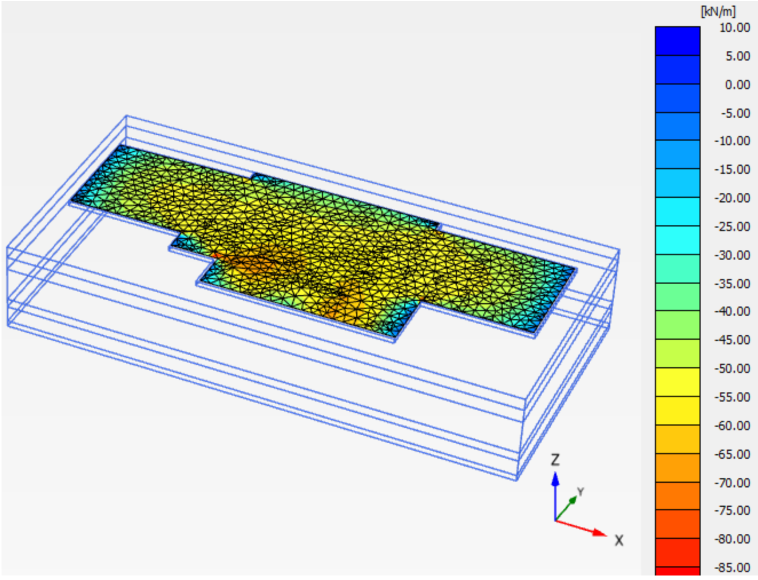

Figure 5.5. Non Uniform Stress Distribution on Project Area

5.6 Differential Settlements' Results

Differential settlement values were given in Figure 5.6. Maximum differential settlement value is 0.43×10^{-3} m for 50 m distance in Hardening Soil Model with Small Strain Stiffness Model. Differential settlement ratio is 0.86/1000 and this value is smaller than 1/1000, which is the limit value of differential settlement criteria. Mohr Coulomb Model and HSMSSS give the differential settlement values directly because these models used soil structure interaction; however, 1 D total settlement analyses cannot include soil structure interaction.

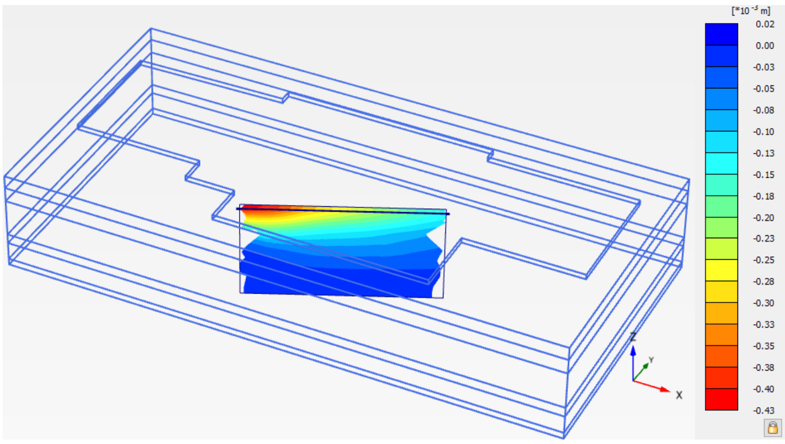

Figure 5.6. Differential Settlement Results in HS-Small Strain Stiffness Model

5.7 Drained Oedometric Stress Strain Modulus for Clay Layer

For cohesive soil obtaining drained stress strain modulus is complicated because in-situ tests are quick but cohesive soil needs time to dissipate water; otherwise, undrained condition affect the test results. Although consolidation tests are suitable for drained stiffness parameters, generally obtained stiffness parameters value are lower than actual value due to difficulties in obtaining undisturbed samples, working on very small volume of soil particles and operator errors. When pressuremeter test results were taken into consideration as undrained stress – strain modulus, these values are four times greater than consolidation drained stress – strain modulus but for normally consolidated medium clays undrained / drained stress – strain modulus ratio is expected to be in the range of 1.07 to 1.34. As a result, cone penetration tests results were used to make compression. Oedometric stress – strain modulus was obtained from multiplying cone resistance with α factor for cohesive soil Drained and undrained oedometric stress strain modulus for silty clay layers were given in Table 5.4.

Table 5.4. Undrained and Drained Oedometric Stress Strain Modulus for Silty Clay

Clay Type	**Cone Penetration Test**			**Consolidation Test**	**Pressuremeter Test**
	E_{oed} (α=5) (kPa)	**E_{oed} (α=6) (kPa)**	**E_{oed} (α=7) (kPa)**	**E_{oed} (kPa)**	**E_u (kPa)**
Silty Clay 1	5821	6985	8150	1660	6875
Silty Clay 2	6428	7714	9000	3200	8190
Silty Clay 3	7000	8400	9800	4166	9570
Silty Clay 4	8928	10714	12500	5500	11900

The α factor ranges from 2 to 12 and it is not consensus. Settlement results for each oedometric stress – strain modulus and maximum – minimum value of clay's undrained / drained stress – strain modulus ratio were given in Table 5.5. Settlement analysis were performed HSMSSS and the α factor was taken as 7 to be compatible with undrained stress – strain modulus.

Table 5.5. Settlement Value for Each Oedometric Stress – Strain Modulus

Oedometric Modulus	**Obtained From**	**Material Model**	**Settlement (m)**	**(E_u/E) min**	**(E_u/E) max**
E_{oed} (α=5)	CPT	HS-Small	0.035	1.54	1.66
E_{oed} (α=6)	CPT	HS-Small	0.027	1.28	1.38
E_{oed} (α=7)	CPT	HS-Small	0.022	1.10	1.19
E_{oed}	Consolidation T.	HS-Small	0.065	2,16	4,14

CHAPTER 6

CONCLUSIONS

6.1. Summary of Findings

The aim of this study was to provide how to evaluate selection of representative soil models, determination of soil parameters, analyzing of stress distribution and obtaining effective depth level of soils to obtain accurate settlement results for geothermal power plant foundation where total settlement and differential settlement criteria are so sensitive. The most important conclusions are summarized as below:

- 1D Stress – Strain analyses and 3D continuum numerical analyses can be used for settlement analyzes for multilayer soil profile.
- Hardening Soil Model with Small Strain satisfies a complete theoretical solution, the equilibrium, compatibility, material constitutive behavior and boundary condition. Moreover, hardening mechanism with small strain accurately represents real soil behaviors, which are elastic and plastic strain contribution, yield surfaces and soil strength parameters. As a result, measured settlement value was most compatible with Hardening Soil Model with Small Strain Stiffness.
- Although the Mohr-Coulomb soil model is used to determine a first approximation of soil behavior, it does not represent the stress-dependency in true soil behavior. According to the analysis result, Mohr-Coulomb soil model's total settlement value approximately three times greater than the actual total settlement value so that it should not be preferred to use in the sensitive analysis of settlement.
- If stress distribution of foundation and last stress increment level of soils are obtained correctly, 1D total settlement analyzes based on in-situ test results will give more accurate settlement results than classical calculation method.
- 1D total settlement analyzes based on consolidation test results gave over settlement results due to the lower oedometric modulus.
- Cone Penetration Test was compatible with Standard Penetration Test for cohesionless soil and Cone Penetration Test was compatible with Pressuremeter

Test for cohesive soil to determine soil stiffness parameters. Reasonably, soil stiffness parameters become stronger with increasing depth for each in situ tests.

- In terms of obtaining non-uniform stress distribution, 3D continuum numeric analyses are reasonable without soil structure interaction analyses, actual stress distributions on soils cannot be obtained so that both total settlement and differential settlement values cannot be obtained correctly.
- Length and width of geothermal power plant foundation are increased as compared to spread footing or continuous footing. For that reason, stress increment level in Boussinesq's method, Westergaard's method and 2:1 method were higher than continuum numerical models. As a result, these methods cannot be suggested for such a case situation.
- According to measured settlement value consolidation time of clays is supposed to short with related to the coefficient of consolidation (0.015 – 0.016 cm^2/sec). The reason is that the silt and sand layers that cut the clay layer work as horizontal drainage and shorten the drainage way distance.
- Unit weight of foundation should be specified as subtracting the unit soil weight from the real unit weight of plate because of the fact that the foundation does not occupy any volume and overlaps with the soil elements. More accurate settlement value was obtained with using this criteria in all analyses.
- The geothermal power plant's foundation type depends on the characteristics of soils and structure loads. Particularly shallow foundation type can be used to decrease structure stresses on soils and balance hydrostatic uplift pressure. For these reasons, the shallow foundation was selected for turbine parts of the geothermal power plant to decreasing total and differential settlement.

6.2. Suggestions

Based on the research done in this thesis several recommendations can be formulated for future research. The recommendations for further research are summarized below:

- In this study, analyzes shows that stress strain modulus value from in-situ tests higher than from consolidation tests. It is advised to control this result is valid for the general case.
- Initial shear modulus obtained with using void ratio and mean effective stress but there are lots of correlation in geotechnical literature. It is advised to make comparison between them to find accurate initial shear modulus for cohesive and cohesionless soils.

REFERENCES

Amer, S., Clarke, B. G. F., Gambin, M., & Orr, T. L. L. (1991). The application of pressuremeter test results to foundation design in Europe. *European Regional Technical Committee 4, Pressuremeters*, 1-24

Ameratunga, J., Sivakugan, N., & Das, B. M. (2016). *Correlations of soil and rock properties in geotechnical engineering* (pp. 8-9). Springer.

ASTM, D. (1998). *1586. Test Method for Penetration Test and Split-Barrel Sampling of Soils, 4*.

Becker, D. E., & Moore, I. D. (2006). *Canadian foundation engineering manual*.

Biarez, J., & Hicher, P. Y. (1994). *Elementary mechanics of soil behaviour: saturated remoulded soils*. AA Balkema.

Bjerrum, L. (1963, October). Allowable settlement of structures. In *Proceedings of the 3rd European Conference on Soil Mechanics and Foundation Engineering, Wiesbaden, Germany* (Vol. 2, pp. 135-137).

Bogdanovi_, L. (1973). Settlement of stiff structures (silos) founded on soft soil with low penetration resistance. *Transactions*.

Bowles, L. E. (1996). *Foundation analysis and design*. McGraw-hill.

Briaud, J. L. (1992). *The pressuremeter*. AA Balkema.

Brinkgreve, R. B. J. (2017). *A. Laera PLAXIS bv*, The Netherlands.

Budhu, M. (2010). *Soil Mechanics and Foundations*, John Wiley & Sons.

Casagrande, A. (1936). The determination of pre-consolidation load and it's practical significance. *In Proc. Int. Conf. Soil Mech. Found. Eng. Cambridge, Mass., 1936* (Vol. 3, p. 60).

Darendeli, M. B., & Stokoe, K. H. (2001). II. (2001). “Development of a new family of normalized modulus reduction and material damping curves*”. Geotechnical Engineering Report.*

Das, B. M. (2013). *Advanced soil mechanics*. Crc Press.

Das, B., & Sivakugan, N. (2007). Settlements of shallow foundations on granular soil an overview. *International Journal of Geotechnical Engineering*, *1*(1), 19-29.

Davis, E. H., & Poulos, H. G. (1968). The use of elastic theory for settlement prediction under three-dimensional conditions. *Geotechnique*, *18*(1), 67-91.

DeBeer, E. E. (1974). Interpretation of the results of static penetration tests. In *Group IV Report: European Symp. on Penetration Testing*.

Dos Santos, J. A., & Correia, A. G. (2001). Reference threshold shear strain of soil. Its application to obtain a unique strain-dependent shear modulus curve for soil. In *Proceedings of the International Conference on Soil Mechanics and Geotechnical Engineering (Vol. 1, pp. 267-270).* AA BALKEMA PUBLISHERS.

Erol, A. O., & Çekinmez, Z. (2014). *Geoteknik mühendisliğinde saha deneyleri*. Yüksel Proje Yayınları.

Kim, T. H., Kim, K. H., & Choi, Y. C. (2015). Assessment of angular distortion of structures adjacent to a road embankment site. *Measurement*, 74, 268-277.

Kulhawy, F. H., & Mayne, P. W. (1990). *Manual on estimating soil properties for foundation design* (No. EPRI-EL-6800). Electric Power Research Inst., Palo Alto, CA (USA); Cornell Univ., Ithaca, NY (USA). Geotechnical Engineering Group.

Likos, W. J. (2016). *Consolidation GLE/CEE 330 Lecture Notes Soil Mechanics,* [PowerPoint slides]. Retrieved from https://slideplayer.com/slide/10533550

Lutenegger, A. J., & DeGroot, D. J. (1995). *Settlement of shallow foundations on granular soils*. University of Massachusetts Transportation Center.

Mair, R. J., & Wood, D. M. (1987). Pressuremeter testing: methods and interpretation. Construction Industry Research and Information Association.

Mayne, P. W., & Poulos, H. G. (1999). Approximate displacement influence factors for elastic shallow foundations. *Journal of Geotechnical and Geoenvironmental Engineering*, *125*(6), 453-460/

Meyerhof, G. G. (1956). Penetration tests and bearing capacity of cohesionless soils. *Journal of the Soil Mechanics and Foundations Division, 82(1), 1-19.*

Monnet, J. (2015). *In Situ Tests in Geotechnical Engineering*. John Wiley & Sons.

Peck, R. B., Hanson, W. E., & Thornburn, T. H. (1974). *Foundation engineering (Vol.10)*. New York: Wiley.

Potts, D. M., Zdravkovic, L., & Zdravković, L. (2001). *Finite element analysis in geotechnical engineering: application (Vol. 2).* Thomas Telford.

Robertson, P. K., & Cabal, K. L. (2012). Guide to Cone Penetration Testing, Greg Drilling & Testing. *INC. Corporate Headquarters, Signal Hill, California*.

Schmertmann, J. H., Hartman, J. P., & Brown, P. R. (1978). Improved strain influence factor diagrams. *Journal of Geotechnical and Geoenvironmental Engineering*, *104* (Tech Note).

Schnaid, F. (2009). *In Situ Testing in Geomechanics*. London: Taylor and Francis Group.

Sınıflama, S., & Kuralları, A. (1986). Türkiye Stratigrafi Komitesi, MTA yayını, 28s.

Smith, I. (2014). *Smith's elements of soil mechanics*. John Wiley & Sons.

Standard, B. (1990). British Standard 1377, Methods of Test for Soils for Civil Engineering Purposes. British Standard Institution, London.

Terzaghi, K. (1944). Theoretical soil mechanics. Chapman and Hali, Limited John Wiler and Sons, Inc; New York.

Terzaghi, K., Peck, R. B., & Mesri, G. (1996). *Soil mechanics in engineering practice*. John Wiley & Sons.

Timoshenko, S., Timoshenko, S., & Goodier, J. N. (1951). *Theory of Elasticity, by S. Timoshenko and JN Goodier*. McGraw-Hill book Company.

Townsend, F. C., Anderson, J. B., & Landy, R. (2001). *Evaluation of FEM engineering parameters from insitu tests* (No. Report no. RPWO-14).

Trofimenkov, J. G. (1974). Penetration Test in URSS-State-of the Art Report. In EUROPEAN SYMPOSIUM ON PENETRATION TESTING (Vol. 1, No. 1974, pp. 147-154).

Truty, A., & Obrzud, R. (2011). *The Hardening soil model–a practical guidebook*. Zace Services Ltd, Software engineering. Lausanne.

Vucetic, M., & Dobry, R. (1991). *Effect of soil plasticity on cyclic response. Journal of geotechnical engineering, 117(1), 89-107.*

Webb, D. L. (1970). *Settlement of structures on deep alluvial sandy sediments in Durban, South Africa.* Paper presented at The British Geotechnical Society Conference on In-Situ Investigations in Soils and Rocks, (pp. 181-8).

APPENDIX A1

BOREHOLE LOGS

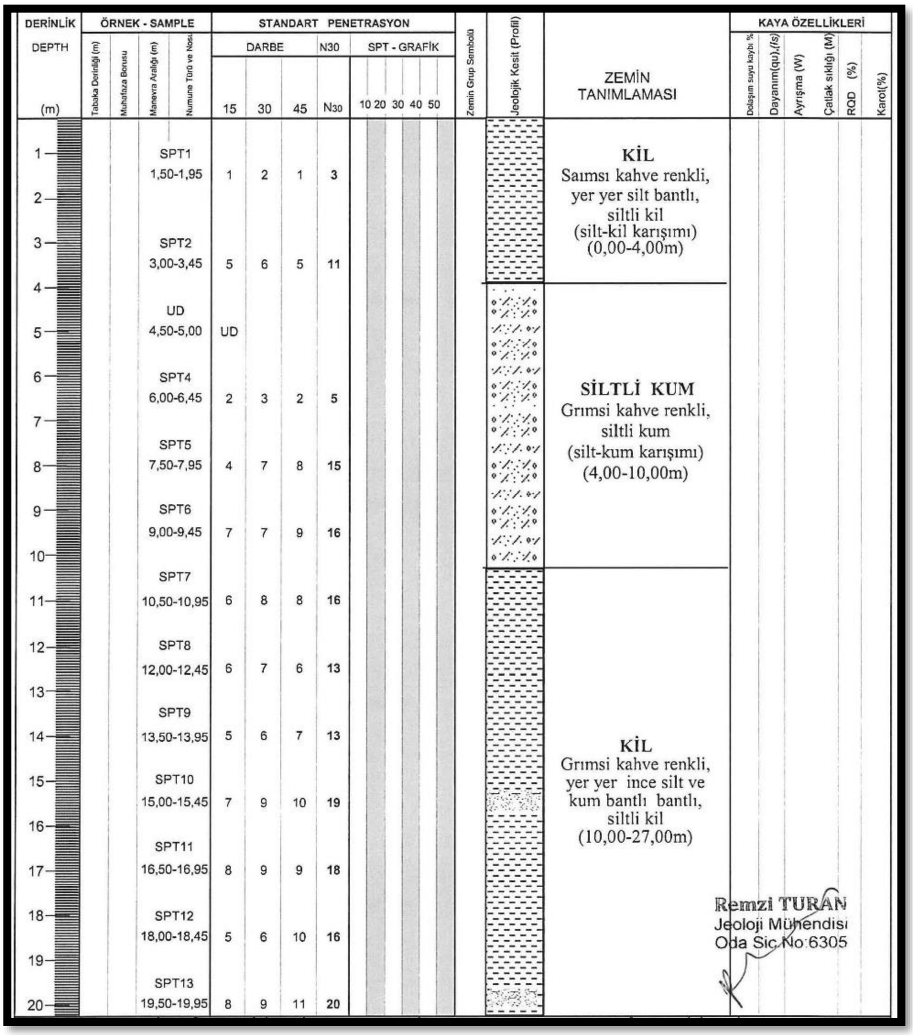

Figure A1.1. Log of Borehole SK 1 from 0 m to 20 m

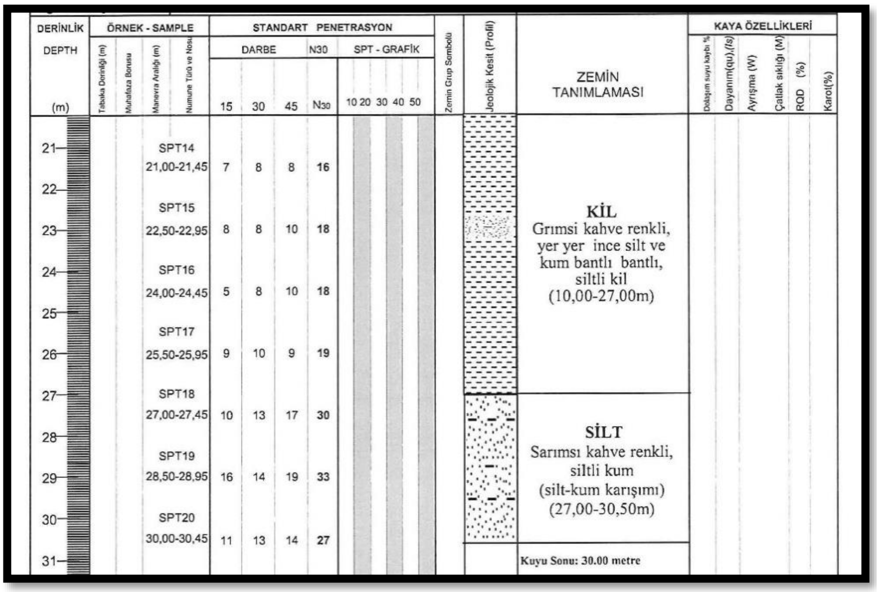

Figure A1.2. Log of Borehole SK 1 from 20 m to 30 m

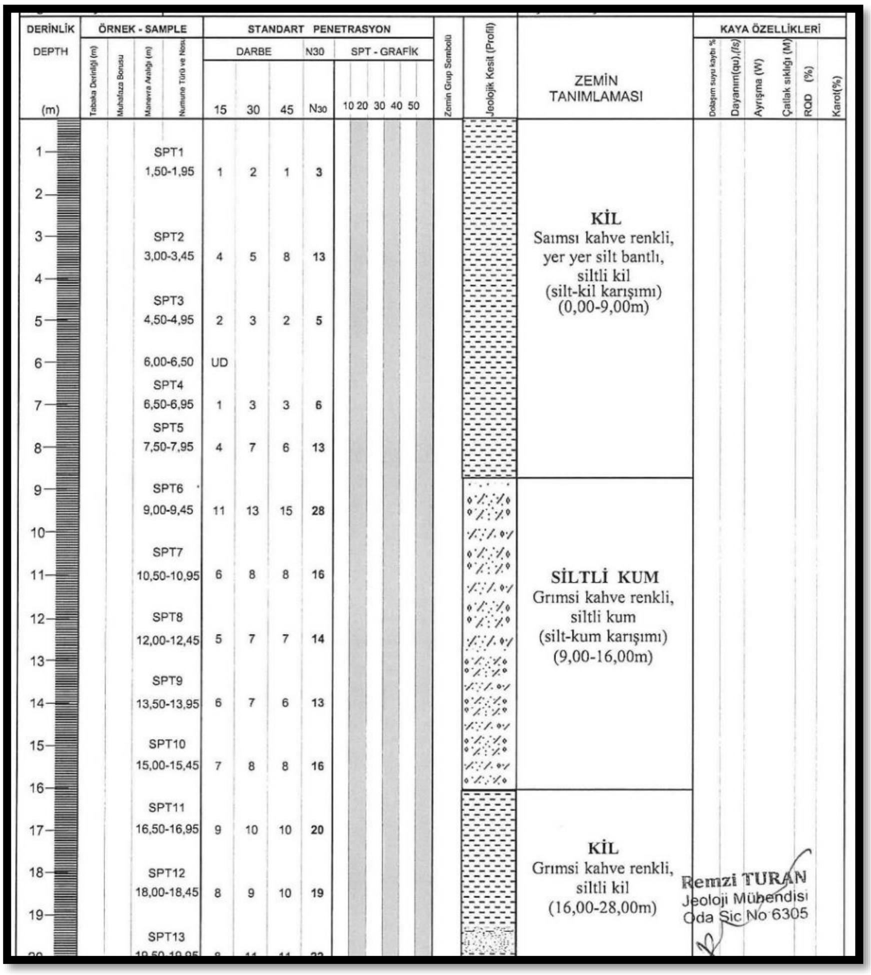

Figure A1.3. Log of Borehole SK 2 from 0 m to 20 m

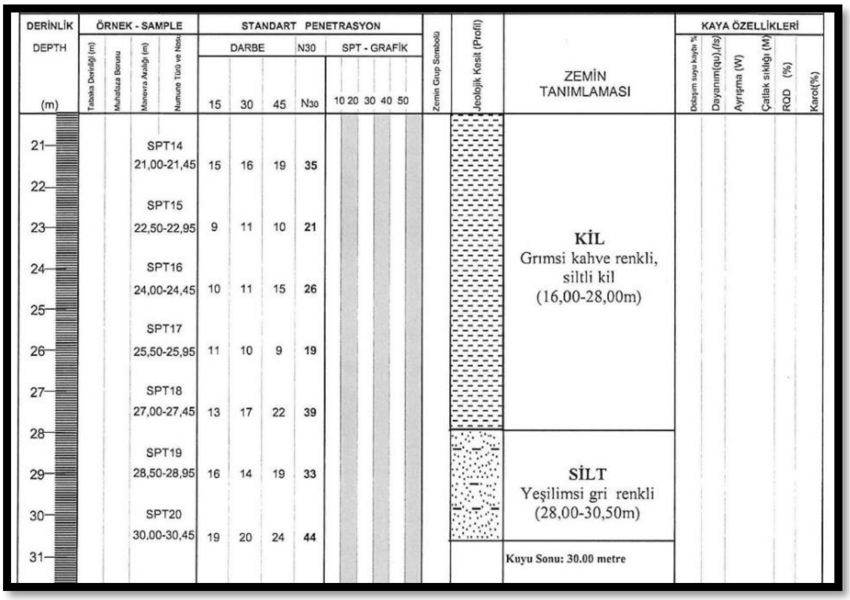

Figure A1.4. Log of Borehole SK 2 from 20 m to 30 m

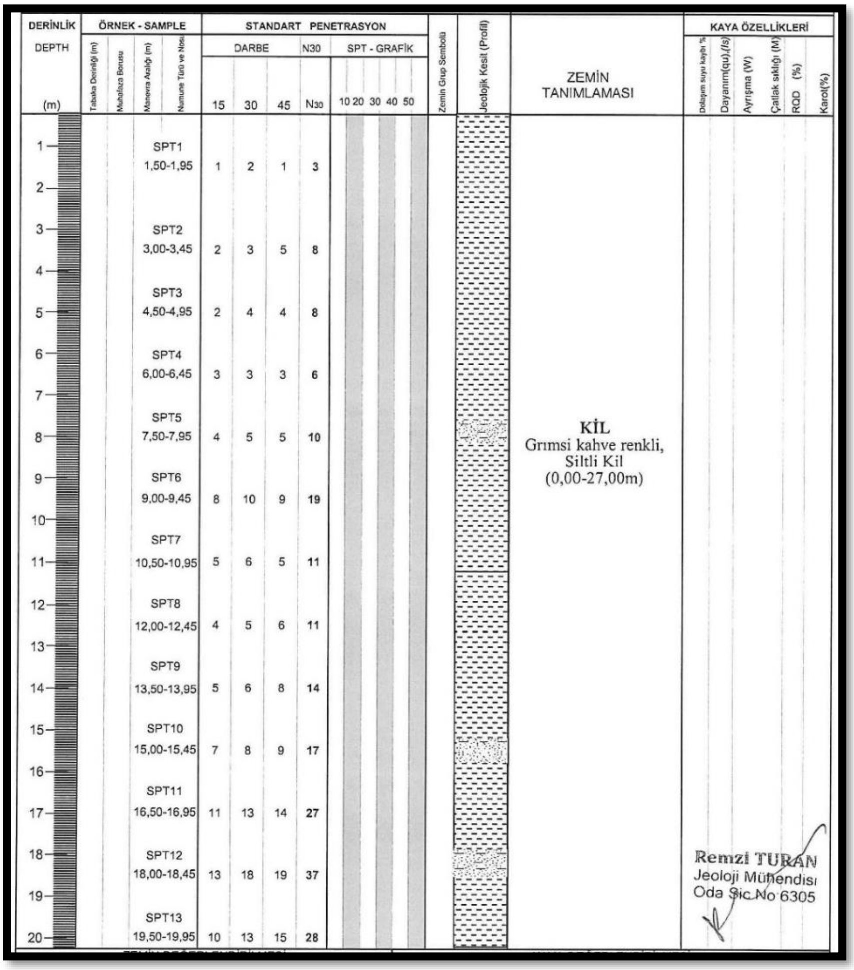

Figure A1.5. Log of Borehole SK 3 from 0 m to 20 m

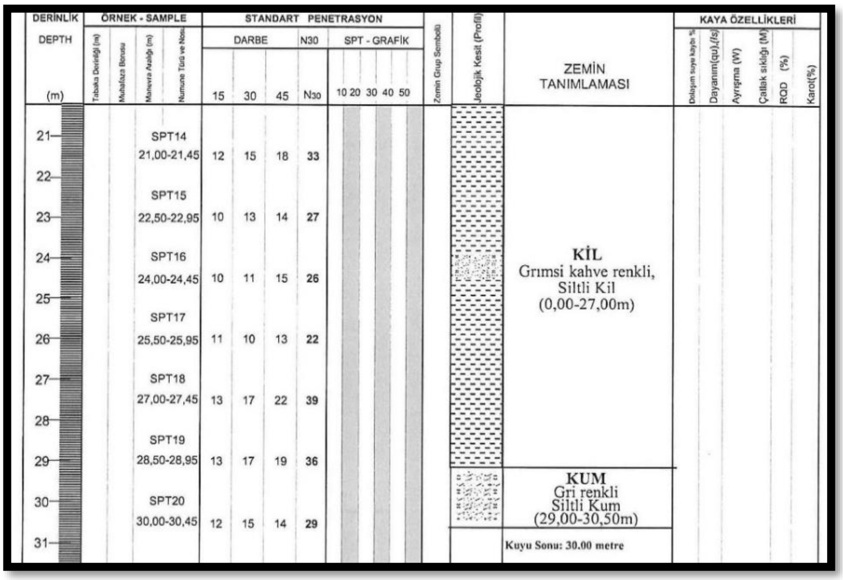

Figure A1.6. Log of Borehole SK 3 from 20 m to 30 m

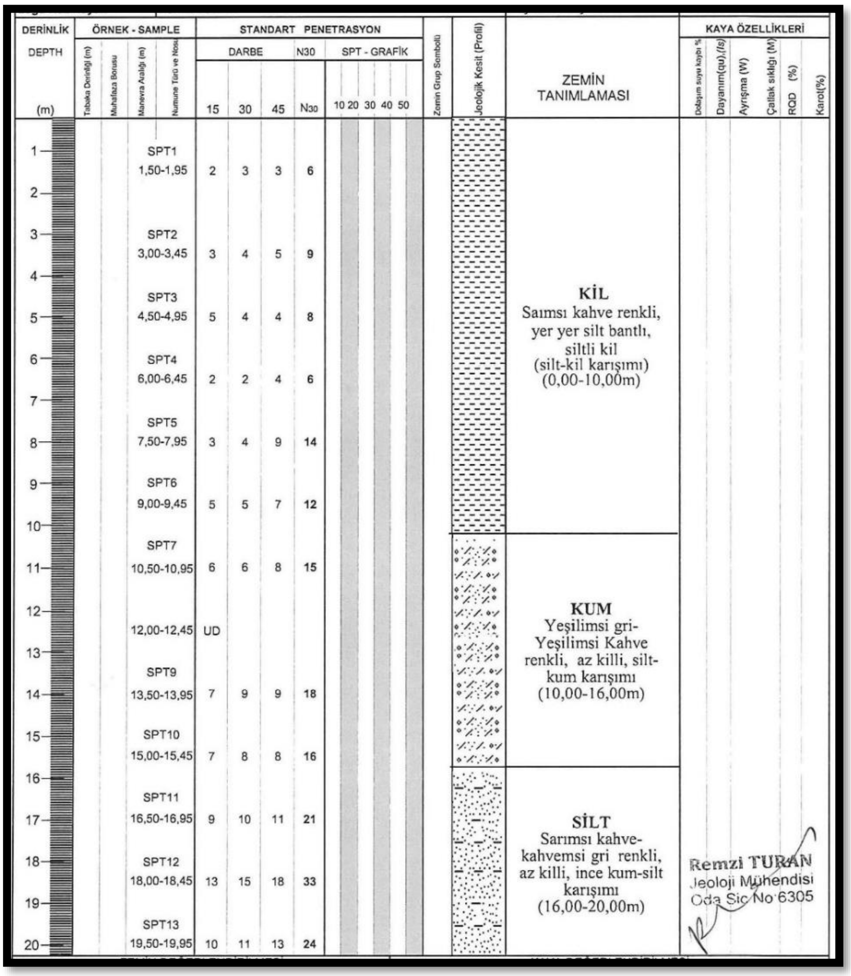

Figure A1.7. Log of Borehole SK 4 from 0 m to 20 m

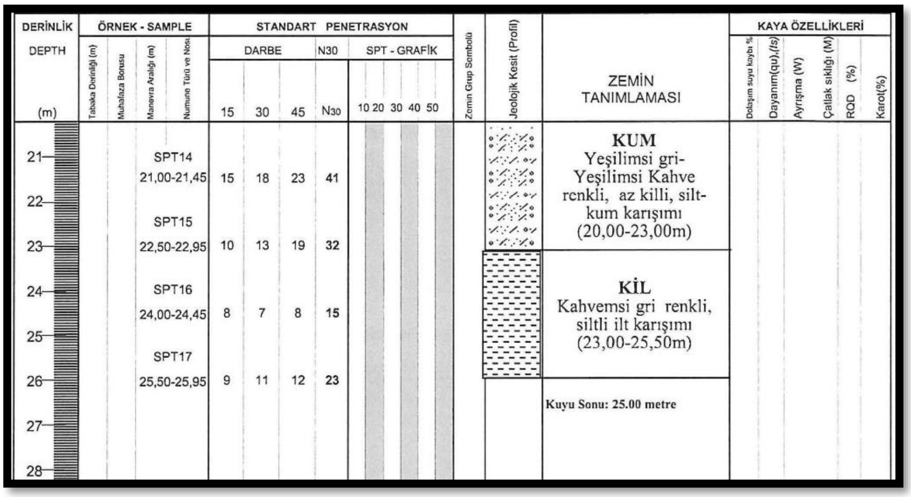

ÖRNEK - SAMPLE		DARBE 15	DARBE 30	DARBE 45	N30
SPT14	21,00-21,45	15	18	23	41
SPT15	22,50-22,95	10	13	19	32
SPT16	24,00-24,45	8	7	8	15
SPT17	25,50-25,95	9	11	12	23

Figure A1.8. Log of Borehole SK 4 from 20 m to 25.5 m

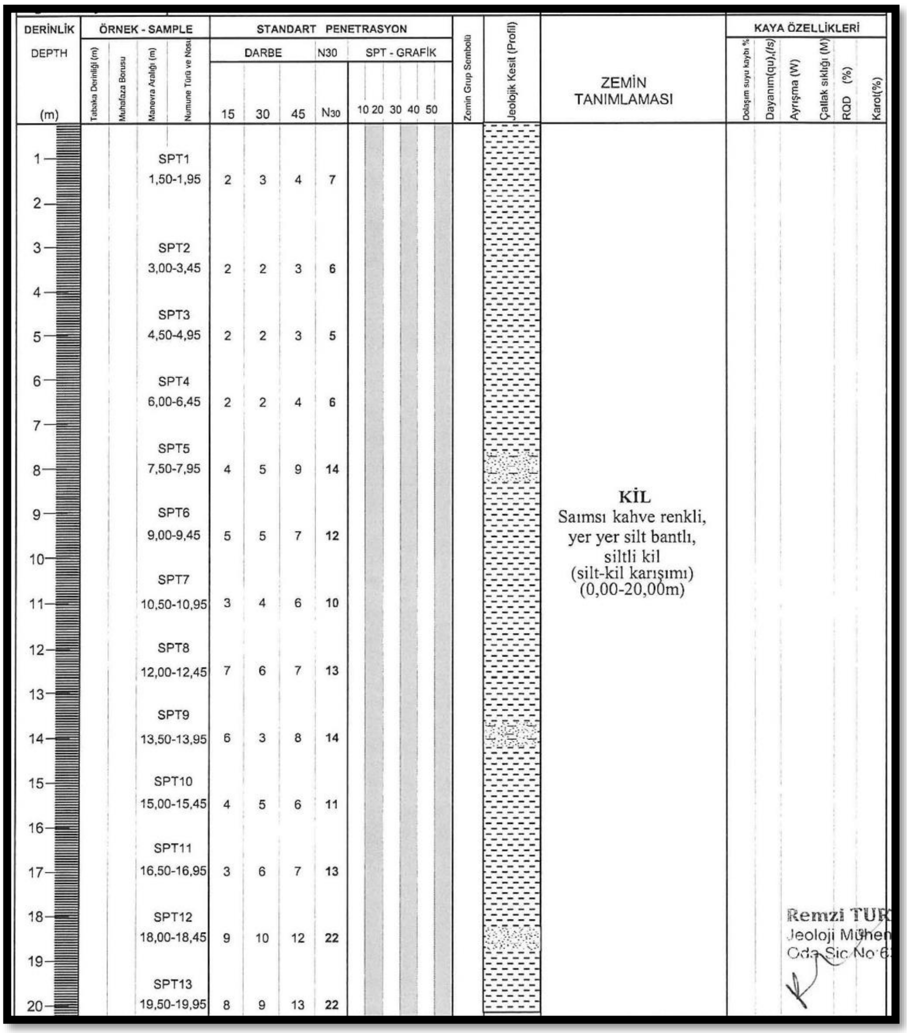

ÖRNEK - SAMPLE		DARBE 15	DARBE 30	DARBE 45	N30
SPT1	1,50-1,95	2	3	4	7
SPT2	3,00-3,45	2	2	3	6
SPT3	4,50-4,95	2	2	3	5
SPT4	6,00-6,45	2	2	4	6
SPT5	7,50-7,95	4	5	9	14
SPT6	9,00-9,45	5	5	7	12
SPT7	10,50-10,95	3	4	6	10
SPT8	12,00-12,45	7	6	7	13
SPT9	13,50-13,95	6	3	8	14
SPT10	15,00-15,45	4	5	6	11
SPT11	16,50-16,95	3	6	7	13
SPT12	18,00-18,45	9	10	12	22
SPT13	19,50-19,95	8	9	13	22

Figure A1.9. Log of Borehole SK 5 from 0 m to 20 m

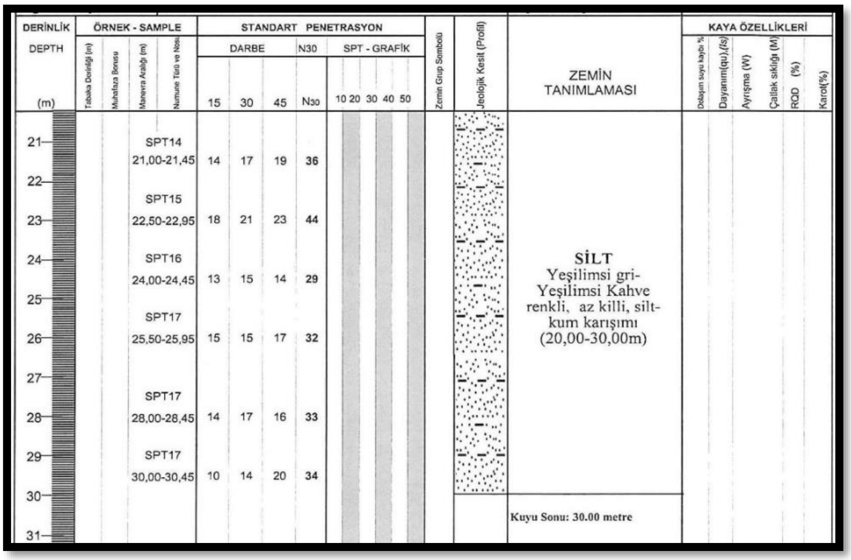

DERİNLİK DEPTH (m)	Numune Türü ve Nosu	Aralık	15	30	45	N30	ZEMİN TANIMLAMASI
21	SPT14	21,00-21,45	14	17	19	36	SİLT Yeşilimsi gri- Yeşilimsi Kahve renkli, az killi, silt-kum karışımı (20,00-30,00m)
22–23	SPT15	22,50-22,95	18	21	23	44	
24	SPT16	24,00-24,45	13	15	14	29	
25–26	SPT17	25,50-25,95	15	15	17	32	
28	SPT17	28,00-28,45	14	17	16	33	
29–30	SPT17	30,00-30,45	10	14	20	34	
30–31							Kuyu Sonu: 30.00 metre

Figure A1.10. Log of Borehole SK 5 from 20 m to 30 m

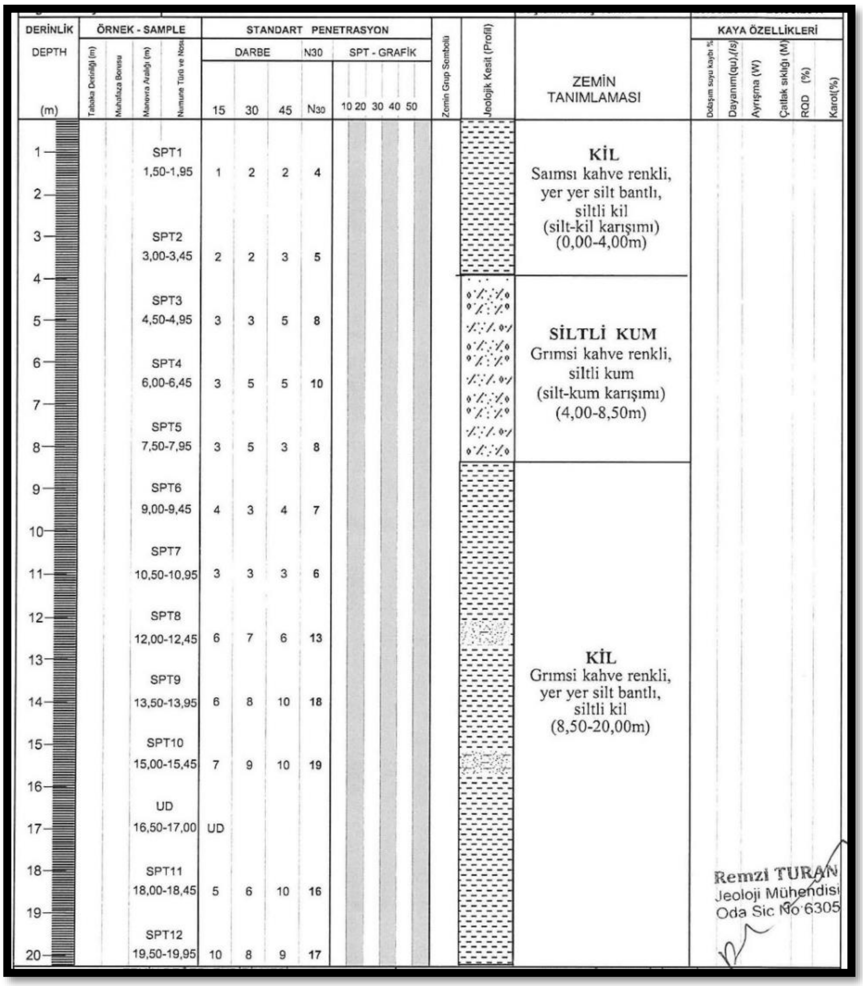

DERİNLİK DEPTH (m)	Numune Türü ve Nosu	Aralık	15	30	45	N30	ZEMİN TANIMLAMASI
1	SPT1	1,50-1,95	1	2	2	4	KİL Saımsı kahve renkli, yer yer silt bantlı, siltli kil (silt-kil karışımı) (0,00-4,00m)
3	SPT2	3,00-3,45	2	2	3	5	
4–5	SPT3	4,50-4,95	3	3	5	8	SİLTLİ KUM Grımsi kahve renkli, siltli kum (silt-kum karışımı) (4,00-8,50m)
6	SPT4	6,00-6,45	3	5	5	10	
7–8	SPT5	7,50-7,95	3	5	3	8	
9	SPT6	9,00-9,45	4	3	4	7	KİL Grımsi kahve renkli, yer yer silt bantlı, siltli kil (8,50-20,00m)
10–11	SPT7	10,50-10,95	3	3	3	6	
12	SPT8	12,00-12,45	6	7	6	13	
13–14	SPT9	13,50-13,95	6	8	10	18	
15	SPT10	15,00-15,45	7	9	10	19	
16–17	UD	16,50-17,00	UD				
18	SPT11	18,00-18,45	5	6	10	16	
19–20	SPT12	19,50-19,95	10	8	9	17	

Remzi TURAN
Jeoloji Mühendisi
Oda Sic No 6305

Figure A1.11. Log of Borehole SK 6 from 0 m to 20 m

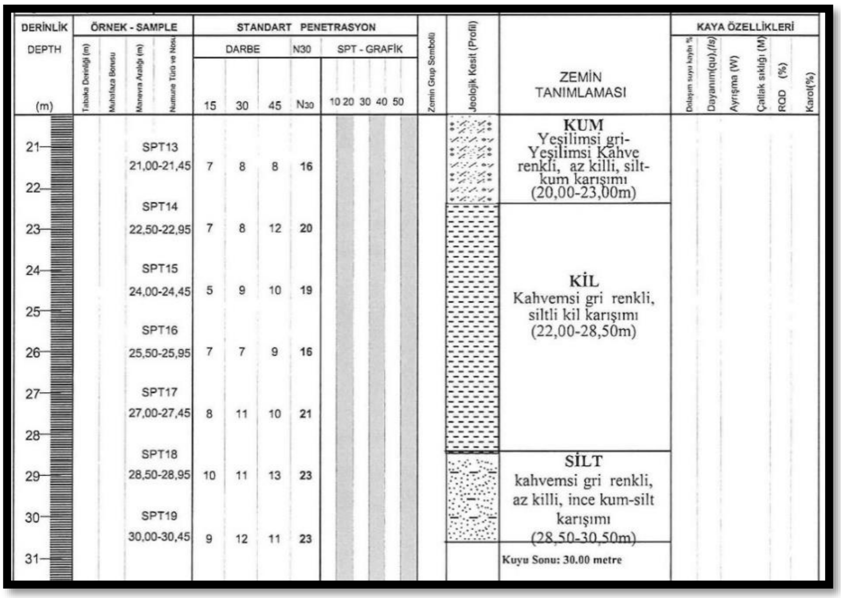

DERİNLİK DEPTH (m)	ÖRNEK - SAMPLE	DARBE 15	DARBE 30	DARBE 45	N30	ZEMİN TANIMLAMASI
21	SPT13 21,00-21,45	7	8	8	16	KUM Yeşilimsi gri-Yeşilimsi Kahve renkli, az killi, silt-kum karışımı (20,00-23,00m)
22	SPT14 22,50-22,95	7	8	12	20	
23–24	SPT15 24,00-24,45	5	9	10	19	KİL Kahvemsi gri renkli, siltli kil karışımı (22,00-28,50m)
25	SPT16 25,50-25,95	7	7	9	16	
27	SPT17 27,00-27,45	8	11	10	21	
28	SPT18 28,50-28,95	10	11	13	23	SİLT kahvemsi gri renkli, az killi, ince kum-silt karışımı (28,50-30,50m)
30	SPT19 30,00-30,45	9	12	11	23	
31						Kuyu Sonu: 30.00 metre

Figure A1.12. Log of Borehole SK 6 from 20 m to 30 m

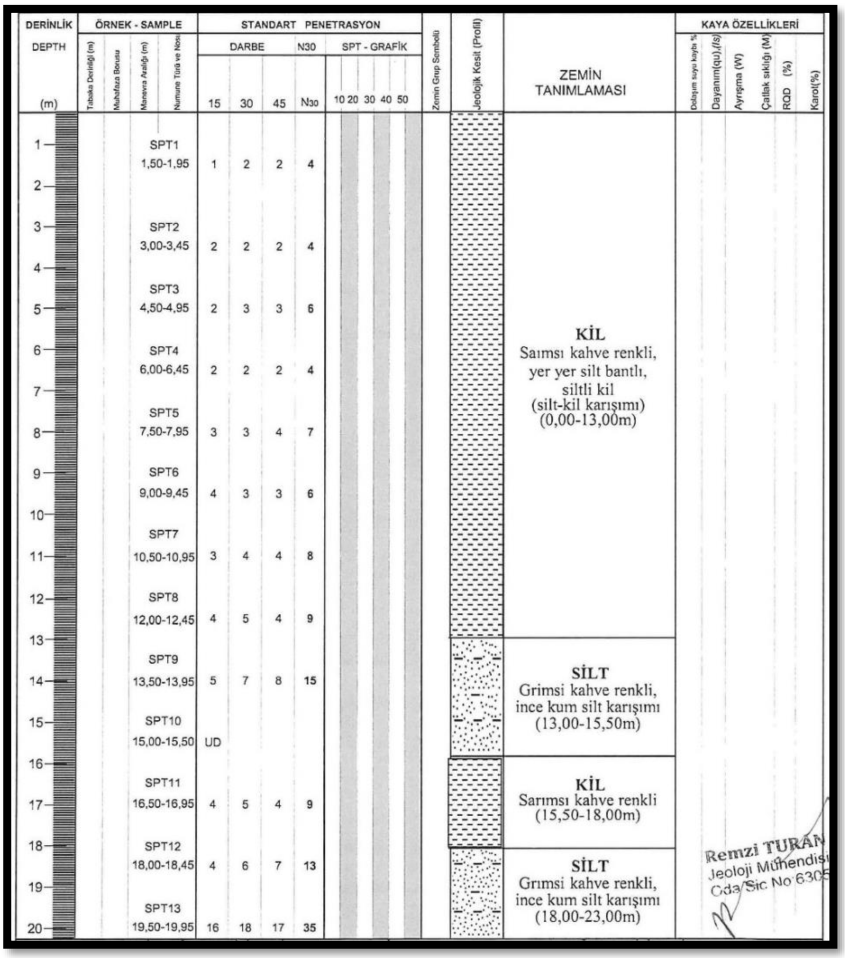

DERİNLİK DEPTH (m)	ÖRNEK - SAMPLE	DARBE 15	DARBE 30	DARBE 45	N30	ZEMİN TANIMLAMASI
1	SPT1 1,50-1,95	1	2	2	4	KİL Saımsı kahve renkli, yer yer silt bantlı, siltli kil (silt-kil karışımı) (0,00-13,00m)
3	SPT2 3,00-3,45	2	2	2	4	
4	SPT3 4,50-4,95	2	3	3	6	
6	SPT4 6,00-6,45	2	2	2	4	
7	SPT5 7,50-7,95	3	3	4	7	
9	SPT6 9,00-9,45	4	3	3	6	
10	SPT7 10,50-10,95	3	4	4	8	
12	SPT8 12,00-12,45	4	5	4	9	
13	SPT9 13,50-13,95	5	7	8	15	SİLT Grimsi kahve renkli, ince kum silt karışımı (13,00-15,50m)
15	SPT10 15,00-15,50	UD				
16	SPT11 16,50-16,95	4	5	4	9	KİL Sarımsı kahve renkli (15,50-18,00m)
18	SPT12 18,00-18,45	4	6	7	13	SİLT Grımsi kahve renkli, ince kum silt karışımı (18,00-23,00m)
19	SPT13 19,50-19,95	16	18	17	35	

Remzi TURAN Jeoloji Mühendisi Oda Sic No 6305

Figure A1.13. Log of Borehole SK 7 from 0 m to 20 m

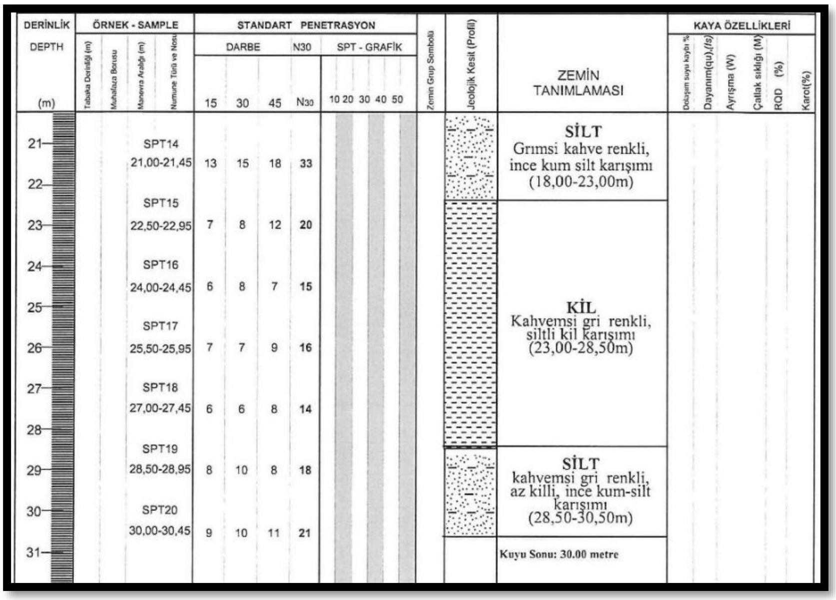

Figure A1.14. Log of Borehole SK 7 from 20 m to 30 m

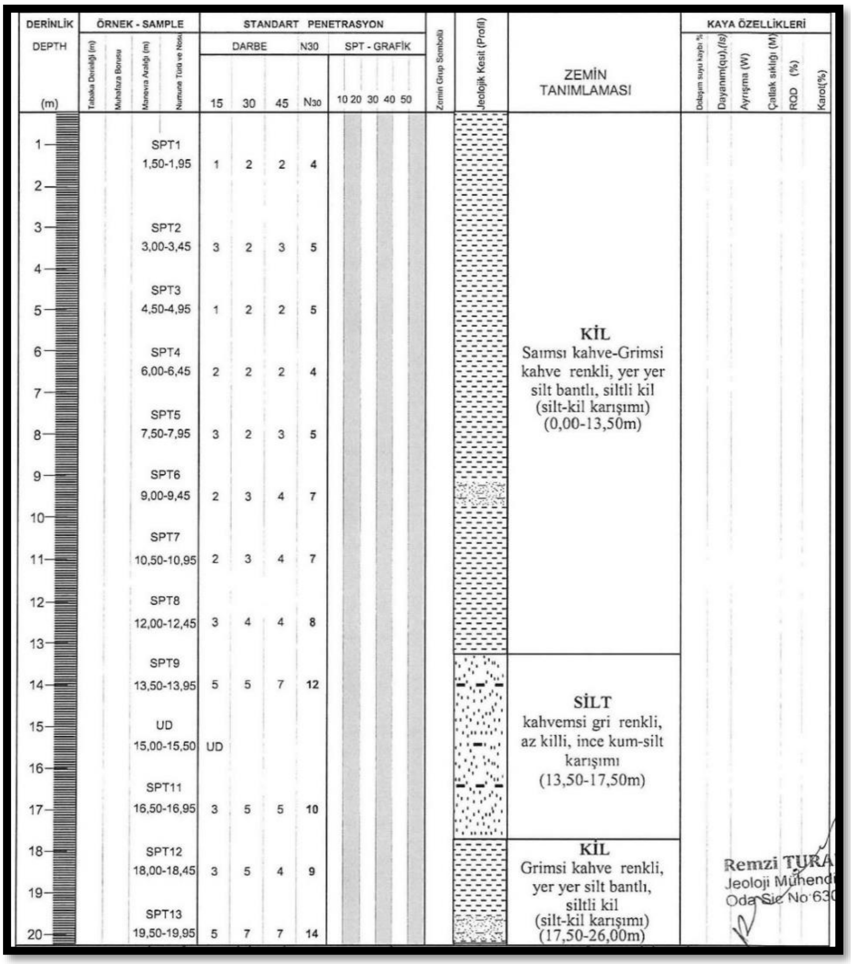

Figure A1.15. Log of Borehole SK 8 from 0 m to 20 m

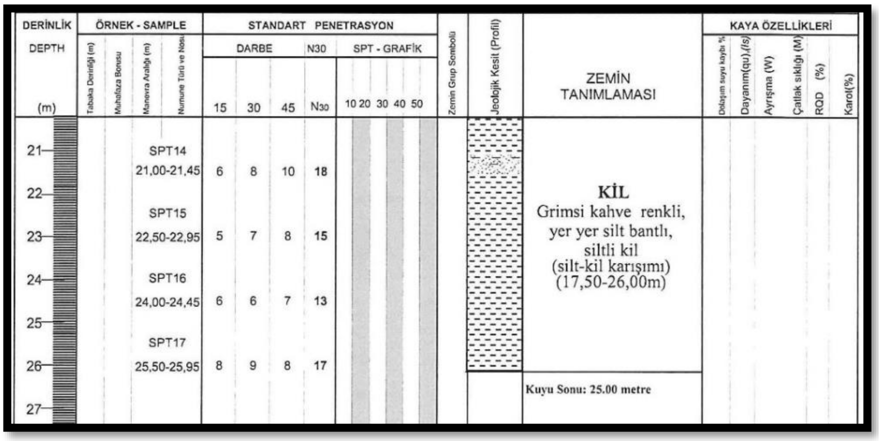

DERİNLİK DEPTH (m)	Numune Türü ve Nosu	Manevra Aralığı (m)	DARBE 15	DARBE 30	DARBE 45	N30
21	SPT14	21,00-21,45	6	8	10	18
22	SPT15	22,50-22,95	5	7	8	15
24	SPT16	24,00-24,45	6	6	7	13
25	SPT17	25,50-25,95	8	9	8	17

ZEMİN TANIMLAMASI: **KİL** Grimsi kahve renkli, yer yer silt bantlı, siltli kil (silt-kil karışımı) (17,50-26,00m)

Kuyu Sonu: 25.00 metre

Figure A1.16. Log of Borehole SK 8 from 20 m to 25 m

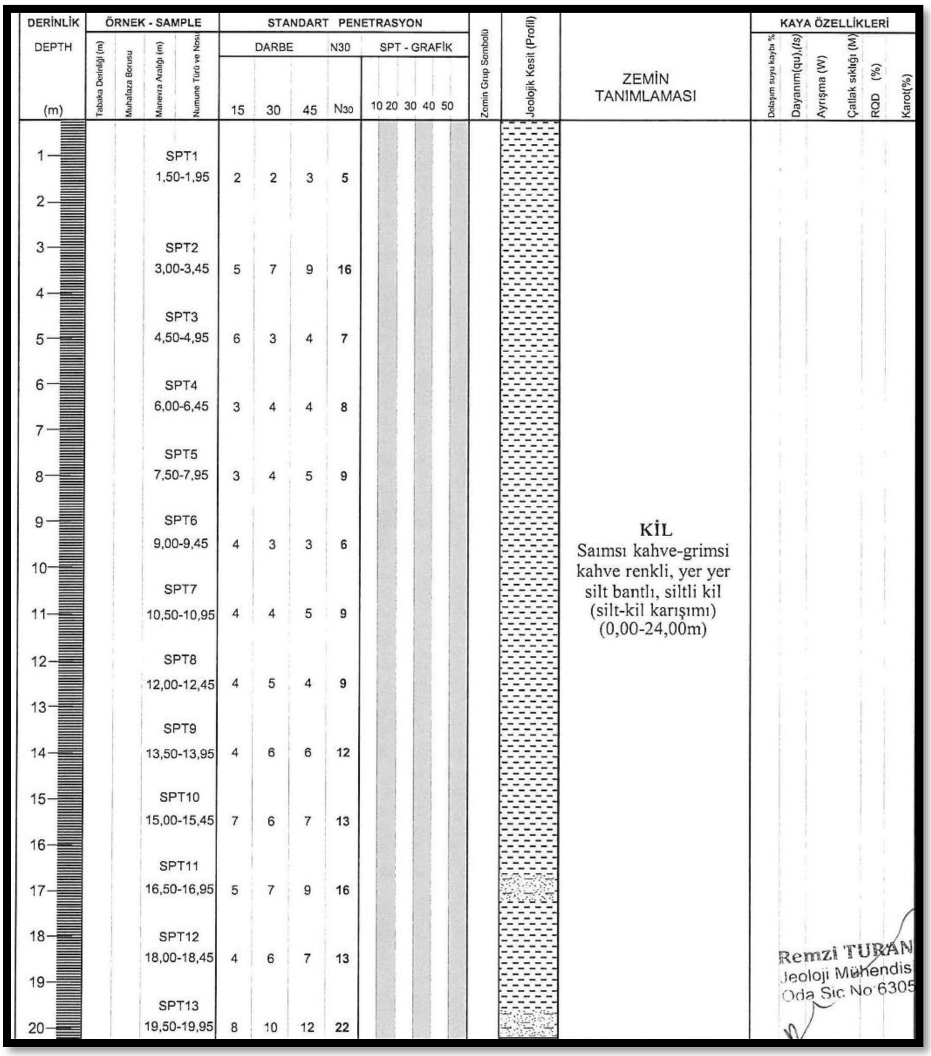

DERİNLİK DEPTH (m)	Numune Türü ve Nosu	Manevra Aralığı (m)	DARBE 15	DARBE 30	DARBE 45	N30
1	SPT1	1,50-1,95	2	2	3	5
3	SPT2	3,00-3,45	5	7	9	16
4	SPT3	4,50-4,95	6	3	4	7
6	SPT4	6,00-6,45	3	4	4	8
7	SPT5	7,50-7,95	3	4	5	9
9	SPT6	9,00-9,45	4	3	3	6
10	SPT7	10,50-10,95	4	4	5	9
12	SPT8	12,00-12,45	4	5	4	9
13	SPT9	13,50-13,95	4	6	6	12
15	SPT10	15,00-15,45	7	6	7	13
16	SPT11	16,50-16,95	5	7	9	16
18	SPT12	18,00-18,45	4	6	7	13
19	SPT13	19,50-19,95	8	10	12	22

ZEMİN TANIMLAMASI: **KİL** Saımsı kahve-grimsi kahve renkli, yer yer silt bantlı, siltli kil (silt-kil karışımı) (0,00-24,00m)

Figure A1.17. Log of Borehole SK 9 from 0 m to 20 m

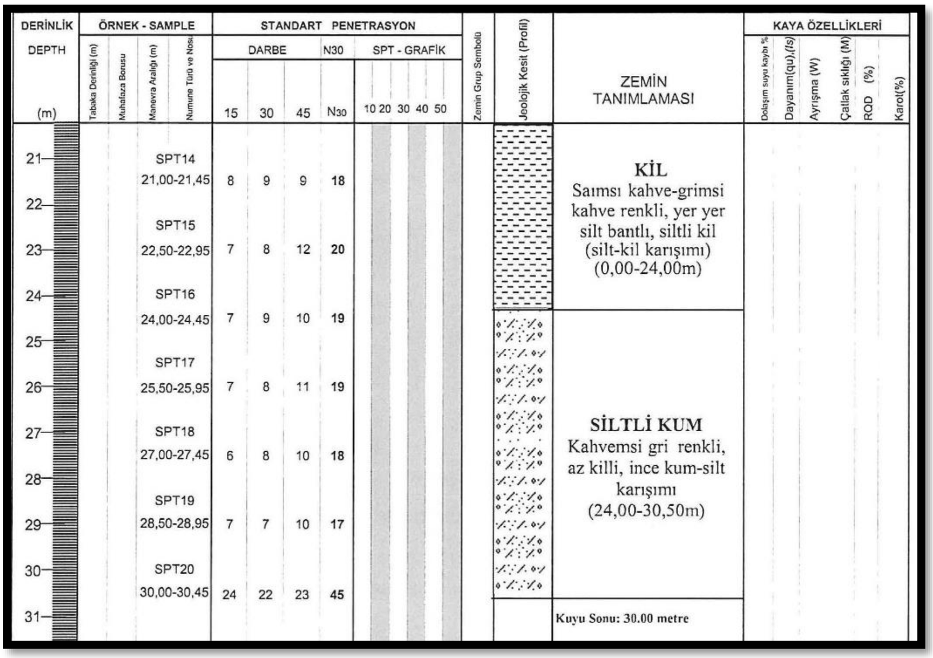

DERİNLİK DEPTH (m)	ÖRNEK - SAMPLE: Numune Türü ve Nosu	STANDART PENETRASYON DARBE 15	30	45	N30	ZEMİN TANIMLAMASI
21	SPT14 21,00-21,45	8	9	9	18	KİL Saımsı kahve-grimsi kahve renkli, yer yer silt bantlı, siltli kil (silt-kil karışımı) (0,00-24,00m)
22–23	SPT15 22,50-22,95	7	8	12	20	
24	SPT16 24,00-24,45	7	9	10	19	SİLTLİ KUM Kahvemsi gri renkli, az killi, ince kum-silt karışımı (24,00-30,50m)
25–26	SPT17 25,50-25,95	7	8	11	19	
27	SPT18 27,00-27,45	6	8	10	18	
28–29	SPT19 28,50-28,95	7	7	10	17	
30	SPT20 30,00-30,45	24	22	23	45	
31						Kuyu Sonu: 30.00 metre

Figure A1.18. Log of Borehole SK 9 from 20 m to 30

APPENDIX A2

THE CORRECTED VALUE OF N_{60}

Sondaj Borehole No	YASS GWT level m	Derinlik Depth (m)	SPT/N	σv', tsf	σv, tsf	%#200	LL	wn, %	SPT/N Darbe sayısı düzeltme katsayıları Correction factors for SPT/N blow counts					$(N_1)_{60}$	α	β	$(N_1)_{60cs}$
									C_N (1)	C_E (2)	C_B (3)	C_R	C_S		(4)	(4)	(4)
SK-1	2.00	1.50	3	0.324	0.270	95.8	52.2		1.70	0.80	1.00	0.75	1.00	3	5.00	1.2	8
SK-1	2.00	3.00	11	0.464	0.540	95.8	52.2	35.4	1.47	0.80	1.00	0.75	1.00	9	5.00	1.2	15
SK-1	2.00	6.00	5	0.704	1.080	9.3	0.0	32.1	1.19	0.80	1.00	0.85	1.00	4	0.64	1.018	4
SK-1	2.00	7.50	15	0.824	1.350	9.3	0.0	25.2	1.10	0.80	1.00	0.95	1.00	12	0.64	1.018	12
SK-1	2.00	9.00	16	0.944	1.620	47.6	0.0	25.2	1.03	0.80	1.00	0.95	1.00	12	5.00	1.2	19
SK-1	2.00	10.50	16	1.064	1.890	98.7	59.4		0.97	0.80	1.00	1.00	1.00	12	5.00	1.2	19
SK-1	2.00	12.00	13	1.184	2.160	98.7	59.4		0.92	0.80	1.00	1.00	1.00	9	5.00	1.2	15
SK-1	2.00	13.50	13	1.304	2.430	98.7	59.4		0.88	0.80	1.00	1.00	1.00	9	5.00	1.2	15
SK-1	2.00	15.00	19	1.424	2.700	98.7	59.4		0.84	0.80	1.00	1.00	1.00	12	5.00	1.2	19
SK-1	2.00	16.50	18	1.544	2.970	98.7	59.4	44.6	0.80	0.80	1.00	1.00	1.00	11	5.00	1.2	18
SK-1	2.00	18.00	16	1.664	3.240	98.7	59.4		0.78	0.80	1.00	1.00	1.00	9	5.00	1.2	15
SK-1	2.00	19.50	20	1.784	3.510	98.7	59.4		0.75	0.80	1.00	1.00	1.00	11	5.00	1.2	18
SK-1	2.00	21.00	16	1.904	3.780	93.7	37.3	31.5	0.72	0.80	1.00	1.00	1.00	9	5.00	1.2	15
SK-1	2.00	22.50	18	2.024	4.050	93.7	37.3		0.70	0.80	1.00	1.00	1.00	10	5.00	1.2	17
SK-1	2.00	24.00	18	2.144	4.320	93.7	37.3		0.68	0.80	1.00	1.00	1.00	9	5.00	1.2	15
SK-1	2.00	25.50	19	2.264	4.590	87.8	58.5	33.0	0.66	0.80	1.00	1.00	1.00	10	5.00	1.2	17
SK-1	2.00	27.00	30	2.384	4.860	87.8	58.5		0.65	0.80	1.00	1.00	1.00	15	5.00	1.2	23
SK-1	2.00	28.50	33	2.504	5.130	62.2	0.0	28.8	0.63	0.80	1.00	1.00	1.00	16	5.00	1.2	24
SK-1	2.00	30.00	27	2.624	5.400	62.2	0.0	28.8	0.62	0.80	1.00	1.00	1.00	13	5.00	1.2	20
													ortalama	10			16

Figure A2.1. N_{60} Values for SK 1

Sondaj Borehole No	YASS GWT level m	Derinlik Depth (m)	SPT/N	σv', tsf	σv, tsf	%#200	LL	wn, %	SPT/N Darbe sayısı düzeltme katsayıları Correction factors for SPT/N blow counts					$(N_1)_{60}$	α	β	$(N_1)_{60cs}$
									C_N (1)	C_E (2)	C_B (3)	C_R	C_S		(4)	(4)	(4)
SK-2	1.80	1.50	3	0.324	0.270	82.0	51.7		1.70	0.80	1.00	0.75	1.00	3	5.00	1.2	8
SK-2	1.80	3.00	13	0.444	0.540	82.0	51.7	30.7	1.50	0.80	1.00	0.75	1.00	11	5.00	1.2	18
SK-2	1.80	4.50	5	0.564	0.810	9.3	51.7		1.33	0.80	1.00	0.85	1.00	4	0.64	1.018	4
SK-2	1.80	6.50	6	0.724	1.170	82.0	34.4	30.3	1.18	0.80	1.00	0.95	1.00	5	5.00	1.2	11
SK-2	1.80	7.50	13	0.804	1.350	97.3	34.4		1.12	0.80	1.00	0.95	1.00	11	5.00	1.2	18
SK-2	1.80	9.00	28	0.924	1.620	97.3	0.0	25.3	1.04	0.80	1.00	0.95	1.00	22	5.00	1.2	31
SK-2	1.80	10.50	16	1.044	1.890	34.6	0.0		0.98	0.80	1.00	1.00	1.00	12	4.96	1.194	19
SK-2	1.80	12.00	14	1.164	2.160	34.6	0.0		0.93	0.80	1.00	1.00	1.00	10	4.96	1.194	16
SK-2	1.80	13.50	13	1.284	2.430	34.6	0.0		0.88	0.80	1.00	1.00	1.00	9	4.96	1.194	15
SK-2	1.80	15.00	20	1.404	2.700	44.1	0.0	28.9	0.84	0.80	1.00	1.00	1.00	13	5.00	1.2	20
SK-2	1.80	16.50	19	1.524	2.970	96.1	36.5		0.81	0.80	1.00	1.00	1.00	12	5.00	1.2	19
SK-2	1.80	18.00	22	1.644	3.240	96.0	36.5		0.78	0.80	1.00	1.00	1.00	13	5.00	1.2	20
SK-2	1.80	19.50	35	1.764	3.510	96.0	36.5		0.75	0.80	1.00	1.00	1.00	21	5.00	1.2	30
SK-2	1.80	21.00	21	1.884	3.780	96.0	36.5	31.5	0.73	0.80	1.00	1.00	1.00	12	5.00	1.2	19
SK-2	1.80	22.50	26	2.004	4.050	96.0	36.5		0.71	0.80	1.00	1.00	1.00	14	5.00	1.2	21
SK-2	1.80	24.00	19	2.124	4.320	96.0	36.5		0.69	0.80	1.00	1.00	1.00	10	5.00	1.2	17
SK-2	1.80	25.50	39	2.244	4.590	96.0	36.5		0.67	0.80	1.00	1.00	1.00	20	5.00	1.2	29
SK-2	1.80	27.00	33	2.364	4.860	96.0	33.4	34.6	0.65	0.80	1.00	1.00	1.00	17	5.00	1.2	25
SK-2	1.80	28.50	34	2.484	5.130	96.0	33.4		0.63	0.80	1.00	1.00	2.00	34	5.00	1.2	45
SK-2	1.80	30.00	35	2.604	5.400	96.0	33.4		0.62	0.80	1.00	1.00	3.00	52	5.00	1.2	67
													ortalama	15			23

Figure A2.2. N_{60} Values for SK 2

Sondaj Borehole No	YASS GWT level m	Derinlik Depth (m)	SPT/N	σv', tsf	σv, tsf	%#200	LL	wn, %	SPT/N Darbe sayısı düzeltme katsayıları Correction factors for SPT/N blow counts					$(N_1)_{60}$	α	β	$(N_1)_{60cs}$
									C_N (1)	C_E (2)	C_B (3)	C_R	C_S		(4)	(4)	(4)
SK-3	2.00	1.50	3	0.324	0.270	93.7	29.0		1.70	0.80	1.00	0.75	1.00	3	5.00	1.2	8
SK-3	2.00	3.00	8	0.464	0.540	93.7	29.0	23.7	1.47	0.80	1.00	0.75	1.00	7	5.00	1.2	13
SK-3	2.00	4.50	8	0.584	0.810	93.7	29.0		1.31	0.80	1.00	0.85	1.00	7	5.00	1.2	13
SK-3	2.00	6.50	6	0.744	1.170	93.7	29.0		1.16	0.80	1.00	0.95	1.00	5	5.00	1.2	11
SK-3	2.00	7.50	10	0.824	1.350	93.7	29.0		1.10	0.80	1.00	0.95	1.00	8	5.00	1.2	14
SK-3	2.00	9.00	19	0.944	1.620	90.8	37.4	33.4	1.03	0.80	1.00	0.95	1.00	14	5.00	1.2	21
SK-3	2.00	10.50	11	1.064	1.890	90.8	37.4		0.97	0.80	1.00	1.00	1.00	8	5.00	1.2	14
SK-3	2.00	12.00	11	1.184	2.160	30.8	37.4		0.92	0.80	1.00	1.00	1.00	8	4.76	1.161	14
SK-3	2.00	13.50	14	1.304	2.430	97.9	37.5	28.0	0.88	0.80	1.00	1.00	1.00	9	5.00	1.2	15
SK-3	2.00	15.00	17	1.424	2.700	97.9	37.5		0.84	0.80	1.00	1.00	1.00	11	5.00	1.2	18
SK-3	2.00	16.50	27	1.544	2.970	81.3	49.9	32.9	0.80	0.80	1.00	1.00	1.00	17	5.00	1.2	25
SK-3	2.00	18.00	37	1.664	3.240	81.3	49.9		0.78	0.80	1.00	1.00	1.00	22	5.00	1.2	31
SK-3	2.00	19.50	28	1.784	3.510	81.3	49.9		0.75	0.80	1.00	1.00	1.00	16	5.00	1.2	24
SK-3	2.00	21.00	33	1.904	3.780	92.8	30.4	29.3	0.72	0.80	1.00	1.00	1.00	19	5.00	1.2	27
SK-3	2.00	22.50	27	2.024	4.050	92.8	30.4		0.70	0.80	1.00	1.00	1.00	15	5.00	1.2	23
SK-3	2.00	24.00	26	2.144	4.320	92.8	30.4		0.68	0.80	1.00	1.00	1.00	14	5.00	1.2	21
SK-3	2.00	25.50	22	2.264	4.590	92.8	30.4		0.66	0.80	1.00	1.00	1.00	11	5.00	1.2	18
SK-3	2.00	27.00	39	2.384	4.860	92.8	30.4		0.65	0.80	1.00	1.00	1.00	20	5.00	1.2	29
SK-3	2.00	28.50	36	2.504	5.130	89.1	31.2	30.9	0.63	0.80	1.00	1.00	2.00	36	5.00	1.2	48
SK-3	2.00	30.00	29	2.624	5.400	89.1	31.2		0.62	0.80	1.00	1.00	3.00	42	5.00	1.2	55
													ortalama	15			22

Figure A2.3. N_{60} Values for SK 3

Sondaj Borehole No	YASS GWT level m	Derinlik Depth (m)	SPT/N	σv', tsf	σv, tsf	%#200	LL	wn, %	SPT/N Darbe sayısı düzeltme katsayıları Correction factors for SPT/N blow counts					$(N_1)_{60}$	α	β	$(N_1)_{60cs}$
									C_N (1)	C_E (2)	C_B (3)	C_R	C_S		(4)	(4)	(4)
SK-4	2.00	1.50	6	0.324	0.270	90.3	51.5	31.1	1.70	0.80	1.00	0.75	1.00	6	5.00	1.2	12
SK-4	2.00	3.00	9	0.464	0.540	90.3	51.5		1.47	0.80	1.00	0.75	1.00	7	5.00	1.2	13
SK-4	2.00	4.50	8	0.584	0.810	90.3	51.5		1.31	0.80	1.00	0.85	1.00	7	5.00	1.2	13
SK-4	2.00	6.00	6	0.704	1.080	90.2	52.5	32.3	1.19	0.80	1.00	0.85	1.00	4	5.00	1.2	9
SK-4	2.00	7.50	13	0.824	1.350	90.2	52.5		1.10	0.80	1.00	0.95	1.00	10	5.00	1.2	17
SK-4	2.00	9.00	12	0.944	1.620	98.2	45.2	43.2	1.03	0.80	1.00	0.95	1.00	9	5.00	1.2	15
SK-4	2.00	10.50	15	1.064	1.890	38.9	0.0		0.97	0.80	1.00	1.00	1.00	11	5.00	1.2	18
SK-4	2.00	13.50	18	1.304	2.430	38.9	0.0	27.0	0.88	0.80	1.00	1.00	1.00	12	5.00	1.2	19
SK-4	2.00	15.00	16	1.424	2.700	38.9	0.0		0.84	0.80	1.00	1.00	1.00	10	5.00	1.2	17
SK-4	2.00	16.50	21	1.544	2.970	38.9	0.0		0.80	0.80	1.00	1.00	1.00	13	5.00	1.2	20
SK-4	2.00	18.00	33	1.664	3.240	51.2	0.0	25.7	0.78	0.80	1.00	1.00	1.00	20	5.00	1.2	29
SK-4	2.00	19.50	24	1.784	3.510	20.4	0.0		0.75	0.80	1.00	1.00	1.00	14	3.68	1.082	18
SK-4	2.00	21.00	41	1.904	3.780	20.4	0.0	23.5	0.72	0.80	1.00	1.00	1.00	23	3.68	1.082	28
SK-4	2.00	22.50	32	2.024	4.050	20.4	0.0		0.70	0.80	1.00	1.00	1.00	17	3.68	1.082	22
SK-4	2.00	24.00	15	2.144	4.320	91.7	32.4		0.68	0.80	1.00	1.00	1.00	8	5.00	1.2	14
SK-4	2.00	25.50	23	2.264	4.590	91.7	32.4	27.4	0.66	0.80	1.00	1.00	1.00	12	5.00	1.2	19
													ortalama	11			18

Figure A2.4. N_{60} Values for SK 4

Sondaj Borehole No	YASS GWT level m	Derinlik Depth (m)	SPT/N	σv', tsf	σv, tsf	%-#200	LL	wn, %	SPT/N Darbe sayısı düzeltme katsayıları Correction factors for SPT/N blow counts C_N (1)	C_E (2)	C_B (3)	C_R	C_S	$(N_1)_{60}$	α (4)	β (4)	$(N_1)_{60cs}$ (4)
SK-5	2.00	1.50	7	0.324	0.270	98.2	48.6	36.9	1.70	0.80	1.00	0.75	1.00	7	5.00	1.2	13
SK-5	2.00	3.00	6	0.464	0.540	98.2	48.6		1.47	0.80	1.00	0.75	1.00	5	5.00	1.2	11
SK-5	2.00	4.50	5	0.584	0.810	98.2	48.6		1.31	0.80	1.00	0.85	1.00	4	5.00	1.2	9
SK-5	2.00	6.50	6	0.744	1.170	98.2	48.6		1.16	0.80	1.00	0.95	1.00	5	5.00	1.2	11
SK-5	2.00	7.50	14	0.824	1.350	98.2	48.6		1.10	0.80	1.00	0.95	1.00	11	5.00	1.2	18
SK-5	2.00	9.00	12	0.944	1.620	98.2	48.6		1.03	0.80	1.00	0.95	1.00	9	5.00	1.2	15
SK-5	2.00	10.50	10	1.064	1.890	99.6	37.1	35.9	0.97	0.80	1.00	1.00	1.00	7	5.00	1.2	13
SK-5	2.00	12.00	13	1.184	2.160	98.9	66.3	44.7	0.92	0.80	1.00	1.00	1.00	9	5.00	1.2	15
SK-5	2.00	13.50	14	1.304	2.430	98.9	66.3		0.88	0.80	1.00	1.00	1.00	9	5.00	1.2	15
SK-5	2.00	15.00	11	1.424	2.700	98.9	66.3		0.84	0.80	1.00	1.00	1.00	7	5.00	1.2	13
SK-5	2.00	16.50	13	1.544	2.970	98.9	66.3		0.80	0.80	1.00	1.00	1.00	8	5.00	1.2	14
SK-5	2.00	18.00	22	1.664	3.240	98.9	66.3		0.78	0.80	1.00	1.00	1.00	13	5.00	1.2	20
SK-5	2.00	19.50	22	1.784	3.510	98.9	66.3		0.75	0.80	1.00	1.00	1.00	13	5.00	1.2	20
SK-5	2.00	21.00	36	1.904	3.780	81.5	0.0		0.72	0.80	1.00	1.00	1.00	20	5.00	1.2	29
SK-5	2.00	22.50	44	2.024	4.050	81.5	0.0	21.1	0.70	0.80	1.00	1.00	1.00	24	5.00	1.2	33
SK-5	2.00	24.00	29	2.144	4.320	81.5	0.0		0.68	0.80	1.00	1.00	1.00	15	5.00	1.2	23
SK-5	2.00	25.50	32	2.264	4.590	77.2	0.0	25.3	0.66	0.80	1.00	1.00	1.00	17	5.00	1.2	25
SK-5	2.00	28.50	33	2.504	5.130	77.2	0.0		0.63	0.80	1.00	1.00	1.00	16	5.00	1.2	24
SK-5	2.00	30.00	34	2.624	5.400	89.0	0.0	30.7	0.62	0.80	1.00	1.00	2.00	33	5.00	1.2	44
													ortalama	12			19

Figure A2.5. N_{60} Values for SK 5

Sondaj Borehole No	YASS GWT level m	Derinlik Depth (m)	SPT/N	σv', tsf	σv, tsf	%-#200	LL	wn, %	SPT/N Darbe sayısı düzeltme katsayıları Correction factors for SPT/N blow counts C_N (1)	C_E (2)	C_B (3)	C_R	C_S	$(N_1)_{60}$	α (4)	β (4)	$(N_1)_{60cs}$ (4)
SK-6	2.00	1.50	4	0.324	0.270	99.0	56.7	37.6	1.70	0.80	1.00	0.75	1.00	4	5.00	1.2	9
SK-6	2.00	3.00	5	0.464	0.540	99.0	56.7		1.47	0.80	1.00	0.75	1.00	4	5.00	1.2	9
SK-6	2.00	4.50	8	0.584	0.810	7.9	0.0	25.7	1.31	0.80	1.00	0.85	1.00	7	0.27	1.012	7
SK-6	2.00	6.00	10	0.704	1.080	7.9	0.0		1.19	0.80	1.00	0.85	1.00	8	0.28	1.012	8
SK-6	2.00	7.50	8	0.824	1.350	7.9	0.0		1.10	0.80	1.00	0.95	1.00	6	0.28	1.012	6
SK-6	2.00	9.00	7	0.944	1.620	87.4	44.9		1.03	0.80	1.00	0.95	1.00	5	5.00	1.2	11
SK-6	2.00	10.50	6	1.064	1.890	87.4	44.9	37.4	0.97	0.80	1.00	1.00	1.00	4	5.00	1.2	9
SK-6	2.00	12.00	13	1.184	2.160	87.4	44.9		0.92	0.80	1.00	1.00	1.00	9	5.00	1.2	15
SK-6	2.00	13.50	18	1.304	2.430	87.4	44.9		0.88	0.80	1.00	1.00	1.00	12	5.00	1.2	19
SK-6	2.00	15.00	19	1.424	2.700	99.3	55.2	42.8	0.84	0.80	1.00	1.00	1.00	12	5.00	1.2	19
SK-6	2.00	18.00	16	1.664	3.240	99.3	55.2		0.78	0.80	1.00	1.00	1.00	9	5.00	1.2	15
SK-6	2.00	19.50	17	1.784	3.510	94.5	37.0	32.5	0.75	0.80	1.00	1.00	1.00	10	5.00	1.2	17
SK-6	2.00	21.00	16	1.904	3.780	44.4	0.0	28.4	0.72	0.80	1.00	1.00	1.00	9	5.00	1.2	15
SK-6	2.00	22.50	20	2.024	4.050	93.2	58.7		0.70	0.80	1.00	1.00	1.00	11	5.00	1.2	18
SK-6	2.00	24.00	19	2.144	4.320	93.2	58.7		0.68	0.80	1.00	1.00	1.00	10	5.00	1.2	17
SK-6	2.00	25.50	16	2.264	4.590	93.2	58.7	35.6	0.66	0.80	1.00	1.00	1.00	8	5.00	1.2	14
SK-6	2.00	27.00	21	2.384	4.860	93.2	58.7		0.65	0.80	1.00	1.00	1.00	10	5.00	1.2	17
SK-6	2.00	28.50	23	2.504	5.130	59.1	0.0		0.63	0.80	1.00	1.00	1.00	11	5.00	1.2	18
SK-6	2.00	30.00	23	2.624	5.400	59.1	0.0		0.62	0.80	1.00	1.00	1.00	11	5.00	1.2	18
													ortalama	8			14

Figure A2.6. N_{60} Values for SK 6

Sondaj Borehole No	YASS GWT level m	Derinlik Depth (m)	SPT/N	σv', tsf	σv, tsf	%-#200	LL	wn, %	SPT/N Darbe sayısı düzeltme katsayıları Correction factors for SPT/N blow counts C_N (1)	C_E (2)	C_B (3)	C_R	C_S	$(N_1)_{60}$	α (4)	β (4)	$(N_1)_{60cs}$ (4)
SK-7	2.00	1.50	4	0.324	0.270	98.6	52.1	36.0	1.70	0.80	1.00	0.75	1.00	4	5.00	1.2	9
SK-7	2.00	3.00	4	0.464	0.540	98.6	52.1		1.47	0.80	1.00	0.75	1.00	3	5.00	1.2	8
SK-7	2.00	4.50	6	0.584	0.810	99.1	52.2	36.5	1.31	0.80	1.00	0.85	1.00	5	5.00	1.2	11
SK-7	2.00	6.00	4	0.704	1.080	99.1	52.2		1.19	0.80	1.00	0.85	1.00	3	5.00	1.2	8
SK-7	2.00	7.50	7	0.824	1.350	99.1	52.2		1.10	0.80	1.00	0.95	1.00	5	5.00	1.2	11
SK-7	2.00	9.00	6	0.944	1.620	95.0	37.6	29.5	1.03	0.80	1.00	0.95	1.00	4	5.00	1.2	9
SK-7	2.00	10.50	8	1.064	1.890	95.0	37.6		0.97	0.80	1.00	1.00	1.00	6	5.00	1.2	12
SK-7	2.00	12.00	9	1.184	2.160	95.0	37.6		0.92	0.80	1.00	1.00	1.00	6	5.00	1.2	12
SK-7	2.00	13.50	15	1.304	2.430	75.7	0.0	28.2	0.88	0.80	1.00	1.00	1.00	10	5.00	1.2	17
SK-7	2.00	16.50	9	1.544	2.970	75.7	0.0	28.2	0.80	0.80	1.00	1.00	1.00	5	5.00	1.2	11
SK-7	2.00	18.00	13	1.664	3.240	75.7	0.0	28.2	0.78	0.80	1.00	1.00	1.00	8	5.00	1.2	14
SK-7	2.00	19.50	35	1.784	3.510	73.3	0.0	27.4	0.75	0.80	1.00	1.00	1.00	20	5.00	1.2	29
SK-7	2.00	21.00	33	1.904	3.780	73.3	0.0		0.72	0.80	1.00	1.00	1.00	19	5.00	1.2	27
SK-7	2.00	22.50	20	2.024	4.050	73.3	0.0		0.70	0.80	1.00	1.00	1.00	11	5.00	1.2	18
SK-7	2.00	24.00	15	2.144	4.320	97.0	66.3	35.0	0.68	0.80	1.00	1.00	1.00	8	5.00	1.2	14
SK-7	2.00	25.50	16	2.264	4.590	97.0	6.3		0.66	0.80	1.00	1.00	1.00	8	5.00	1.2	14
SK-7	2.00	27.00	14	2.384	4.860	97.0	66.3		0.65	0.80	1.00	1.00	1.00	7	5.00	1.2	13
SK-7	2.00	28.50	18	2.504	5.130	79.0	0.0		0.63	0.80	1.00	1.00	1.00	9	5.00	1.2	15
SK-7	2.00	30.00	21	2.624	5.400	79.0	0.0		0.62	0.80	1.00	1.00	1.00	10	5.00	1.2	17
													ortalama	8			14

Figure A2.7. N_{60} Values for SK 7

Sondaj Borehole No	YASS GWT level m	Derinlik Depth (m)	SPT/N	σv', tsf	σv, tsf	%-#200	LL	wn, %	SPT/N Darbe sayısı düzeltme katsayıları Correction factors for SPT/N blow counts C_N (1)	C_E (2)	C_B (3)	C_R	C_S	$(N_1)_{60}$	α (4)	β (4)	$(N_1)_{60cs}$ (4)
SK-8	2.00	1.50	4	0.324	0.270	95.2	44.1		1.70	0.80	1.00	0.75	1.00	4	5.00	1.2	9
SK-8	2.00	3.00	5	0.464	0.540	95.2	44.1	29.3	1.47	0.80	1.00	0.75	1.00	4	5.00	1.2	9
SK-8	2.00	4.50	5	0.584	0.810	95.2	44.1		1.31	0.80	1.00	0.85	1.00	4	5.00	1.2	9
SK-8	2.00	6.00	4	0.704	1.080	95.2	44.1		1.19	0.80	1.00	0.85	1.00	3	5.00	1.2	8
SK-8	2.00	7.50	5	0.824	1.350	91.8	34.3	33.0	1.10	0.80	1.00	0.95	1.00	4	5.00	1.2	9
SK-8	2.00	9.00	7	0.944	1.620	91.8	34.3		1.03	0.80	1.00	0.95	1.00	5	5.00	1.2	11
SK-8	2.00	10.50	7	1.064	1.890	73.2	26.3	30.8	0.97	0.80	1.00	1.00	1.00	5	5.00	1.2	11
SK-8	2.00	12.00	8	1.184	2.160	73.2	26.3		0.92	0.80	1.00	1.00	1.00	5	5.00	1.2	11
SK-8	2.00	13.50	12	1.304	2.430	94.1	0.0		0.88	0.80	1.00	1.00	1.00	8	5.00	1.2	14
SK-8	2.00	16.50	10	1.544	2.970	94.1	0.0	34.5	0.80	0.80	1.00	1.00	1.00	6	5.00	1.2	12
SK-8	2.00	18.00	9	1.664	3.240	98.7	46.3		0.78	0.80	1.00	1.00	1.00	5	5.00	1.2	11
SK-8	2.00	19.50	14	1.784	3.510	98.7	46.3		0.75	0.80	1.00	1.00	1.00	8	5.00	1.2	14
SK-8	2.00	21.00	18	1.904	3.780	98.7	46.3	24.8	0.72	0.80	1.00	1.00	1.00	10	5.00	1.2	17
SK-8	2.00	22.50	15	2.024	4.050	98.7	46.3		0.70	0.80	1.00	1.00	1.00	8	5.00	1.2	14
SK-8	2.00	24.00	13	2.144	4.320	97.0	30.4	38.5	0.68	0.80	1.00	1.00	1.00	7	5.00	1.2	13
SK-8	2.00	25.50	17	2.264	4.590	97.0	30.4		0.66	0.80	1.00	1.00	1.00	9	5.00	1.2	15
													ortalama	6			12

Figure A2.8. N_{60} Values for SK 8

Sondaj Borehole No	YASS GWT level m	Derinlik Depth (m)	SPT/N	σv', tsf	σv, tsf	%-#200	LL	wn, %	SPT/N Darbe sayısı düzeltme katsayıları Correction factors for SPT/N blow counts C_N (1)	C_E (2)	C_B (3)	C_R	C_S	$(N_1)_{60}$	α (4)	β (4)	$(N_1)_{60cs}$ (4)
SK-9	1.80	1.50	5	0.324	0.270	82.8	32.6		1.70	0.80	1.00	0.75	1.00	5	5.00	1.2	11
SK-9	1.80	3.00	16	0.444	0.540	82.8	32.6		1.50	0.80	1.00	0.75	1.00	14	5.00	1.2	21
SK-9	1.80	4.50	7	0.564	0.810	82.8	32.6	35.9	1.33	0.80	1.00	0.85	1.00	6	5.00	1.2	12
SK-9	1.80	6.00	8	0.684	1.080	82.8	32.6		1.21	0.80	1.00	0.85	1.00	6	5.00	1.2	12
SK-9	1.80	7.50	9	0.804	1.350	82.8	32.6		1.12	0.80	1.00	0.95	1.00	7	5.00	1.2	13
SK-9	1.80	9.00	6	0.924	1.620	82.8	32.6		1.04	0.80	1.00	0.95	1.00	4	5.00	1.2	9
SK-9	1.80	10.50	9	1.044	1.890	99.4	37.2	38.1	0.98	0.80	1.00	1.00	1.00	7	5.00	1.2	13
SK-9	1.80	12.00	9	1.164	2.160	99.4	37.2		0.93	0.80	1.00	1.00	1.00	6	5.00	1.2	12
SK-9	1.80	13.50	12	1.284	2.430	99.4	37.2		0.88	0.80	1.00	1.00	1.00	8	5.00	1.2	14
SK-9	1.80	15.00	13	1.404	2.700	99.4	37.2		0.84	0.80	1.00	1.00	1.00	8	5.00	1.2	14
SK-9	1.80	16.50	16	1.524	2.970	96.9	65.3	42.9	0.81	0.80	1.00	1.00	1.00	10	5.00	1.2	17
SK-9	1.80	18.00	13	1.644	3.240	96.9	65.3		0.78	0.80	1.00	1.00	1.00	8	5.00	1.2	14
SK-9	1.80	19.50	22	1.764	3.510	96.9	65.3		0.75	0.80	1.00	1.00	1.00	13	5.00	1.2	20
SK-9	1.80	21.00	18	1.884	3.780	96.9	65.3		0.73	0.80	1.00	1.00	1.00	10	5.00	1.2	17
SK-9	1.80	22.50	20	2.004	4.050	96.9	65.3		0.71	0.80	1.00	1.00	1.00	11	5.00	1.2	18
SK-9	1.80	24.00	19	2.124	4.320	96.9	65.3		0.69	0.80	1.00	1.00	1.00	10	5.00	1.2	17
SK-9	1.80	25.50	19	2.244	4.590	23.4	0.0	23.1	0.67	0.80	1.00	1.00	1.00	10	4.11	1.103	15
SK-9	1.80	27.00	18	2.364	4.860	23.4	0.0		0.65	0.80	1.00	1.00	1.00	9	4.11	1.103	14
SK-9	1.80	28.50	17	2.484	5.130	23.4	0.0		0.63	0.80	1.00	1.00	2.00	17	4.11	1.103	22
SK-9	1.80	30.00	45	2.604	5.400	84.8	0.0	31.6	0.62	0.80	1.00	1.00	3.00	66	5.00	1.2	84
													ortalama	12			18

Figure A2.9. N_{60} Values for SK 9

APPENDIX B1

CONE PENETRATION TEST 1

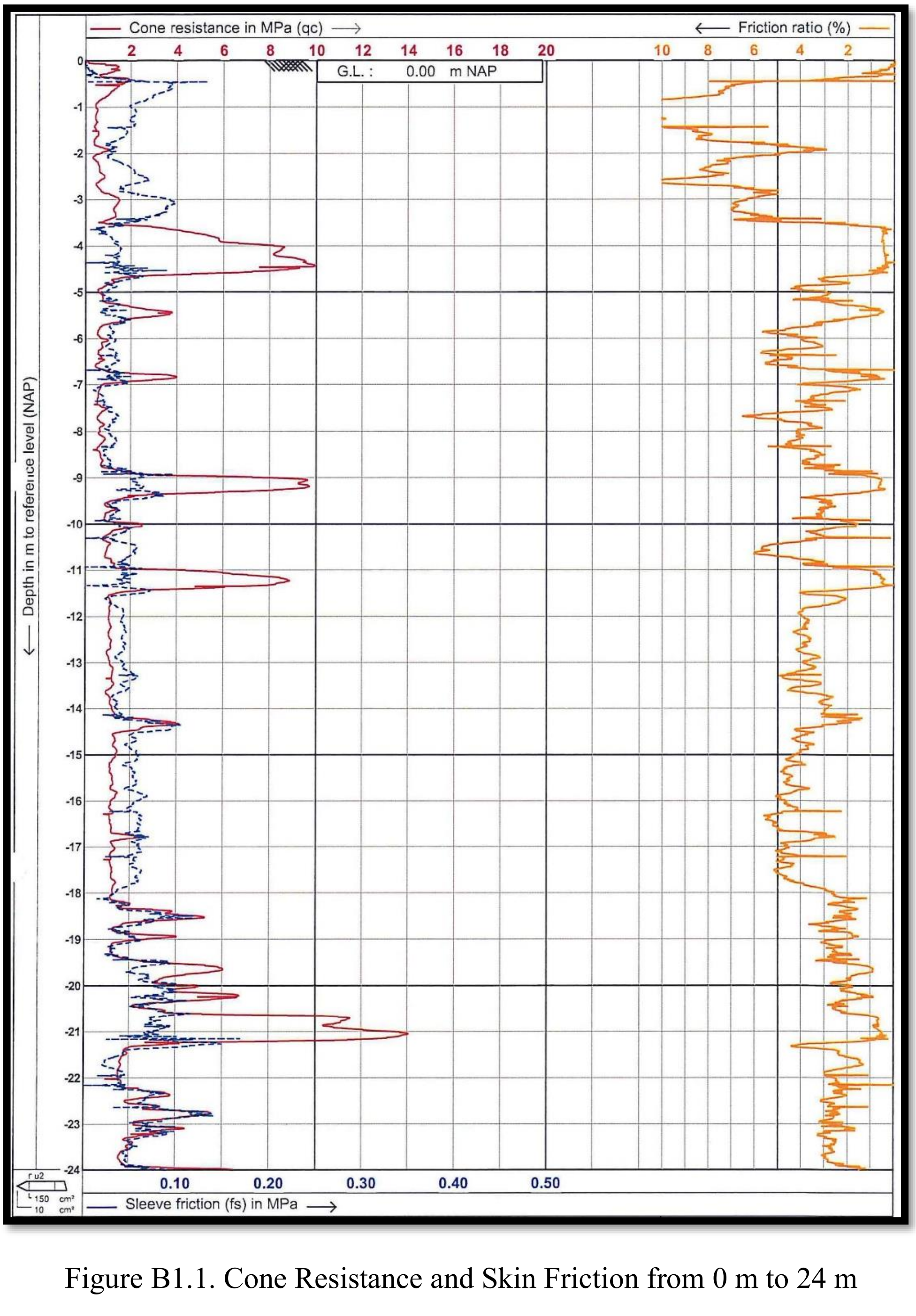

Figure B1.1. Cone Resistance and Skin Friction from 0 m to 24 m

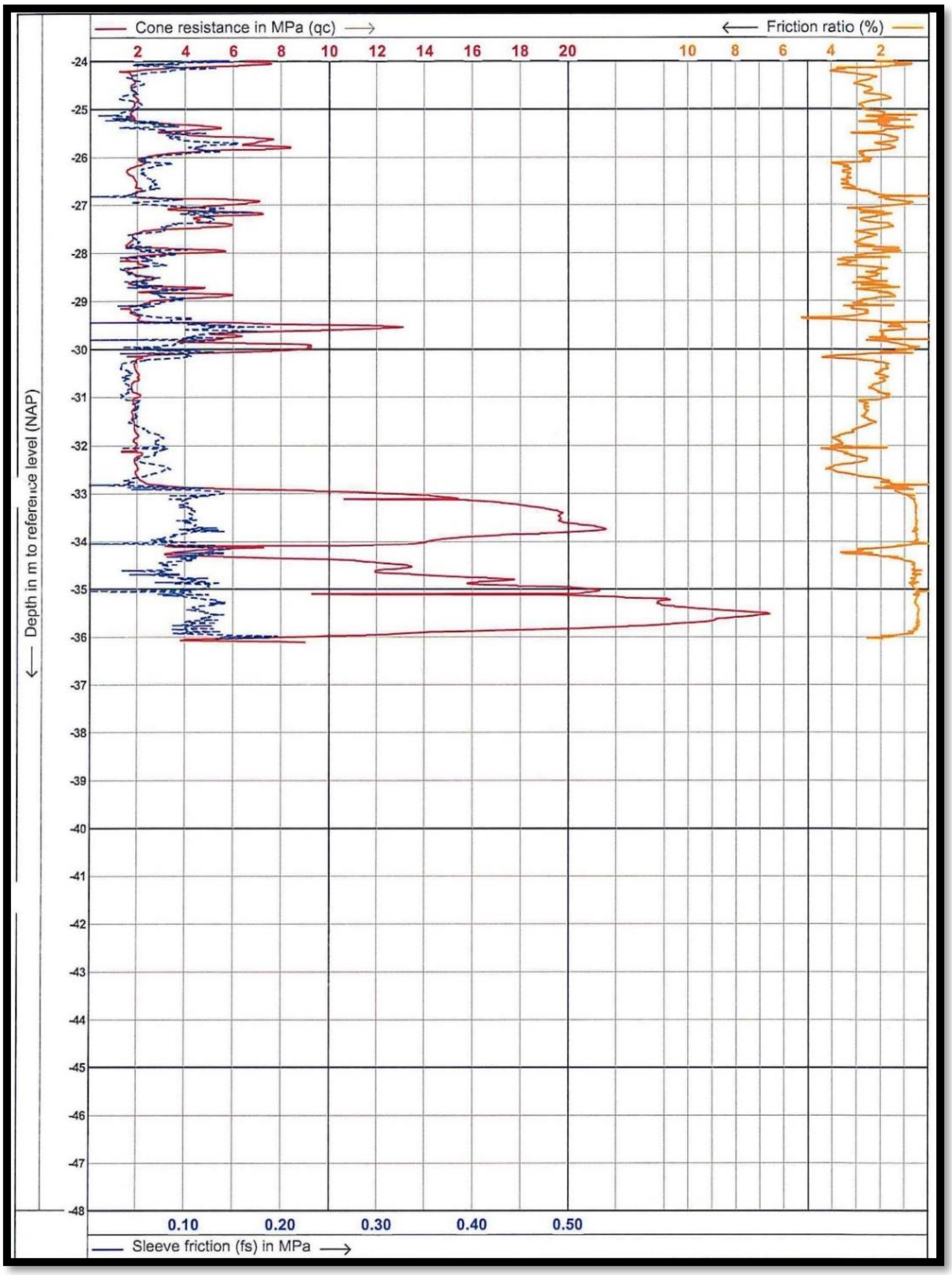

Figure B1.2. Cone Resistance and Skin Friction from 24 m to 36 m

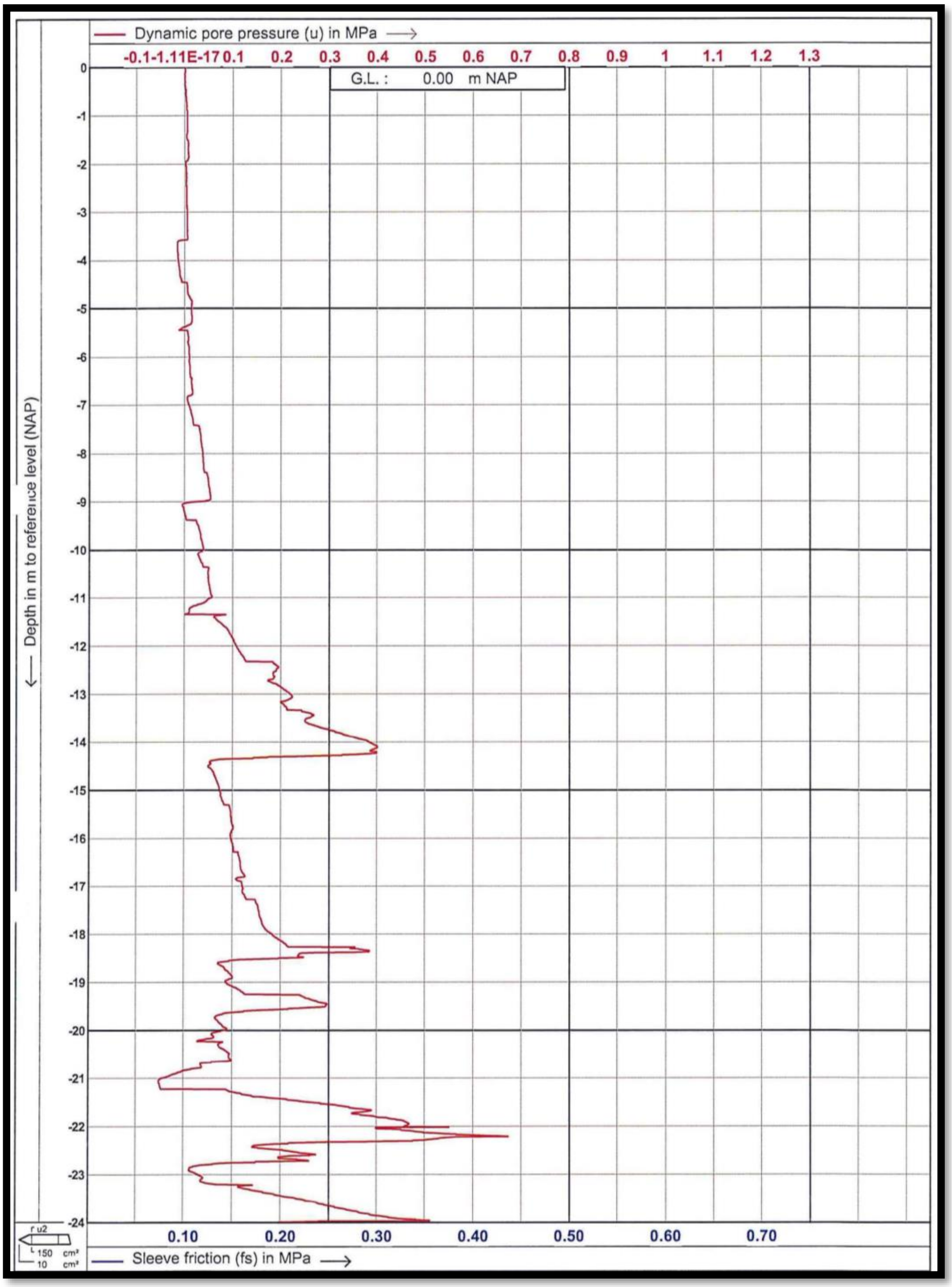

Figure B1.3. Dynamic Pore Pressure from 0 m to 24 m

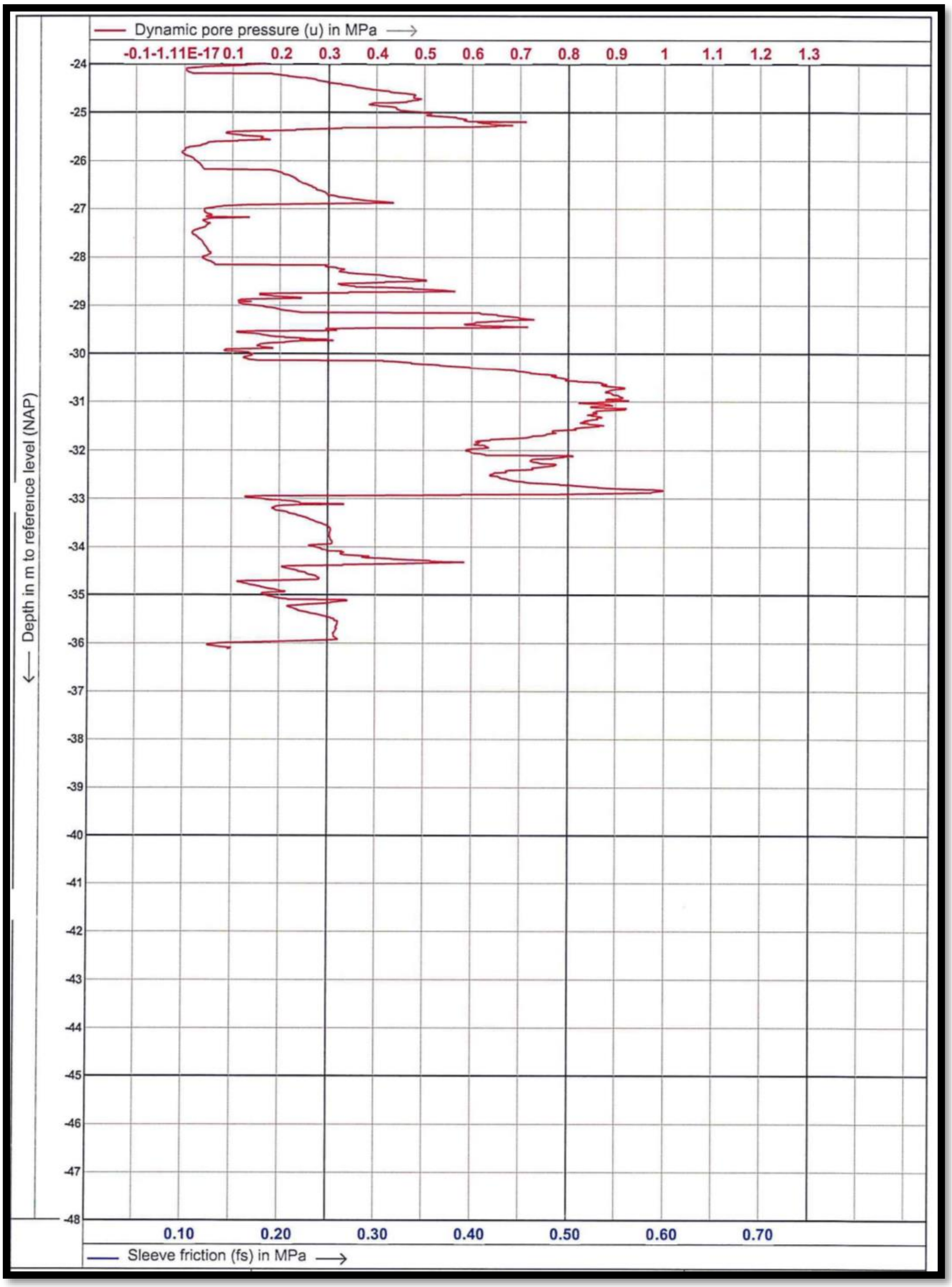

Figure B1.4. Dynamic Pore Pressure from 24 m to 36 m

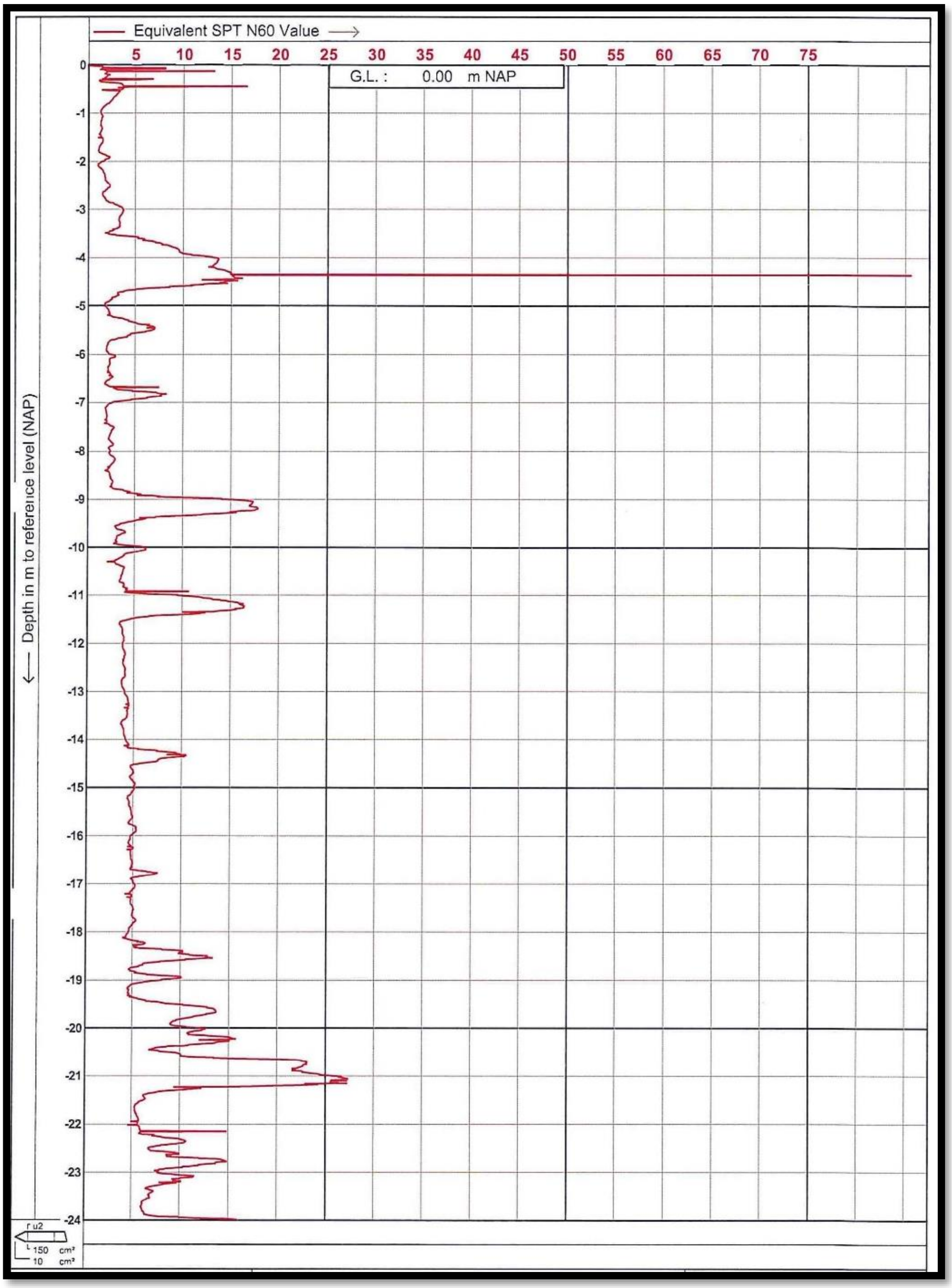

Figure B1.5. Equivalent SPT N60 Value from 0 m to 24 m

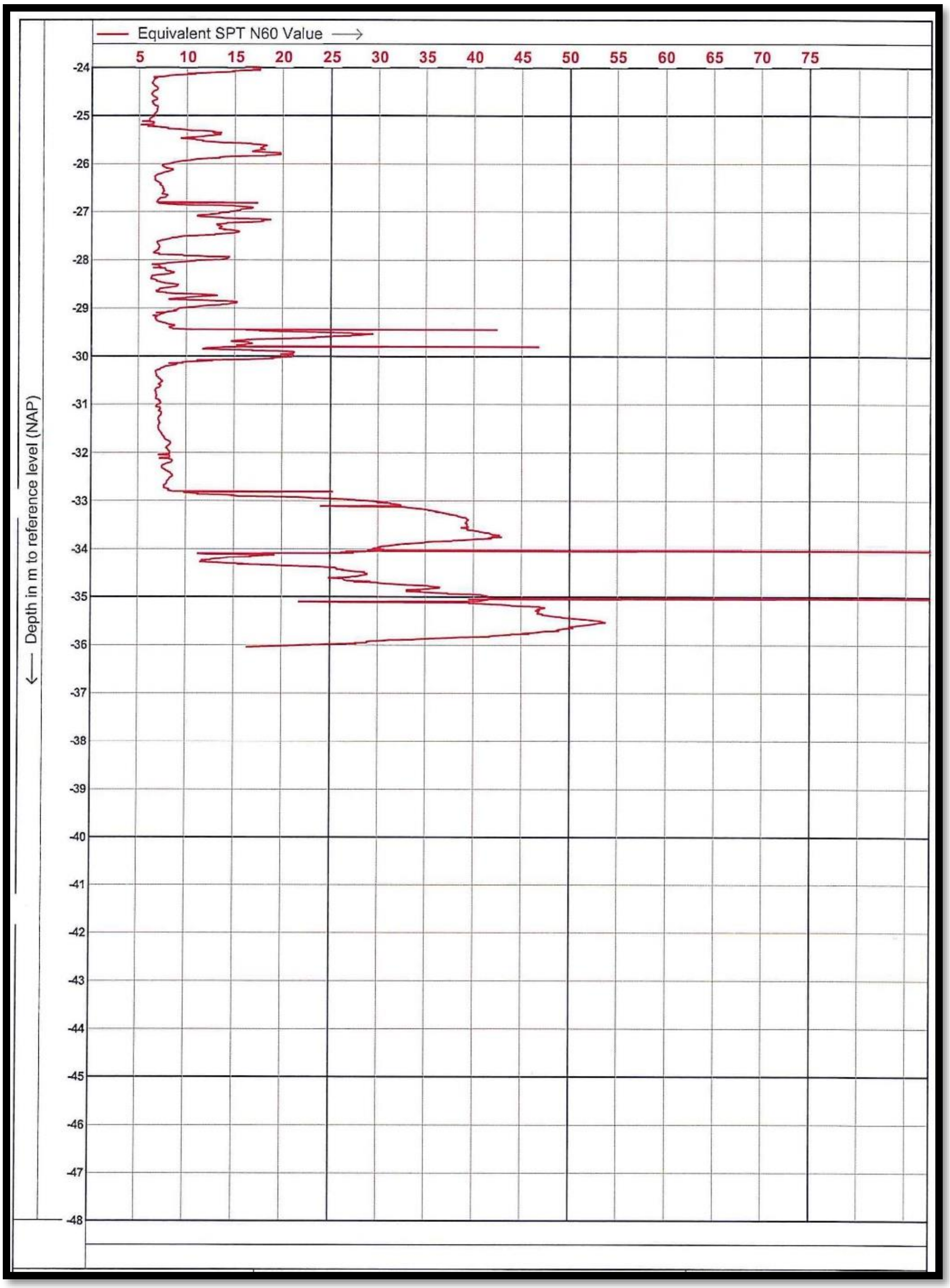

Figure B1.6. Equivalent SPT N60 Value from 24 m to 36 m

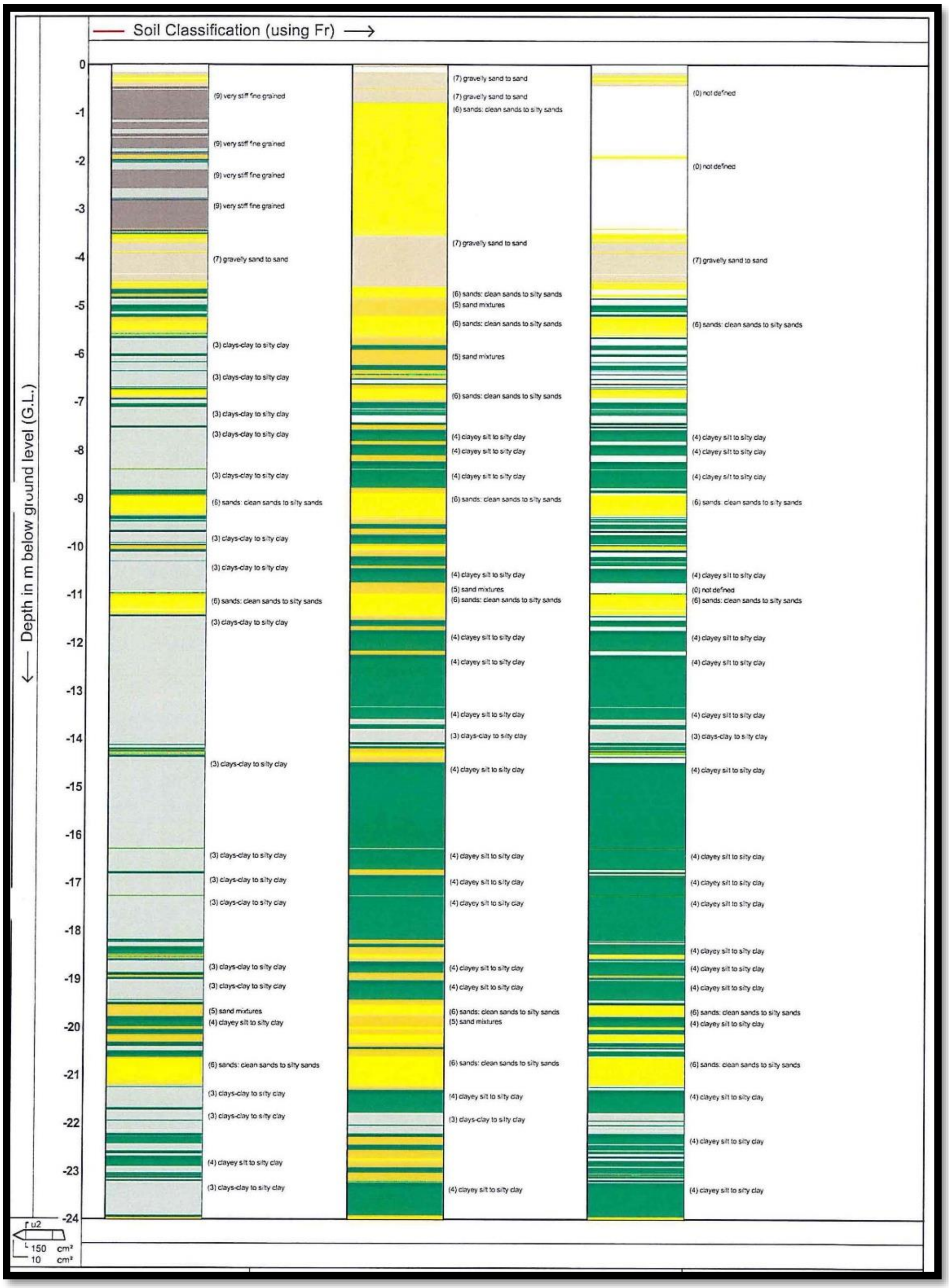

Figure B1.7. Soil Classification from 0 m to 24 m

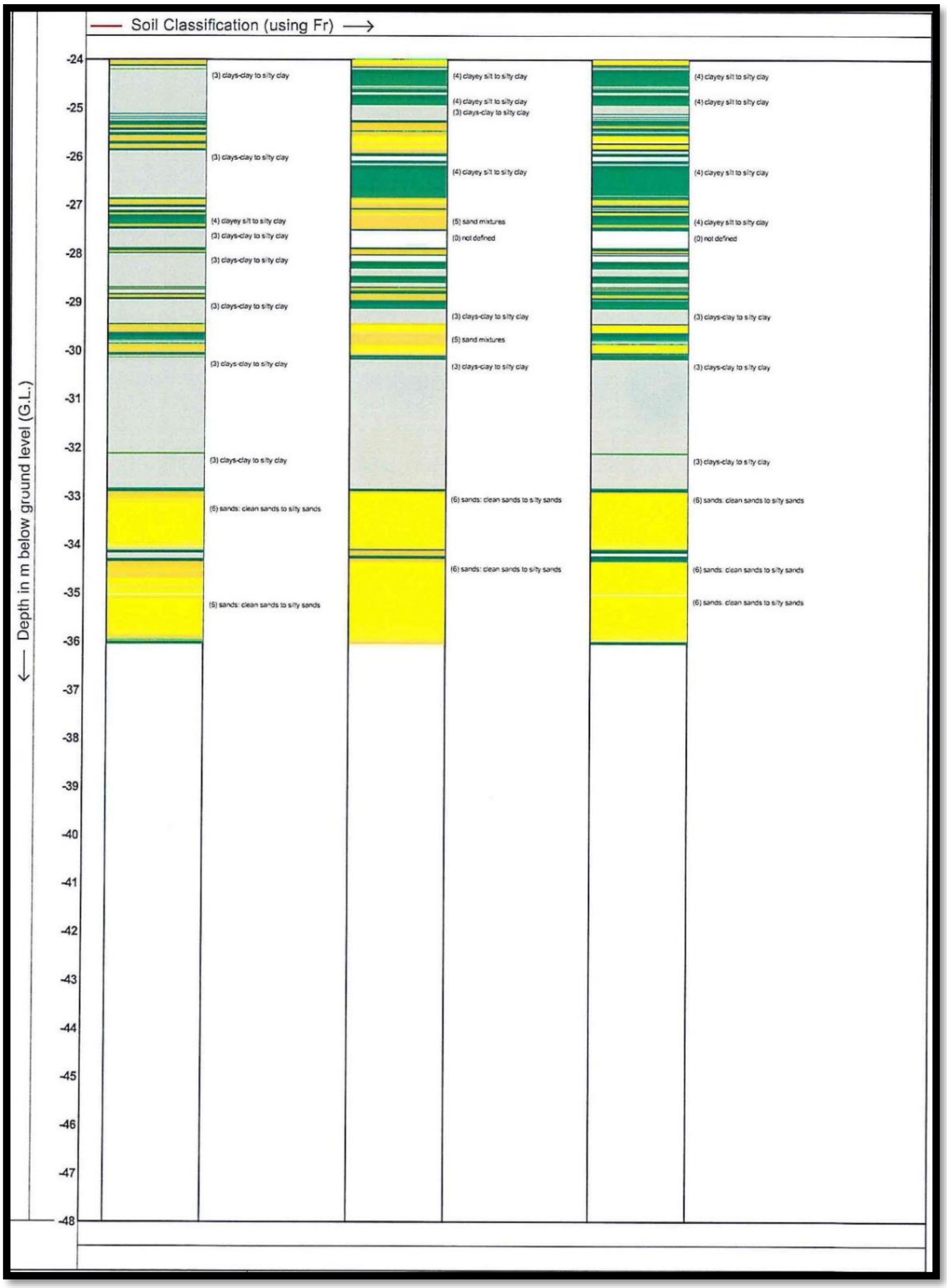

Figure B1.8. Soil Classification from 24 m to 36 m

APPENDIX B2

CONE PENETRATION TEST 2

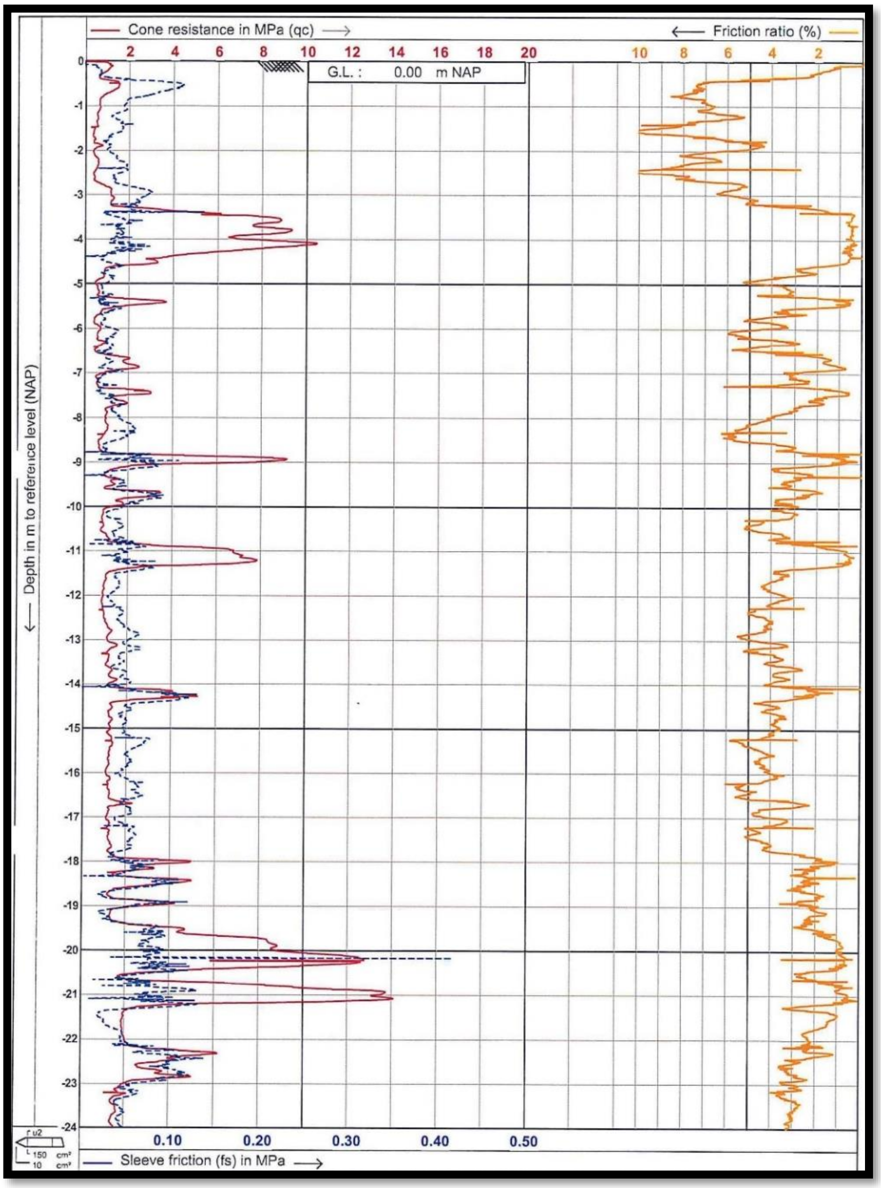

Figure B2.1. Cone Resistance and Skin Friction from 0 m to 24 m

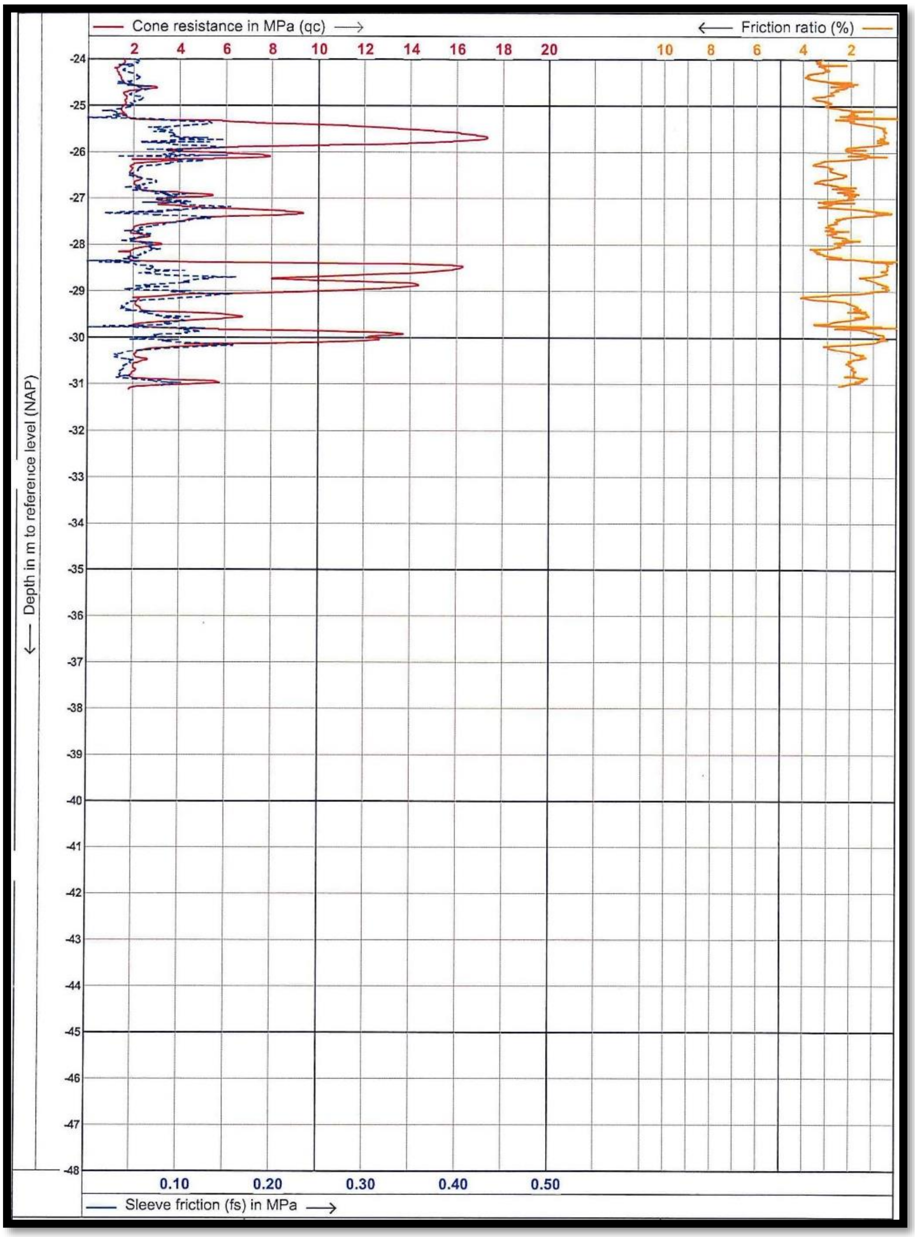

Figure B2.2. Cone Resistance and Skin Friction from 24 m to 36 m

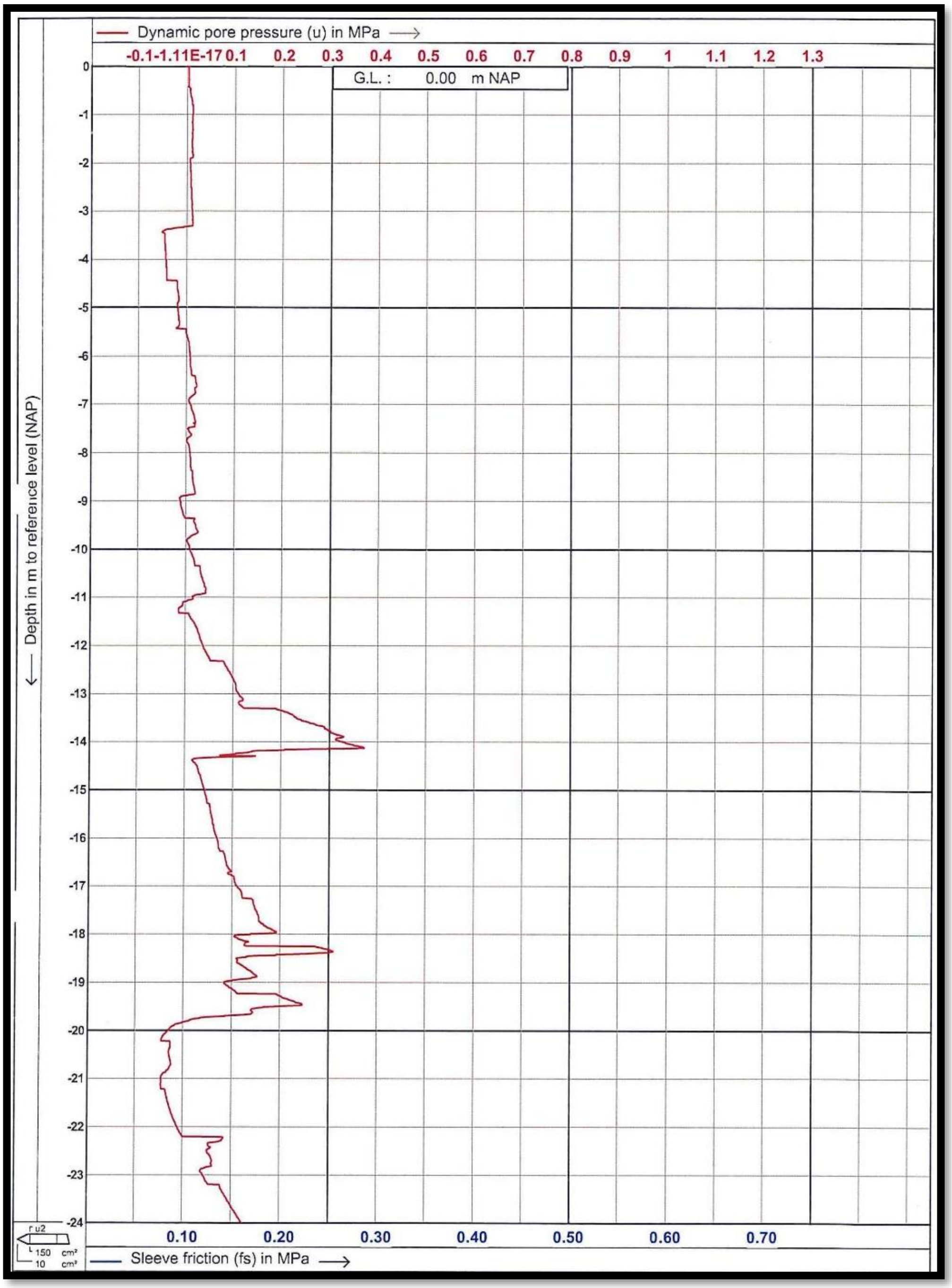

Figure B2.3. Dynamic Pore Pressure from 0 m to 24 m

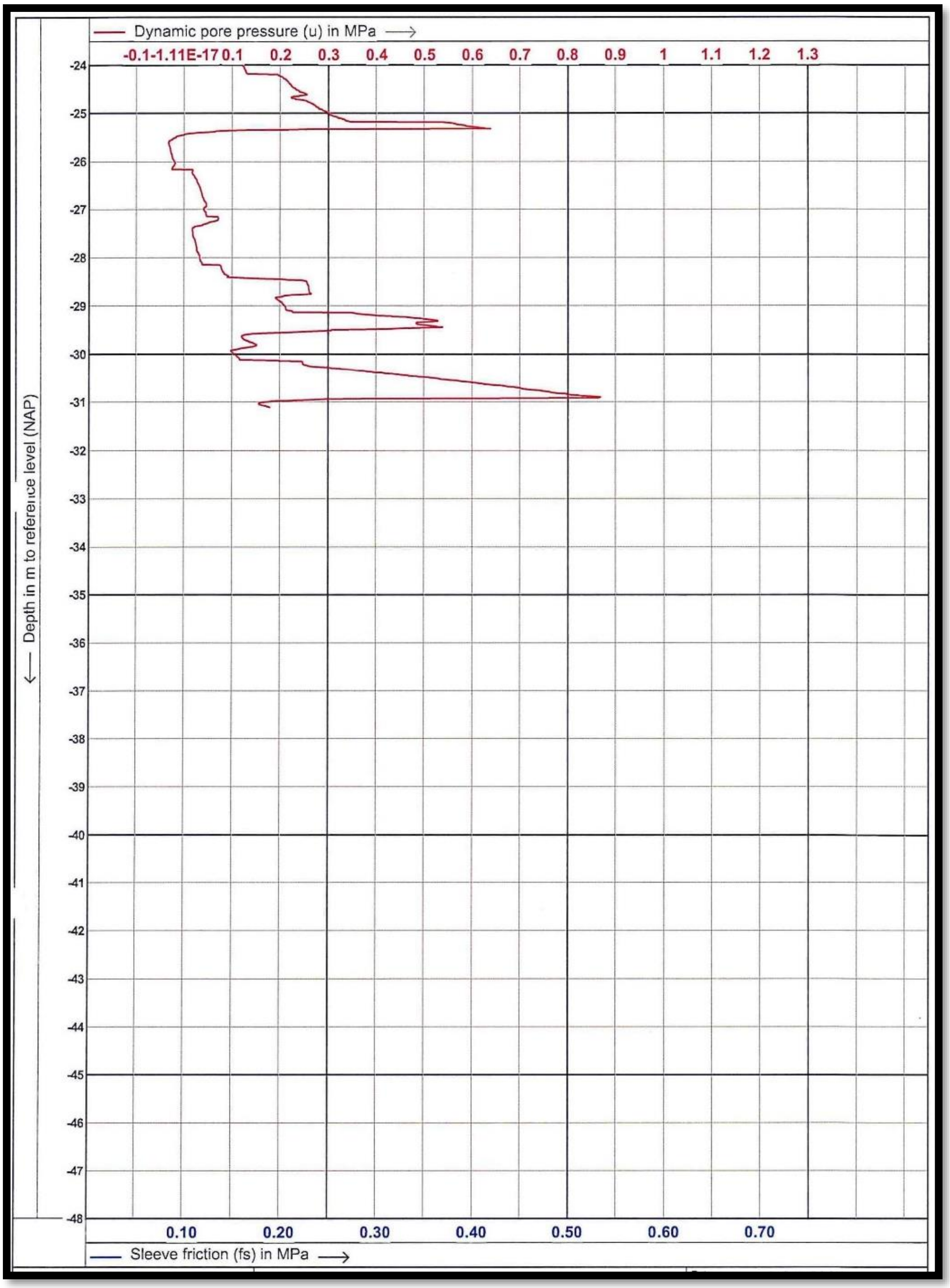

Figure B2.4. Dynamic Pore Pressure from 24 m to 36 m

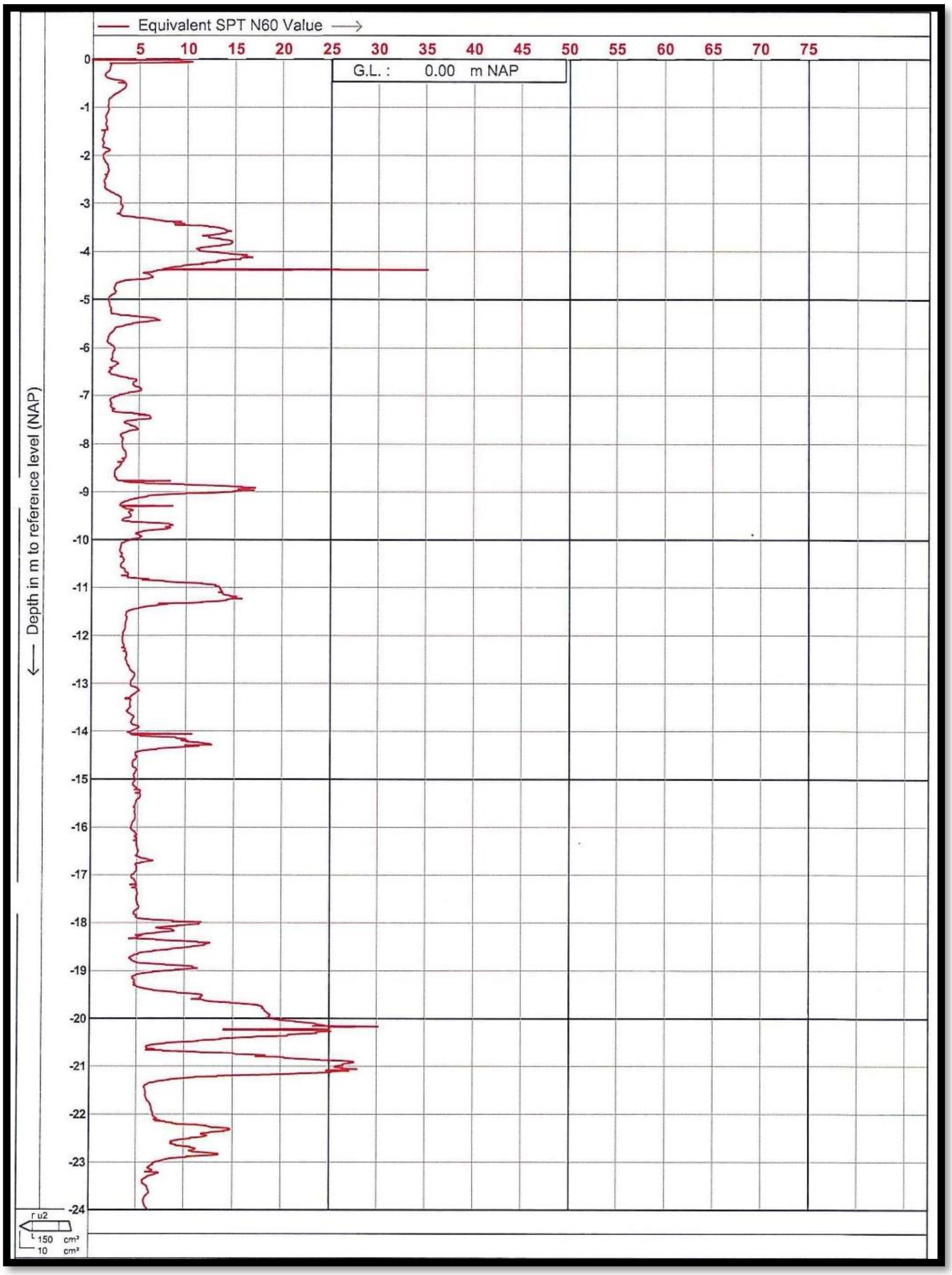

Figure B2.5. Equivalent SPT N60 Value from 0 m to 24 m

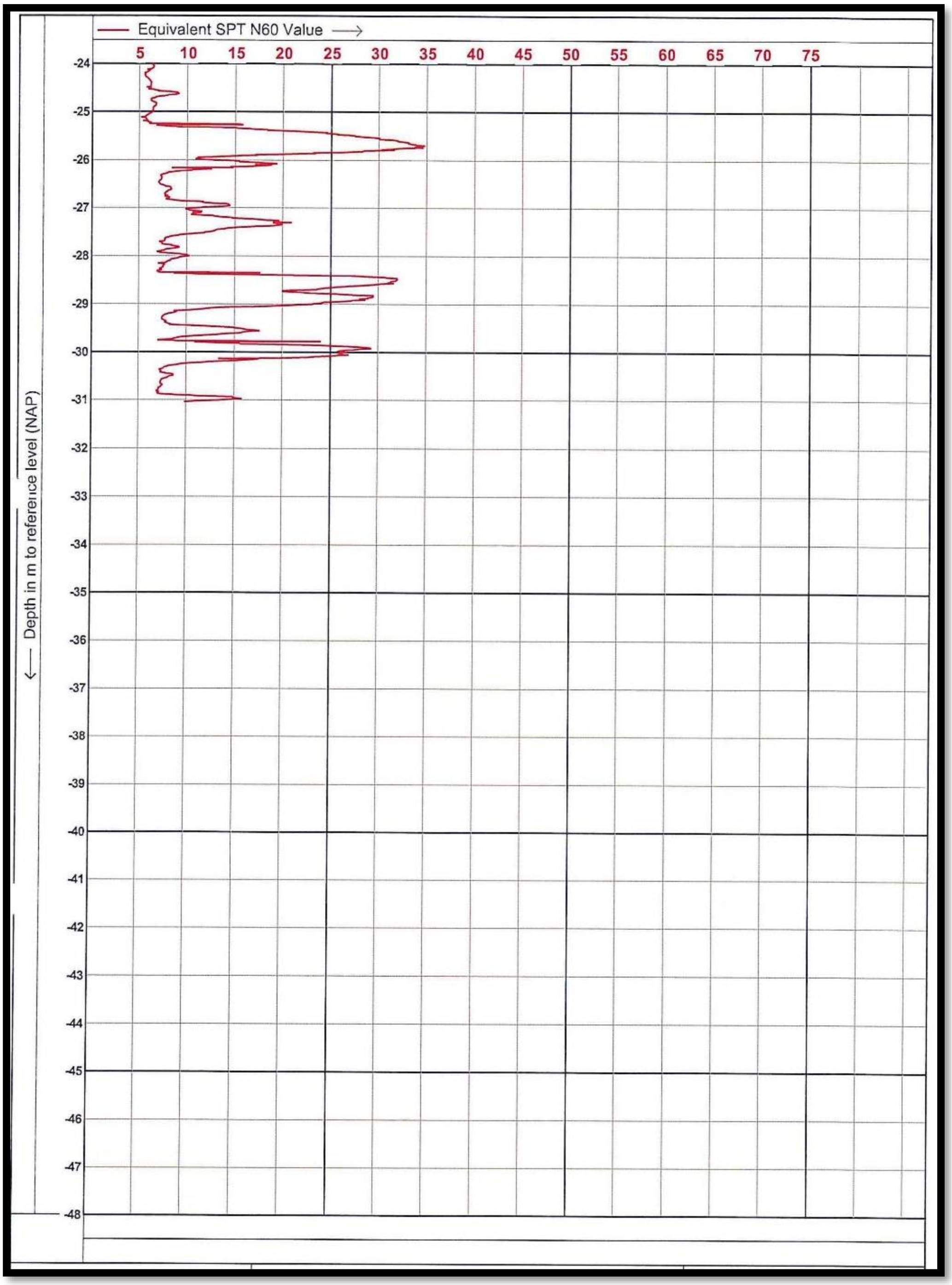

Figure B2.6. Equivalent SPT N60 Value from 24 m to 30 m

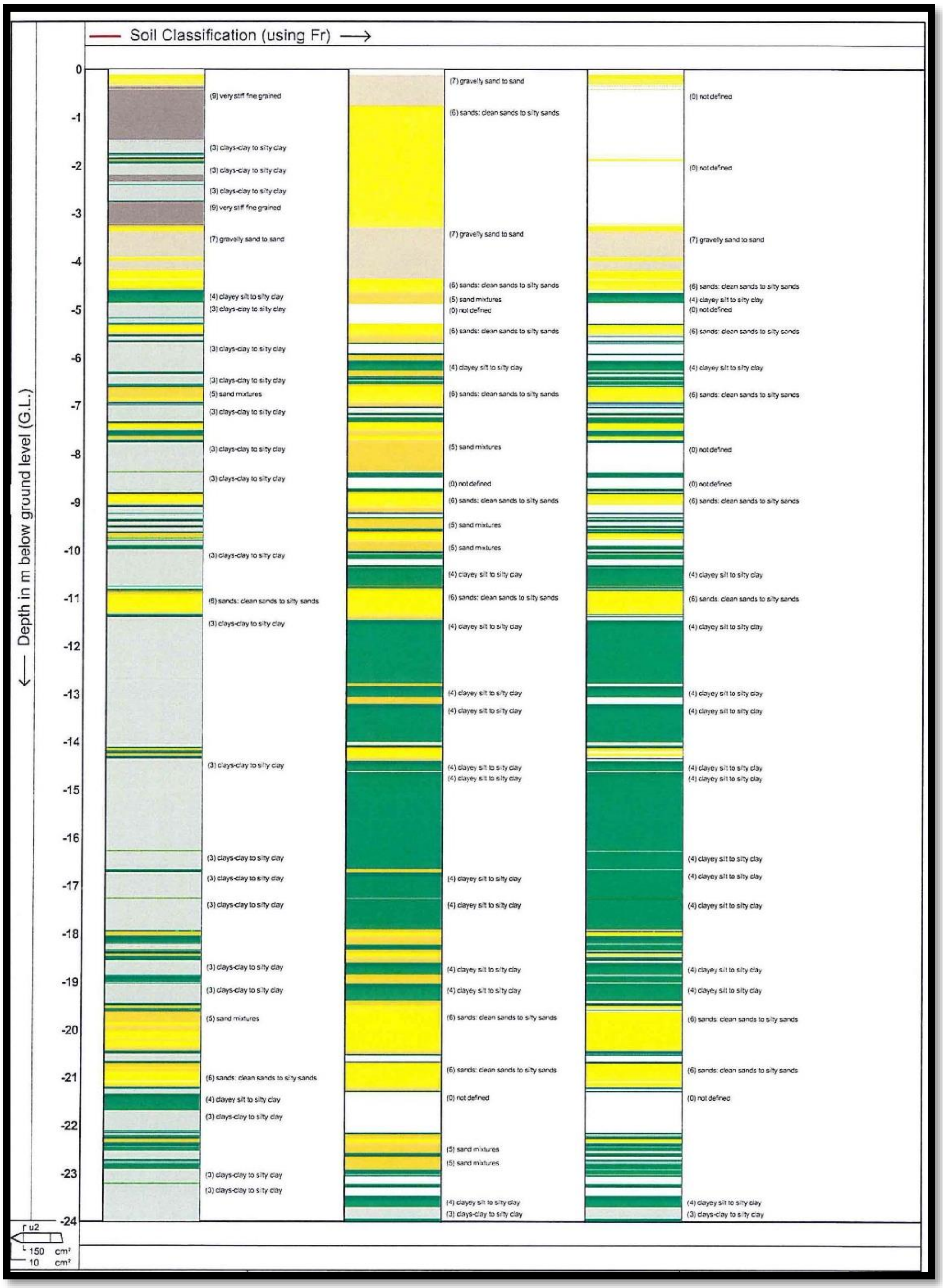

Figure B2.7. Soil Classification from 0 m to 24 m

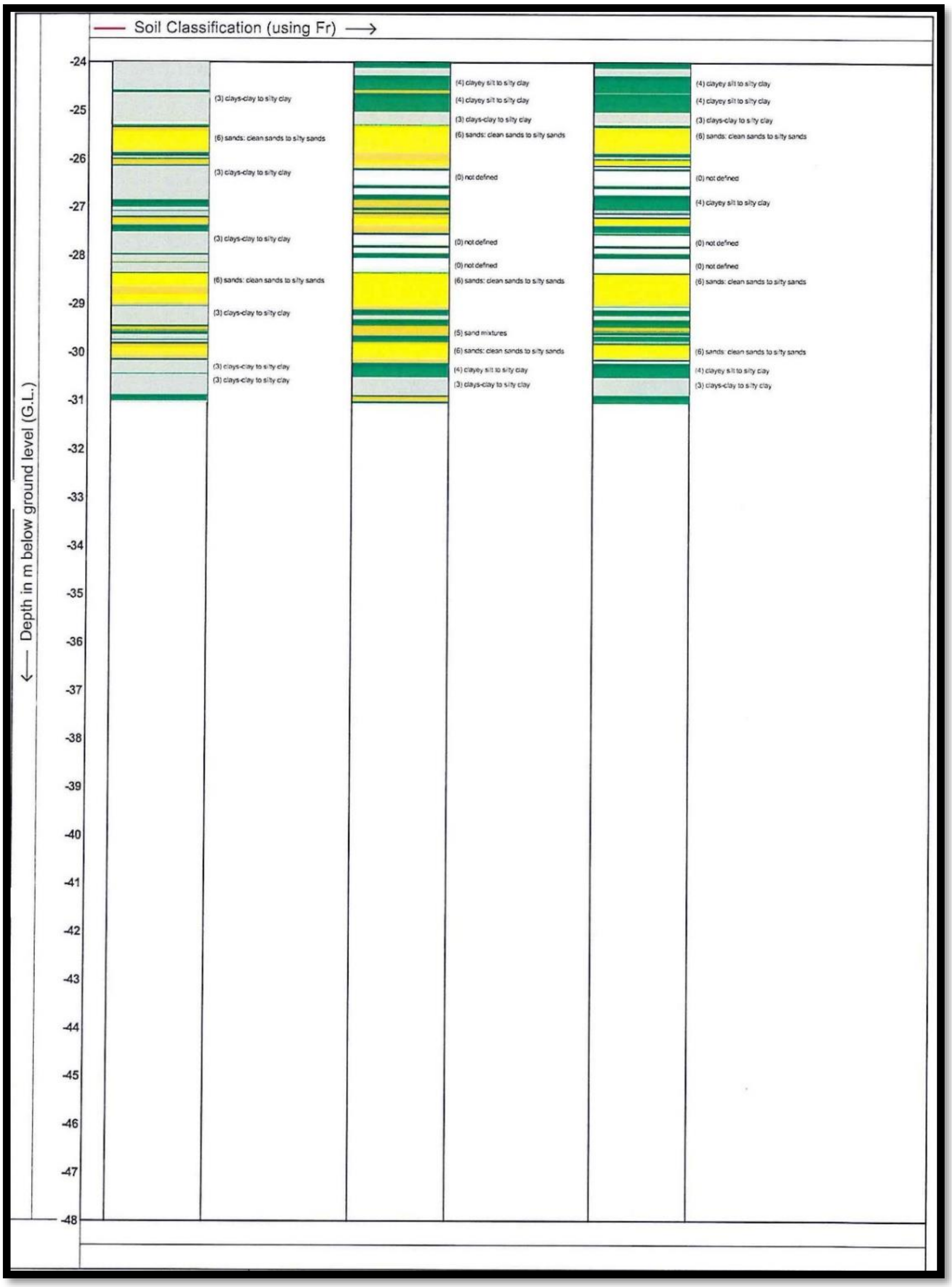

Figure B2.8. Soil Classification from 24 m to 31 m

APPENDIX C

PRESSUREMETER TEST

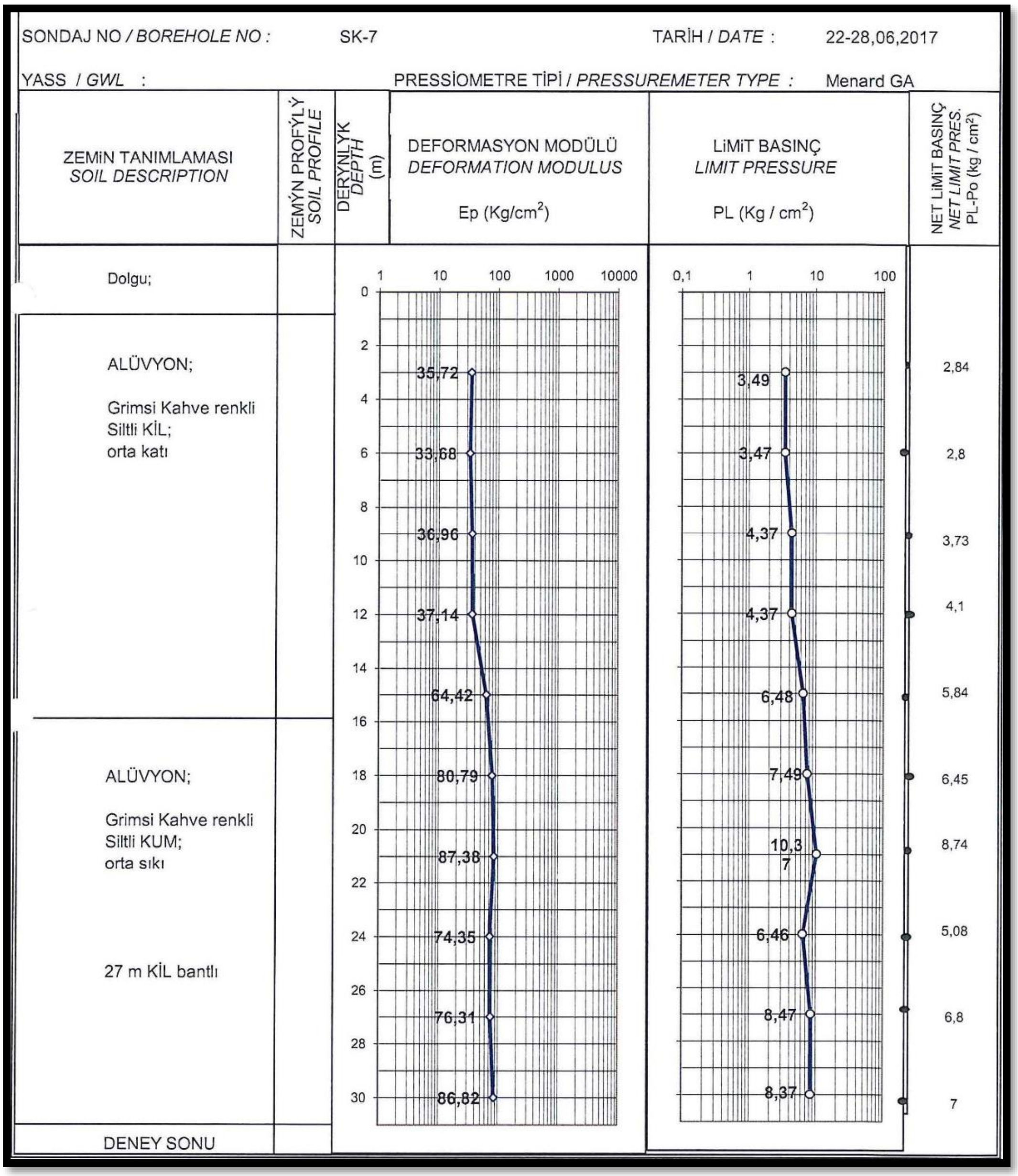

Figure C.1. Pressuremeter Test Results at SK-7

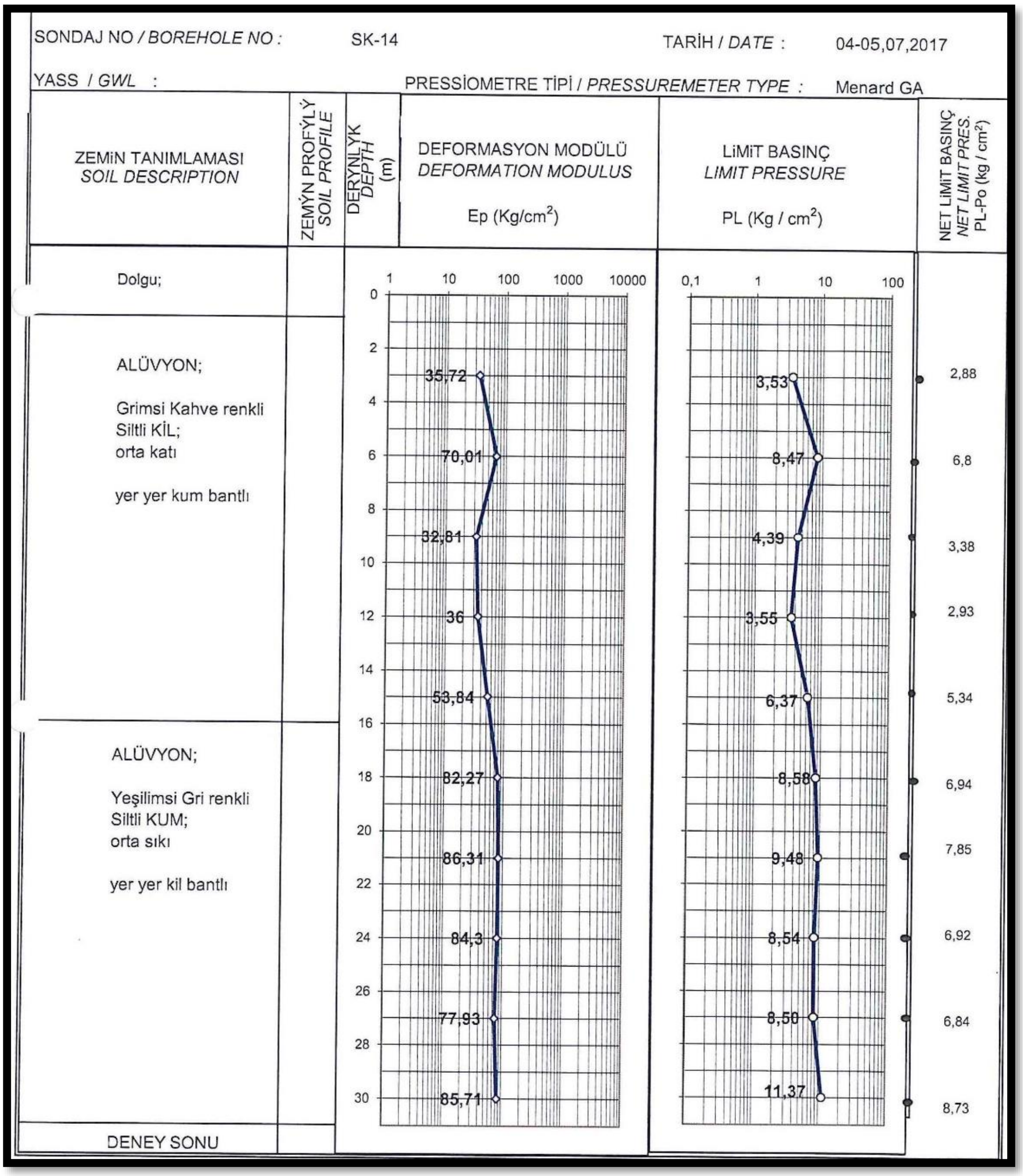

Figure C.2. Pressuremeter Test Results at SK-14

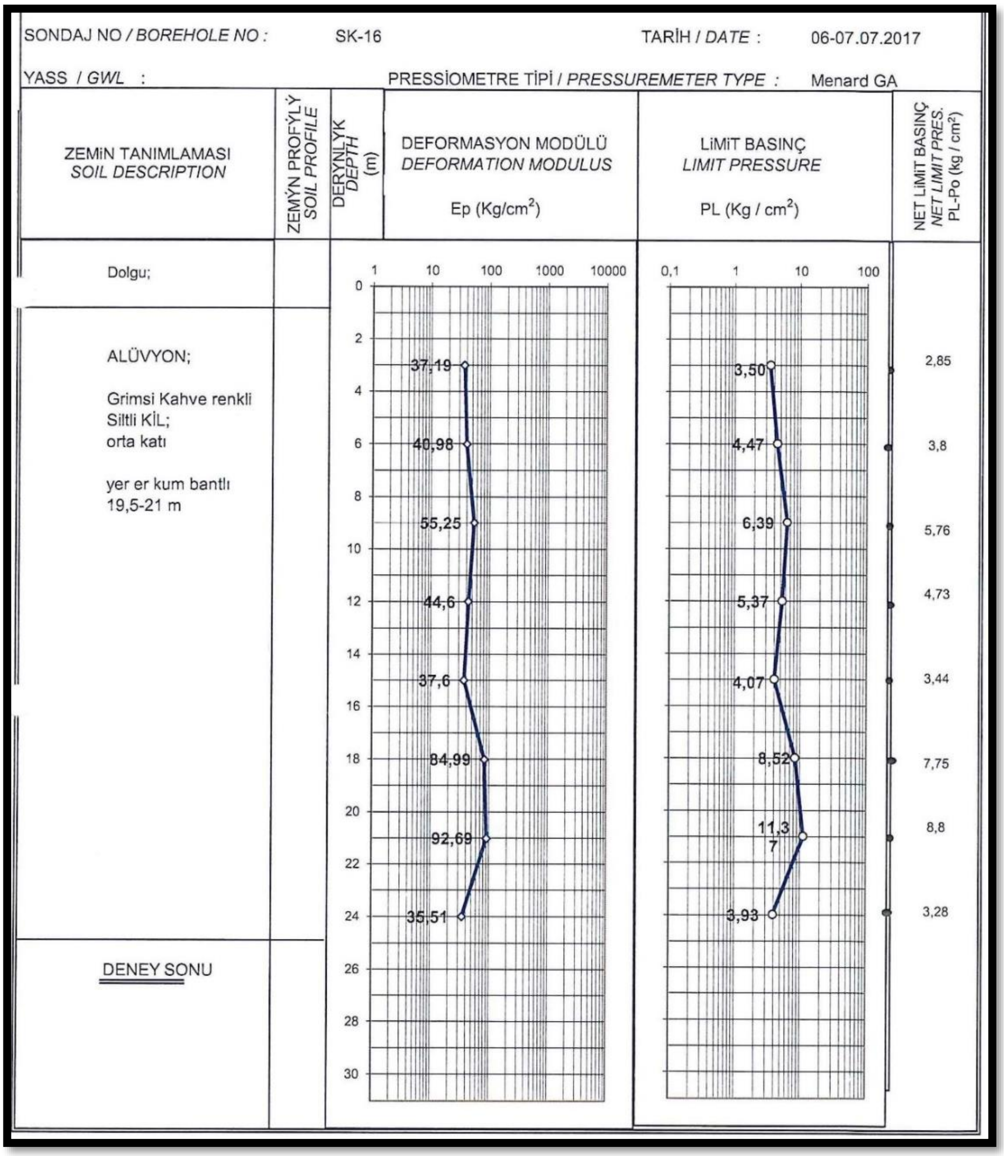

Figure C.3. Pressuremeter Test Results at SK-16

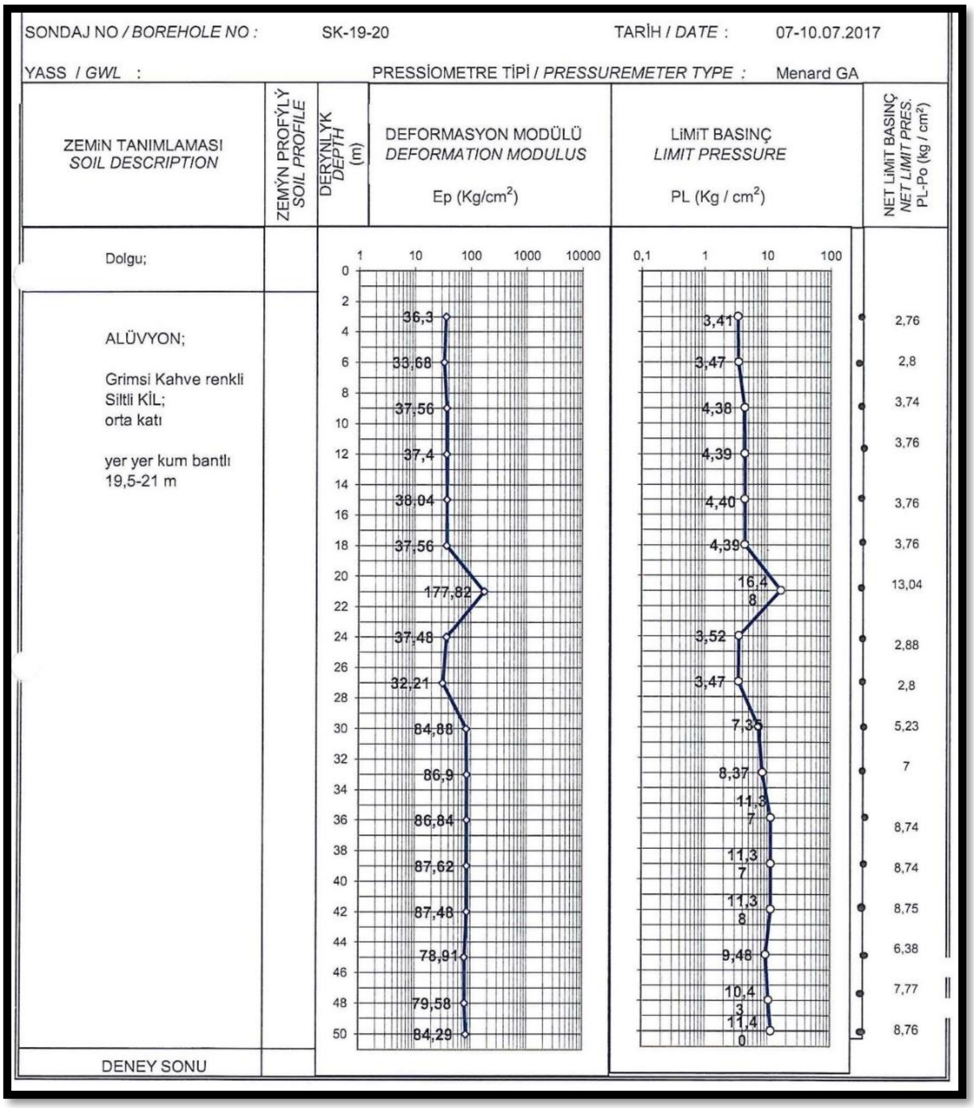

Figure C.4. Pressuremeter Test Results at SK-19-20

APPENDIX D

PLATE LOAD TEST

Plate Load Test: Plot of Settlement v. Pressure Page : 1

Location:	The Geothermal Project	Ground Elevation :	
Site :	ACC - Turbine Generator	Plate Diameter : 76.00cm	
Plate Depth :	0,50m	Date :	11.10.2017
Weather :	Sunny	Dry / Wet:	Dry
Test No:	**PMT**		

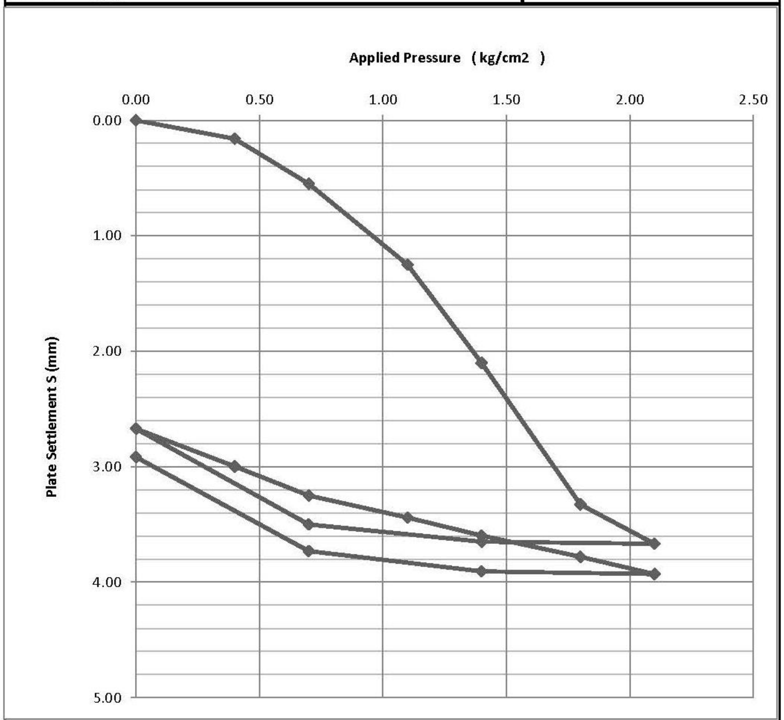

Remarks

Deformation Module: *Ev = [0,75 x D x ($\Delta\sigma$ / ΔS)], kg/cm^2

	σ_{02} kgf/cm^2	σ_{01} kgf/cm^2	$\Delta\sigma$ kgf/cm^2	S_2 cm	S_1 cm	ΔS cm	**$*E_{v1}$ Mpa**	**$*E_{v2}$ Mpa**
$*E_{v1}$	1.80	1.10	0.70	0.333	0.263	0.070	**57.00**	
$*E_{v2}$	1.40	0.70	0.70	0.365	0.350	0.015		**266.00**
	E_{v2}/E_{v1} =	**4.67**						

Deformation Module: *Ev = [0,75 x D x ($\Delta\sigma$ / ΔS)], kg/cm^2

	σ_{02} kgf/cm^2	σ_{01} kgf/cm^2	$\Delta\sigma$ kgf/cm^2	S_2 cm	S_1 cm	ΔS cm	**$*E_{v3}$ Mpa**	**$*E_{v4}$ Mpa**
$*E_{v3}$	1.80	1.10	0.70	0.378	0.344	0.034	**117.35**	
$*E_{v4}$	1.40	0.70	0.70	0.391	0.373	0.018		**221.67**
	E_{v4}/E_{v3} =	**1.89**						

Performed by : Hakan ELMAS

Checked By:Mümin Şen

Figure D.1. Plate Load Test Results

APPENDIX E

CONSOLIDATION TESTS

KONSOLİDASYON DENEY RAPORU

Ring No.	1	Ring+Yas Num Ağır.(g	193,08	Özgül Ağırlık Gs (gr/cm³)	2,70		Rapor No: EF17/16516
						SONDAJ NO: SK-2	SAYFA NO: 17
							Rapor Tarihi 02.08.2017
Çap (cm)	6,35	Ring+Kuru Num Ağır.(g	160,46	19		NUMUNE NO: UD	PAFTA 0
				$H_s = W_s / g_s A$ (cm)	1,041	DERİNLİK: 6,00-6,50	ADA 0
Kesit Alanı A (cm²)	31,65	Ring Ağırlığı (gr)	71,51	Boşluk Oranı $e_o=(h_o-h_s)/h_s=$	0,922		PARSEL 0
Yükseklik $h_{o(cm)}$	2,00	Kuru Num Ağ.W_s (gr)	88,95	Su muhtevası $Wo=W_{su}/W_s$	36,67%		İLİ AYDIN
Hacim,V_o(cm³)	63,31	Su ağırlığı W_{su} gr)	32,62	Doygunluk Derecesi			İLÇE İNCİRLİOVA / OSMANBÜKÜ MAH
		Birim Ağır.(gr/cm³)	1,920	$Sr = G_s\ Wo/e_o$ (%)	107,44%		BRN:13046622

Tatbik Edilen Basınç kg/cm²	Oturma cm	Numune Yüksekliği $h=h_o-e$ cm	Boşluk Yüksekliği $h_v=h-h_s$	Boşluk Oranı $e=h_v/h_s$	Boşluk Oranı Değişimi	Basınç Artışı kg/cm²	Sıkıştırma Kat Sayısı $a_v= e/s$ cm²/kg	Hacımsal Sıkışma Katsayısı $mv=av/(1+e)$ cm²/kg	Oturma Zamanı sn t_{50}	Oturma Zamanı sn t_{90}	Konsolidasyon Katsayısı Cv(cm²/sn) $0.049\ h^2$ t_{50}	Konsolidasyon Katsayısı Cv(cm²/sn) $0.212\ h^2$ t_{90}	Permeabilite $k=mv.cv.g_w$ cm/sn 10^{-4}	Düşünceler
0	0	2	0,9592	0,9216										
0,25	0,0703	1,9297	0,8889	0,8541	0,0675	0,25	0,2702	0,1406		45		0,0175	24,6654056	
0,5	0,1222	1,8778	0,8370	0,8042	0,0499	0,25	0,1995	0,1076		45		0,0166	17,8714409	
1	0,1832	1,8168	0,7760	0,7456	0,0586	0,5	0,1172	0,0650		45		0,0156	10,1029473	
2	0,2605	1,7395	0,6987	0,6713	0,0743	1	0,0743	0,0425		60		0,0107	4,5488943	
4	0,3486	1,6514	0,6106	0,5867	0,0846	2	0,0423	0,0253		60		0,0096	2,4401170	
8	0,4252	1,5748	0,5340	0,5131	0,0736	4	0,0184	0,0116		60		0,0088	1,0161362	
1	0,4355	1,5645	0,5237	0,5032	-0,0099	1	-0,0099							
0,25	0,3922	1,6078	0,5670	0,5448	0,0416	0,25	0,1664							

0,25	0,5	1	2	4	8	1	0,25
0,8541	0,8042	0,7456	0,6713	0,5867	0,5131	0,5032	0,5448

Figure E.1. Consolidation Test Results for SK-2

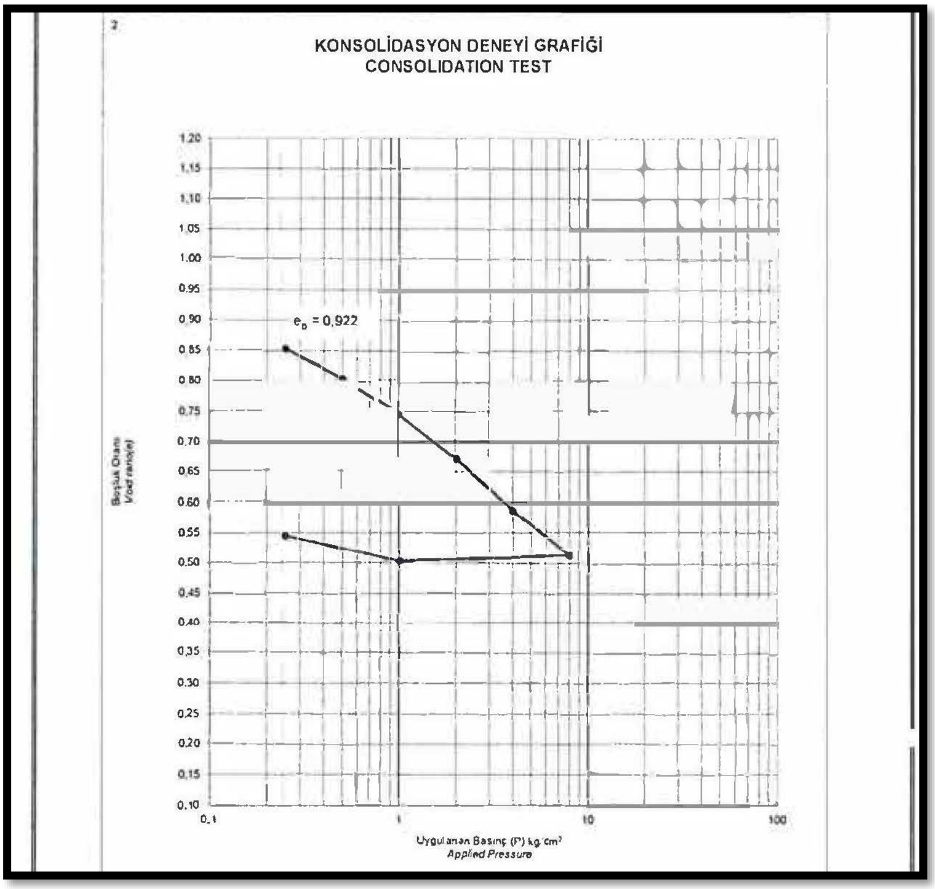

Figure E.2. Consolidation Test Graph for SK-2

KONSOLİDASYON DENEY RAPORU

Ring No.	1	Ring+Yas Num Ağır.(g	189,14	Ozgul Ağırlık Gs (gr/cm³)	2,72
Çap (cm)	6,35	Ring+Kuru Num Ağır.(g	167,46	19	
				$H_s = W_k / g_s A$ (cm)	1,114
Kesit Alanı A (cm²)	31,65	Ring Ağırlığı (gr)	71,51	Boşluk Oranı $e_o=(h_o-h_s)/h_s=$	0,755
Yukseklik $h_{o(cm)}$	2,00	Kuru Num Ağ W_k (gr)	95,95	Su muhtevası $Wo=W_{su}/W_k$	22,60%
Hacim,V_o(cm³)	63,31	Su ağırlığı W_{su} (gr)	21,68	Doygunluk Derecesi	
		Birim Ağır.(gr/cm³)	1,858	$Sr = G_s Wo/e_o$ (%)	77,34%

SONDAJ NO:	SK-6			Rapor No	EF17/16516
NUMUNE NO:	UD	PAFTA	0	SAYFA NO.	21
DERİNLİK:	16,50-17,00	ADA	0	Rapor Tarihi	02.08.2017
		PARSEL	0		
		İLİ	AYDIN		
		İLÇE	İNCİRLİOVA / OSMANBÜKÜ MAH.		
		BRN:13046622			

Tatbik Edilen Basınç kg/cm²	Oturma cm	Numune Yüksekliği $h=h_o-e$ cm	Boşluk Yüksekliği $h_b=h-h_k$	Boşluk Oranı $e=h_b/h_k$	Boşluk Oranı Değişimi e	Basınç Artışı kg/cm²	Sıkıştırma Kat Sayısı $a_v= e/s$ cm²/kg	Hacimsal Sıkışma Katsayısı $mv=av/(1+e)$ cm²/kg	Oturma Zamanı sn t_{50}	Oturma Zamanı sn t_{90}	Konsolidasyon Katsayısı Cv(cm²/sn) $0.049 h^2 / t_{50}$	Konsolidasyon Katsayısı Cv(cm²/sn) $0.212 h^2 / t_{90}$	Permeabilite $k=mv.cv.g_w$ cm/sn 10^{-4}	Düşünceler
0	0	2	0,8856	0,7946										
0,25	0,0710	1,9290	0,8146	0,7309	0,0637	0,25	0,2548	0,1420		45		0,0175	24,8929374	
0,5	0,1328	1,8672	0,7528	0,6755	0,0555	0,25	0,2218	0,1281		45		0,0164	21,0485054	
1	0,1906	1,8094	0,6950	0,6236	0,0519	0,5	0,1037	0,0619		45		0,0154	9,5490356	
2	0,2624	1,7376	0,6232	0,5592	0,0644	1	0,0644	0,0397		60		0,0107	4,2332516	
4	0,3458	1,6542	0,5398	0,4843	0,0748	2	0,0374	0,0240		60		0,0097	2,3203147	
8	0,4614	1,5386	0,4242	0,3806	0,1037	4	0,0259	0,0175		60		0,0084	1,4613219	
1	0,4386	1,5614	0,4470	0,4011	0,0205	1	0,0205							
0,25	0,3888	1,6112	0,4568	0,4457	0,0447	0,25	0,1787							

0,25	0,5	1	2	4	8	1	0,25
0,7309	0,6755	0,6236	0,5592	0,4843	0,3806	0,4011	0,4457

Figure E.3. Consolidation Test Results for SK-6

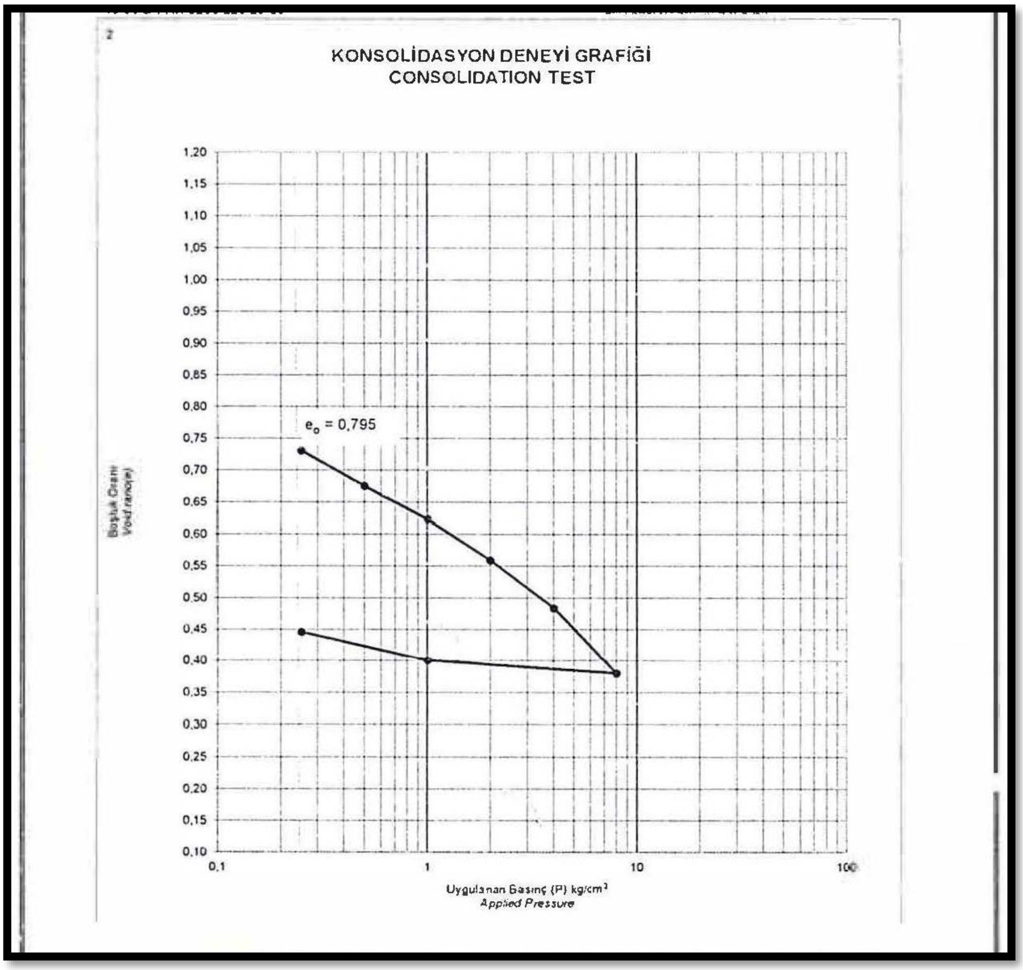

Figure E.4. Consolidation Test Results for SK-6

KONSOLİDASYON DENEY RAPORU

Ring No	1	Ring+Yaş Num Ağır.(c	191.16	Özgül Ağırlık Gs (gr/cm^3)	2,69		Rapor No: EF17/16516
							SAYFA NO: 12
						SONDAJ NO: SK-25	Rapor Tarihi 02.08.2017
Çap (cm)	6,35	Ring+Kuru Num Ağır.(g	160,03	19		NUMUNE NO: UD	PAFTA 0
				$H_s = W_s / g_s A$ (cm)	1.040	DERİNLİK: 4,50-5,00	ADA 0
Kesit Alanı A (cm^2)	31,65	Ring Ağırlığı (gr)	71,51	Boşluk Oranı $e_o=(h_o-h_s)/h_s=$	0,924		PARSEL 0
Yükseklik $h_{o(cm)}$	2,00	Kuru Num.Ağ.W_s (gr)	88.52	Su muhtevası $Wo=W_{su}/W_s$	35,17%		İLİ AYDIN
Hacim.V_o(cm^3)	63,31	Su ağırlığı W_{su} (gr)	31,13	Doygunluk Derecesi			İLÇE İNCİRLİOVA / OSMANBÜKÜ MAH.
		Birim Ağır.(gr/cm^3)	1,890	Sr = G_s Wo/e_o (%)	102,40%		BRN:13046622

Tatbik Edilen Basınç kg/cm^2	Oturma cm	Numune Yüksekliği $h=h_o-e$ cm	Boşluk Yüksekliği $h_b=h-h_s$	Boşluk Oranı $e=h_b/h_s$	Boşluk Oranı Değişimi e	Basınç Artışı kg/cm^2	Sıkıştırma Kat Sayısı $a_v = e/s$ cm^2/kg	Hacımsal Sıkışma Katsayısı mv=av/(1+e) cm^2/kg	Oturma Zamanı sn t_{50}	Oturma Zamanı sn t_{90}	Konsolidasyon Katsayısı Cv(cm^2/sn) 0.049 h^2 / t_{50}	Konsolidasyon Katsayısı Cv(cm^2/sn) 0.212 h^2 / t_{90}	Permeabilite k=mv.cv.g_w cm/sn 10^{-4}	Düşünceler
0	0	2	0,9604	0,9238										
0,25	0,0820	1,9180	0,8784	0,8449	0,0789	0,25	0,3155	0,1640		45		0,0173	28,4226391	
0,5	0,1142	1,8858	0,8462	0,8139	0,0310	0,25	0,1239	0,0672		45		0,0168	11,2507603	
1	0,1732	1,8268	0,7872	0,7572	0,0568	0,5	0,1135	0,0626		45		0,0157	9,8376582	
2	0,2444	1,7556	0,7160	0,6887	0,0685	1	0,0685	0,0390		60		0,0109	4,2444825	
4	0,3784	1,6216	0,5820	0,5598	0,1289	2	0,0644	0,0382		60		0,0093	3,5458578	
8	0,4943	1,5057	0,4661	0,4483	0,1115	4	0,0279	0,0179		60		0,0080	1,4313348	
1	0,4564	1,5436	0,5040	0,4848	0,0365	1	0,0365							
0,25	0,4018	1,5982	0,5586	0,5373	0,0525	0,25	0,2101							

0,25	0,5	1	2	4	8	1	0,25
0,8449	0,8139	0,7572	0,6887	0,5598	0,4483	0,4848	0,5373

Figure E.5. Consolidation Test Results for SK-25

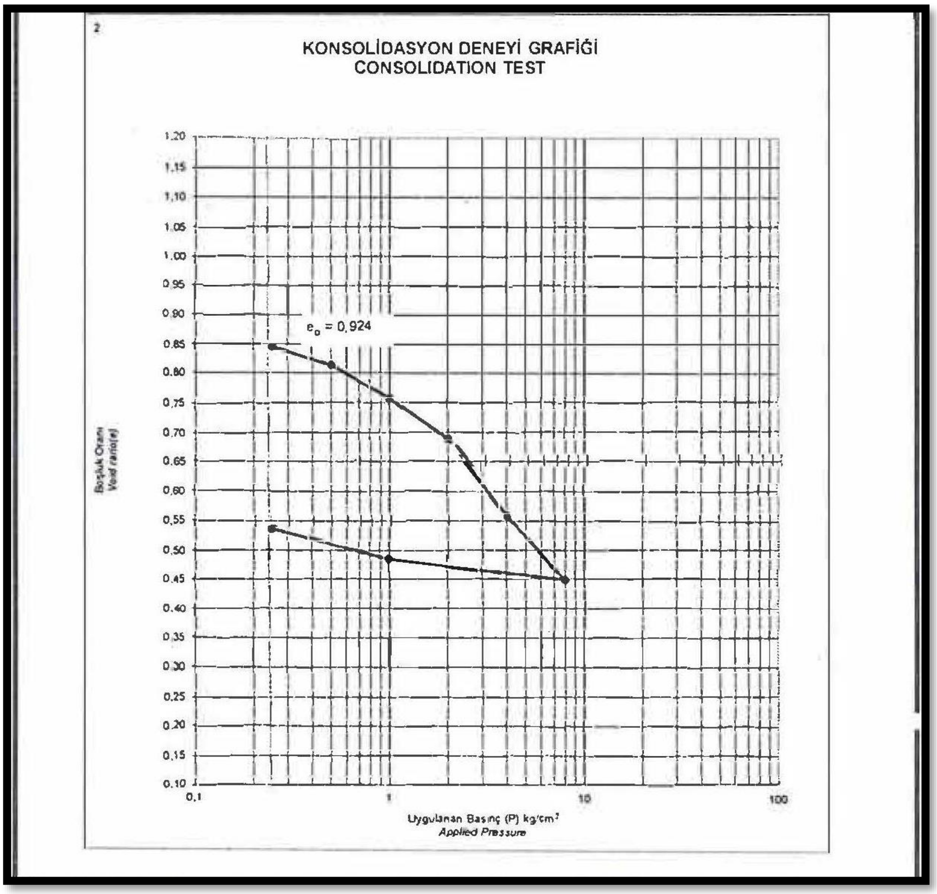

Figure E.6. Consolidation Test Results for SK-25

APPENDIX F

SOIL EXPERIMENTS

SONDAJ BORING NO	NUMUNE SAMPLE NO	DERİNLİK DEPTH (m)	Wn %	γ_n kN/m3	γ_K kN/m3	Gs	LL	PL	PI	RÖTRE LİMİT %	10 (+) (%)	200 (-) (%)	ZEMİN SINIFLANDIRMA TS 1500	Hidrometre kil %	Hidrometre silt %	KESME KUTUSU DENEYİ DIRECT SHEAR TEST c kPa	KESME KUTUSU ø Deg.	ÜÇ EKSENLİ BASINÇ DENEYİ TRIAXIAL COMPRESSION TEST c kPa	ÜÇ EKSENLİ ø Deg		TEK EKSENLİ BASINÇ DAYANIMI (ZEMİN) UNCONFINED COMP. TEST q_u kPa	q_r kPa	NOKTA YÜKÜ DAYANIMI İNDEKSİ ISRM 1981 Is (50) kg/cm²	TEK EKSENLİ BASINÇ DAYANIMI (KAYA) TS EN 1926 Mpa	KONSOLİDASYON DENEYİ CONSOLIDATION TEST Şişme Basıncı kPa	Şişme Swell (%)	PROKTOR SIKIŞTIRMA DENEYİ PROCTOR TEST γK Max g/cm³	Wopt %	Tabii Boşluk Oranı e %	Tabii Porosite n %
SK-1	SPT	3,00-3,45	35,35				52,18	20,60	31,58		0,00	95,82	CH																	
SK-1	UD	4,50-5,00	32,08	18,26			N.P.	N.P.	N.P.		0,00	9,27	SP-SM			0	26			UU										
SK-1	SPT	9,00-9,45	25,17				N.P.	N.P.	N.P.		0,00	47,61	SM																	
SK-1	SPT	16,50-16,95	44,56				59,44	28,00	31,44		0,00	98,66	CH																	
SK-1	SPT	21,00-21,45	31,50				37,26	18,89	18,37		0,33	93,73	CI																	
SK-1	SPT	25,50-25,95	33,02				58,46	24,71	33,75		0,00	87,77	CH																	
SK-1	SPT	28,50-28,95	28,81				N.P	N.P	N.P		0,00	62,23	ML																	
SK-2	SPT	3,00-3,45	30,66				51,69	20,19	31,50		0,00	82,02	CH																	
SK-2	UD	6,00-6,50	30,34	18,14		2,70	34,38	21,35	13,03		0,00	97,26	CL					33	4	UU					X	X				
SK-2	SPT	9,00-9,45	25,33				N.P	N.P	N.P		0,00	34,60	SM																	
SK-2	SPT	15,00-15,45	28,86				N.P.	N.P.	N.P.		6,69	44,06	SM																	
SK-2	SPT	21,00-21,45	31,48				36,47	19,21	17,26		0,36	96,09	CI																	
SK-2	SPT	27,00-27,45	34,61				33,41	20,08	13,33		0,36	96,09	CL																	
SK-3	SPT	3,00-3,45	23,72				29,01	20,00	9,01		0,00	93,73	CL																	
SK-3	SPT	9,00-9,45	33,38				37,39	21,92	15,47		0,24	90,77	CI																	
SK-3	SPT	13,50-13,95	28,02				37,51	23,29	14,23		0,00	97,90	CI																	
SK-3	SPT	16,50-16,95	32,88				49,91	20,61	29,31		0,00	81,31	CI																	
SK-3	SPT	21,00-21,45	29,31				30,42	21,47	8,95		0,00	92,84	CL																	
SK-3	SPT	28,50-28,95	30,92				31,20	21,05	10,15		0,00	89,05	CL																	

Figure F.1. Soil Experiment Results for SK1 – SK3

NUMUNE SAMPLE			Wn	γ_n	γ_K	Gs	ATTERBERG LİMİTLERİ TS 1900-2&2006				ELEK ANALİZİ SIEVE ANALYSIS		ZEMİN SINIFLANDIRMA TS 1500	Hidrometre		KESME KUTUSU DENEYİ DIRECT SHEAR TEST TS 1900-2 04.2006		ÜÇ EKSENLİ BASINÇ DENEYİ TRIAXIAL COMPRESSION TEST TS 1900-2 06.2006			TEK EKSENLİ BASINÇ DAYANIMI(ZEMİN) UNCONFINED COMP. TEST TS 1900-2 05.2006		NOKTA YÜKÜ DAYANIMI İNDEKSİ ISRM 1981	TEK EKSENLİ BASINÇ DAYANIMI (KAYA)	KONSOLİDASYON DENEYİ CONSOLIDATION TEST TS 1900-2 02.2006		PROKTOR SIKIŞTIRMA DENEYİ PROCTOR TEST		Tabii Boşluk Oranı	Tabii Porosite	Doygunluk Yüzdesi	PERMEABİLİTE DENEYİ PERMEABILITY TEST
SONDAJ BORING NO	NUMUNE SAMPLE NO	DERİNLİK DEPTH (m)	%	kN/m3	kN/m3	TS	LL	PL	PI	RÖTRE LİMİT %	10 (+) (%)	200 (-) (%)		kil %	silt %	c kPa	ø Deg.	c kPa	ø Deg		q_u kPa	qr kPa	$Is_{(50)}$ kg/cm^2	TS EN 1926 Mpa	Şişme Basıncı kPa	Şişme Swell (%)	γK Max g/cm^3	Wopt %	e %	n %	S %	K cm /
SK-4	SPT	1,50-1,95	31,05				51,49	20,34	31,16		0,00	90,30	CH																			
SK-4	SPT	6,00-6,45	32,26				52,45	20,97	31,48		0,00	90,17	CH																			
SK-4	SPT	9,00-9,45	43,23				45,18	18,32	26,86		0,00	98,17	CI																			
SK-4	UD	12,00-12,50	27,01	18,58			NP	NP	NP		0,16	38,91	SM			0	29			UU												
SK-4	SPT	18,00-18,45	25,71				NP	NP	NP		0,00	51,62	ML																			
SK-4	SPT	21,00-21,45	23,49				NP	NP	NP		0,00	20,40	SM																			
SK-4	SPT	25,00-25,45	27,39				32,42	17,37	15,05		0,00	91,07	CL																			
SK-5	SPT	1,50-1,95	36,89				48,64	18,40	30,24		0,14	98,18	CI																			
SK-5	SPT	10,50-10,95	35,87			2,70	37,08	21,05	16,03		0,00	99,59	CI	14,44	85,15																	
SK-5	SPT	16,50-10,95	44,66				66,25	24,17	42,08		0,00	98,93	CH																			
SK-5	SPT	22,50-22,95	21,11				N.P	N.P	N.P		0,00	81,52	ML																			
SK-5	SPT	25,50-25,95	25,29				N.P	N.P	N.P		0,32	77,18	ML																			
SK-5	SPT	30,00-30,45	30,71				N.P	N.P	N.P		0,14	89,00	ML																			
SK-6	SPT	1,50-1,95	37,55				56,72	23,89	32,82		0,00	99,03	CH																			
SK-6	SPT	4,50-4,95	25,67				N.P	N.P	N.P		0,00	7,88	SP-SM																			
SK-6	SPT	10,50-10,95	37,44				44,92	19,02	25,90		0,00	87,35	CI																			
SK-6	UD	16,50-17,00	42,83	18,01			55,15	24,09	31,06		0,00	99,34	CH					86	3	UU					X	X						
SK-6	SPT	19,50-19,95	32,50				37,03	18,31	18,72		0,00	94,59	CI																			
SK-6	SPT	21,00-21,45	28,40				NP	NP	NP		0,00	44,44	SM																			
SK-6	SPT	25,50-25,95	35,60				58,73	26,32	32,41		0,00	93,20	CH																			
SK-6	SPT	30,00-30,45	25,60				NP	NP	NP		0,00	59,14	ML																			

Figure F.2. Soil Experiment Results for SK4 – SK6

NUMUNE SAMPLE SONDAJ BORING NO	NUMUNE SAMPLE NO	DERİNLİK DEPTH (m)	Wn %	γ_n kN/m3	γ_K kN/m3	Gs	ATTERBERG LİMİTLERİ LL	PL	PI	RÖTRE LİMİT %	ELEK ANALİZİ SIEVE ANALYSIS 10 (+) (%)	200 (-) (%)	ZEMİN SINIFLANDIRMA TS 1500	Hidrometre kil %	silt %	KESME KUTUSU DENEYİ DIRECT SHEAR TEST c kPa	Ø Deg.	ÜÇ EKSENLİ BASINÇ DENEYİ TRIAXIAL COMPRESSION TEST c kPa	Ø Deg		TEK EKSENLİ BASINÇ DAYANIMI(ZEMİN) UNCONFINED COMP. TEST q_u kPa	q_r kPa	NOKTA YÜKÜ DAYANIMI İNDEKSİ ISRM 1981 $Is_{(50)}$ kg/cm²	TEK EKSENLİ BASINÇ DAYANIMI (KAYA) TS EN 1926 Mpa	KONSOLİDASYON DENEYİ CONSOLIDATION TEST Şişme Basıncı kPa	Şişme Swell (%)	PROKTOR SIKIŞTIRMA DENEYİ PROCTOR TEST γK Max g/cm³	Wopt %	Tabii Boşluk Oranı e %	Tabii Porosite n %	Doygunluk Yüzdesi S %	PERMEABİLİTE DENEYİ PERMEABILITY TEST K cm/
SK-7	SPT	1,50-1,95	36,01				52,06	19,85	32,21		0,22	98,60	CH																			
SK-7	SPT	4,50-4,95	36,52				52,22	20,86	31,36		0,00	99,06	CH																			
SK-7	SPT	9,00-9,45	29,48				37,61	23,44	14,18		0,00	95,00	CI																			
SK-7	UD	15,00-15,50	28,20	17,86			N.P.	N.P.	N.P.		0,00	75,66	ML			4	23			UU												
SK-7	SPT	19,50-19,95	27,35				N.P.	N.P.	N.P.		0,00	73,26	ML																			
SK-7	SPT	24,00-24,45	35,03				66,27	23,13	43,13		0,00	97,00	CH																			
SK-7	SPT	30,00-30,45	27,33				N.P	N.P	N.P		0,00	79,00	ML																			
SK-8	SPT	3,00-3,45	29,28				44,09	21,11	22,98		0,00	95,16	CI																			
SK-8	SPT	7,50-7,95	33,00				34,25	17,17	17,07		0,00	91,83	CL																			
SK-8	SPT	10,50-10,95	30,84			2,70	26,32	18,06	8,26		0,00	73,16	CL	7,22	65,94																	
SK-8	UD	15,00-15,50	34,51	17,81			N.P.	N.P.	N.P.		0,00	94,11	ML			4	22			UU												
SK-8	SPT	21,00-21,45	34,82				46,26	17,42	28,85		0,51	98,70	CI																			
SK-8	SPT	24,00-24,45	38,49				30,44	20,00	10,44		0,47	97,00	CL																			
SK-9	SPT	4,50-4,95	35,85				32,64	19,71	12,93		0,59	82,79	CL																			
SK-9	SPT	10,50-10,95	38,13				37,17	20,69	16,48		0,00	99,37	CI																			
SK-9	SPT	16,50-16,95	42,88				65,28	24,18	41,10		0,00	98,87	CH																			
SK-9	SPT	25,50-25,95	23,05				N.P	N.P	N.P		0,00	23,43	SM																			
SK-9	SPT	30,00-30,45	31,63				N.P	N.P	N.P		0,18	84,83	ML																			

Figure F.3. Soil Experiment Results for SK7 – SK9